

**Deep Uncertainty in
Multi-Objective Optimization
Leveraging Robustness Analysis to Improve
Adaptive Policy Design for River Basin
Management - A Case Study**

by

Paul Ludwig Branzk

A thesis submitted to the Faculty of Technology, Policy and
Management in partial fulfillment of the requirements for the degree of

Master of Science
in
Engineering and Policy Analysis
Technology, Policy, and Management

Thesis Chair:

Prof.dr.ir. P.H.A.J.M. van Gelder

Supervisor:

Prof. Jazmin Zatarain Salazar

Prof.dr.ir. P.H.A.J.M. van Gelder

Technical University of Delft
Delft, Netherlands

Declaration

I hereby declare that except where specific reference is made to the work of others, the contents of this thesis are original and have not been submitted in whole or in part for consideration for any other degree or qualification in this, or any other university. This thesis is my own work and contains nothing which is the outcome of work done in collaboration with others, except as specified in the text.

Paul Ludwig Branzk
August 2024

Abstract

Transboundary river basins are increasingly subjected to pressures from climate change, economic expansion, and population growth. These challenges are compounded by Deep Uncertainties and the complexities of managing water resources that cross administrative borders. The thesis aims to improve decision support for river basin management under Deep Uncertainty. Robustness Analysis is leveraged to improve the adaptive policy design of reservoir operating policies. Open Exploration generates future states of the world. Using Feature Scoring, PRIM, and Logistic Regression Modeling, Scenario Discovery pinpoints vulnerabilities that result in Adaptation Tipping Points described by streamflow patterns. Results identified decreasing precipitation and low seasonal amplitudes as the most significant uncertainty factors influencing system performance. In combination with the evaporation rate, they accurately predict policy failure. A precipitation threshold of 0.965 and a seasonal amplitude threshold of 1.05 effectively describe streamflow patterns that describe the Adaptation Tipping Point across the Best Hydropower, Best Environment, and Best Tradeoff policy. Specifically, a resultant streamflow pattern at these thresholds accurately signals imminent policy inefficiencies that necessitate policy adaptation.

Table of contents

| | |
|--|-----------|
| List of figures | xi |
| List of tables | xix |
| Nomenclature | xxi |
| Executive Summary | xxiii |
| 1 Introduction | 1 |
| 2 Theoretical Background | 5 |
| 2.1 River Basin Management | 5 |
| 2.1.1 Problem Context | 5 |
| 2.1.2 Decision Context | 6 |
| 2.2 Deep Uncertain River Basins | 7 |
| 2.2.1 Decision-making Under Deep Uncertainty | 7 |
| 2.2.2 Robust Planning | 8 |
| 2.2.3 Dynamic Planning | 9 |
| 2.2.4 Comparing Robust and Dynamic Planning Approaches | 12 |
| 2.2.5 Decision Support Tools for Deep Uncertainty | 14 |
| 2.3 Modeling River Basin Management | 15 |
| 2.3.1 Mass-Balance Approach | 15 |
| 2.3.2 Decision Problem | 16 |
| 2.3.3 The Three Curses of Modeling | 17 |
| 2.4 Evolutionary Multi-Objective Direct Policy Search | 18 |
| 2.4.1 Direct Policy Search | 18 |
| 2.4.2 Multi-Objective Evolutionary Algorithms | 18 |
| 2.4.3 EMODPS and Deep Uncertainty | 19 |
| 2.5 Research Questions | 19 |
| 3 Case Study Area | 23 |
| 3.1 Zambezi River System | 23 |
| 3.2 Zambezi Model | 24 |

| | | |
|----------|--|-----------|
| 3.2.1 | Model Structure | 26 |
| 3.2.2 | Policy Functions | 26 |
| 3.2.3 | Objectives | 28 |
| 4 | Method | 31 |
| 4.1 | Methodology | 31 |
| 4.1.1 | Identification of Policy Alternatives | 31 |
| 4.1.2 | Robustness Analysis | 31 |
| 4.1.3 | Improvement of Adaptive Policy Design | 32 |
| 4.2 | Method | 33 |
| 4.2.1 | Uncertainty Characterization | 33 |
| 4.2.2 | Open Exploration | 34 |
| 4.2.3 | Scenario Discovery | 35 |
| 4.3 | Assessment Metrics | 37 |
| 4.3.1 | Quality Indicators | 37 |
| 4.3.2 | Visual Analysis | 38 |
| 4.4 | Experimental Settings | 39 |
| 5 | Analysis | 41 |
| 5.1 | Zambezi Base Case Run | 41 |
| 5.1.1 | Reference Set | 41 |
| 5.1.2 | Convergence | 42 |
| 5.1.3 | Multi-objective Tradeoffs | 44 |
| 5.2 | Uncertainty Characterization | 45 |
| 5.2.1 | Manipulation of Streamflow Data | 45 |
| 5.2.2 | Temperature | 48 |
| 5.2.3 | Irrigation Demand | 48 |
| 5.3 | Exploratory Modeling | 49 |
| 5.3.1 | Selection of Policy Levers | 49 |
| 5.3.2 | Sampling the Uncertainty Space | 49 |
| 5.3.3 | Open Exploration | 50 |
| 5.4 | Scenario Discovery | 53 |
| 5.4.1 | Defining Signpost Conditions | 53 |
| 5.4.2 | Quantification of Adaptation Tipping Points | 56 |
| 6 | Results | 63 |
| 6.1 | Key Uncertainties in the Zambezi River Basin | 63 |
| 6.1.1 | Hydroclimatic Uncertainties | 63 |
| 6.1.2 | Socio-economic Uncertainties | 64 |
| 6.2 | Critical Signpost Conditions for the Zambezi River Basin | 66 |
| 6.2.1 | Feature Scoring | 66 |
| 6.2.2 | PRIM | 72 |
| 6.3 | Adaptation Tipping Points for the Zambezi River Basin | 79 |
| 6.3.1 | Identification of Adaptation Tipping Point Thresholds | 81 |

| | | |
|----------|---|------------|
| 6.3.2 | Streamflow Patterns of Adaptation Tipping Points | 84 |
| 7 | Discussion | 89 |
| 8 | Conclusion and Recommendations | 95 |
| 8.1 | Conclusion | 95 |
| 8.2 | Recommendation | 96 |
| 8.3 | Limitations | 97 |
| 8.4 | Future Work | 98 |
| | References | 101 |
| | Appendix A Zambezi Model | 109 |
| A.1 | Zambezi Model Model Structure | 110 |
| A.2 | Reservoir Class Structure | 111 |
| A.3 | Catchment Class Structure | 112 |
| A.4 | Policy Class Structure | 112 |
| A.5 | Utils Class Structure | 112 |
| A.6 | Smash Class Structure | 113 |
| | Appendix B Base Case Reference Set | 115 |
| B.1 | Base Case Pareto-Sets | 115 |
| B.2 | Pareto-Sets across five different seeds | 115 |
| | Appendix C Uncertainty Characterization | 119 |
| C.1 | Flow Duration Curves: Historical vs. Synthetic | 120 |
| C.2 | Rescaled Mean Precipitation Catchment Inflows | 121 |
| C.3 | Rescaled Inter-annual Variability Catchment Inflows | 122 |
| C.4 | Fitted Fourier Series over Monthly Average Historical Catchment Inflows | 123 |
| C.5 | Rescaled Seasonal Amplitudes Catchment Inflows | 124 |
| C.6 | Rescaled Seasonal Shift Catchment Inflows | 125 |
| | Appendix D Scenario Discovery | 127 |
| D.1 | Scenarios of Interest | 127 |
| D.2 | PRIM Density-Coverage Tradeoff Plots (Best Hydropower Policy) | 130 |
| D.3 | PRIM Density-Coverage Tradeoff Plots (Best Environment Policy) | 132 |
| D.4 | PRIM Density-Coverage Tradeoff Plots (Best Irrigation Policy) | 133 |
| D.5 | PRIM Density-Coverage Tradeoff Plots (Best Tradeoff Policy) | 134 |
| D.6 | PRIM Scenario Box Tables | 135 |
| | Appendix E Adaptation Tipping Points | 145 |
| E.1 | Logistic Regression Contour Plot Best Hydropower (Hydropower Deficit) | 145 |
| E.2 | Logistic Regression Model Parameters (Best Hydropower Policy) | 146 |
| E.3 | Logistic Regression Model Parameters (Best Environment Policy) | 147 |
| E.4 | Logistic Regression Model Parameters (Best Irrigation Policy) | 148 |

| | | |
|------|--|-----|
| E.5 | Logistic Regression Model Parameters (Best Tradeoff Policy) | 149 |
| E.6 | Logistic Regression Contour Plots (Signpost Condition Set 1) | 150 |
| E.7 | Logistic Regression Contour Plots (Signpost Condition Set 2) | 152 |
| E.8 | Logistic Regression Contour Plots (Signpost Condition Set 3) | 154 |
| E.9 | Adaptation Tipping Point Streamflow Plot for ATP-Conditions | 156 |
| E.10 | Adaptation Tipping Point Streamflow Tables for Max ATP-Condition | 156 |

List of figures

| | | |
|-----|---|-------|
| 1 | The Zambezi River Basin. | xxiii |
| 2 | Proposed Methodology. | xxiv |
| 3 | ATP Streamflow Decrease. | xxv |
| 2.1 | XLRM Framework Diagram for River Basin Management. Policy levers (L) describe reservoir release decisions to improve the system (R) under varying external conditions (X) captured by performance metrics (M). | 7 |
| 2.2 | Progressive Transition Table of Levels of Uncertainty from (Marchau et al., 2019). Levels range from deterministic systems to total ignorance, with four different levels in between. The main criteria are context, system model, system outcomes, and weights. | 8 |
| 2.3 | Dynamic Adaptive Policy Pathway Map. It illustrates a metro map commonly used for Dynamic Adaptive Policy Pathway planning. It depicts various policy actions over time, starting from the current policy. It outlines potential future paths, each representing a response to changing conditions captured by the Signpost. Policies adapt when current policy actions reach adaptation tipping points. | 11 |
| 3.1 | Map of the Zambezi River Basin. The map highlights eight irrigation districts, three main ecological sides, and five water reservoirs. The basin spans across eight riparian countries - Angola, Botswana, Malawi, Mozambique, Namibia, Tanzania, Zambia, and Zimbabwe. | 24 |
| 3.2 | Conceptual Diagram of the Zambezi River Basin Model. The model has three main components: five water reservoirs, three ecological sides, and eight irrigation districts. The main rivers are the Kafue and Zambezi Rivers, with additional inflows from seven catchment areas. | 25 |
| 4.1 | Conceptualized Methodology Workflow. The workflow is structured into three main components. a) Conventional EMODPS describes the Zambezi model, resulting in Pareto-optimal policies. b) Robustness Analysis includes the identification of key uncertainties through Open Exploration and Scenario Discovery. c) Improving the Adaptive Policy Design focuses on the identification of Signpost and Adaptation Tipping Points | 32 |

| | | |
|-----|--|----|
| 5.1 | Pair Plot and Density Distribution of Reference Set. A comprehensive visualization of MinMax normalized Pareto-optimal solutions across three objectives derived from five seeds. Diagonal panels display density plots for each objective, with lower values indicating better performance. Off-diagonal scatter plots illustrate pairwise tradeoffs between the objectives. | 42 |
| 5.2 | Quality Indicators for Basecase Run. The figure illustrates four key performance metrics across five seeds over 200,000 NFEs. a) Generational Distance measures convergence towards the Pareto front. b) Hypervolume highlights the quality and diversity of solution space. c) Additive Epsilon Indicator reflects solution accuracy. d) Epsilon Progress displays epsilon improvements, indicating convergence. | 43 |
| 5.3 | Parallel Coordinate Plot. It displays Tradeoffs among Hydropower, Environment, and Irrigation. Each line represents a different solution from the reference set, with the vertical position on each axis indicating the MinMax normalized performance score. Lower values are preferred. The color gradient from light purple to dark blue represents the hydropower objective value; the darker, the better. | 44 |
| 5.4 | Kariba Catchment Exceedance Probability Under Different Scenarios. The left panel displays the effect of different mean precipitation multiplier values (m_{μ}). The right panel shows the effect of different interannual variability multiplier values (m_{σ}). | 46 |
| 5.5 | Kariba Catchment Seasonal Variability. The left panel displays different seasonal amplitude values of m_{C1} and m_{C2} . The right panel shows the effect of different seasonal phase shift values of $d\phi_1$ and $d\phi_2$ | 47 |
| 5.6 | Open Exploration Scenario Outcomes. The figure illustrates the distribution and tradeoffs of objective values for hydropower, environment, and irrigation under 25,000 uncertainty conditions. Diagonal panels show frequency distributions of objective deficits, with color intensity indicating occurrence frequency: darker shades for more common outcomes and lighter for rarer ones. The upper panels depict scatter plots comparing two objectives. The color coding differentiates four policies. | 51 |
| 5.7 | Feature Scoring Heatmap for Best Hydropower Policy. The heatmap displays the importance of uncertainty factors in relation to the objective outcomes, with lighter colors indicating higher importance. | 54 |
| 5.8 | PRIM Density - Coverage Tradeoff Plot. Each scatter dot represents a scenario box described by uncertainty factors. The color coding indicates the total number. Density displays how accurate the box is in identifying failure scenarios. Coverage indicates how reliable the scenario box is in covering all failure scenarios. | 55 |

| | | |
|------|---|----|
| 5.9 | Logistic Regression Contour Plot for Best Hydropower Policy. The probability of policy failure is shown across three signpost conditions. The contour line color indicates failure probability, with lighter shades representing higher risks. Dark dots describe policy failure. | 58 |
| 5.10 | Comparison of Monthly Average Streamflow and Adaptation Tipping Point for the Kafue Flats catchment. The monthly streamflow Adaptation Tipping Point indicates the upper limit of the generated streamflow patterns. Once actual streamflow data falls below this graph, the Best Hydropower policy should adapt. | 59 |
| 6.1 | Feature Scoring Summary across Four Policies. The heatmap displays the importance of uncertainty factors in relation to the objective outcomes, with lighter colors indicating higher importance. | 67 |
| 6.2 | Feature Scoring Heatmap for Best Hydropower policy. The heatmap displays the importance of uncertainty factors in relation to the objective outcomes, with lighter colors indicating higher importance. | 68 |
| 6.3 | Feature Scoring Heatmap for Best Environment policy. The heatmap displays the importance of uncertainty factors in relation to the objective outcomes, with lighter colors indicating higher importance. | 69 |
| 6.4 | Feature Scoring Heatmap for Best Irrigation policy. The heatmap displays the importance of uncertainty factors in relation to the objective outcomes, with lighter colors indicating higher importance. | 70 |
| 6.5 | Feature Scoring Heatmap for Best Tradeoff policy. The heatmap displays the importance of uncertainty factors in relation to the objective outcomes, with lighter colors indicating higher importance. | 71 |
| 6.6 | Summary of PRIM Density - Coverage Tradeoff Plots for Best Hydropower Policy. Subplots describe the scenario of interest, which PRIM tries to describe under the Best Hydropower policy. | 74 |
| 6.7 | Summary of PRIM Density - Coverage Tradeoff Plots for Best Irrigation Policy. Subplots describe the scenario of interest, which PRIM tries to describe under the Best Irrigation policy. | 76 |
| 6.8 | Summary of PRIM Density - Coverage Tradeoff Plots for Best Tradeoff Policy. Subplots describe the scenario of interest, which PRIM tries to describe under the Best Tradeoff policy. | 78 |
| 6.9 | Logistic Regression Contour Plots for Best Hydropower Policy. The contour line color indicates failure probability, with lighter shades representing higher risks. Dark dots describe policy failure. | 81 |
| 6.10 | Logistic Regression Contour Plots for Best Environment Policy. The contour line color indicates failure probability, with lighter shades representing higher risks. Dark dots describe policy failure. | 82 |
| 6.11 | Logistic Regression Contour Plots for Best Tradeoff Policy. The contour line color indicates failure probability, with lighter shades representing higher risks. Dark dots describe policy failure. | 83 |

| | | |
|------|---|-----|
| 6.12 | Comparison of Monthly Average Streamflow and adaptation tipping point patterns for the Kafue Flats catchment. | 85 |
| 6.13 | Streamflow Pattern of the Chosen Adaptation Tipping Point Scenario with Absolute Decrease Values. The heatmap indicates the monthly decrease in streamflow across all relevant catchments compared to historical averages. The color intensity represents the absolute difference, with darker shades indicating higher values. | 86 |
| A.1 | UML Overview of the Zambezi Base Case Model. | 110 |
| A.2 | UML Overview of the Reservoir Class. | 111 |
| A.3 | UML Overview of the Catchment Class. | 112 |
| A.4 | UML Overview of the Policy Class. | 112 |
| A.5 | UML Overview of the Utils Class. | 112 |
| A.6 | UML Overview of the Smash Class. | 113 |
| B.1 | Pareto optimal solutions over five seeds across three objectives. Lower objective values indicate better performance. Values are normalized using MinMaxScaler. | 115 |
| B.2 | Pair plots of the five seeds using scatter plots. Pareto optimal solutions for five seeds from a) Seed 0 to e) Seed 4. The three objectives are hydropower, environment, and irrigation. Lower objective values indicate better performance. Values are normalized using MinMaxScaler. | 116 |
| B.3 | Pair plots of the five seeds using kernel density estimates. Pareto optimal solutions for five seeds from a) Seed 0 to e) Seed 4. The three objectives are hydropower, environment, and irrigation. Lower objective values indicate better performance. Values are normalized using MinMaxScaler. | 117 |
| C.1 | Flow Duration Curves of Historic and Synthetic Inflow Data of seven Catchments within the Zambezi River Basin. Panels (a) to (f) display the FDCs for each catchment respectively. Synthetic and historic streamflow data is log-transformed. Each curve represents an FDC over one year. In total, data consists of 20 years. | 120 |
| C.2 | Flow Duration Curves of Historic and Rescaled Mean Precipitation Inflow Data of seven Catchments within the Zambezi River Basin. The areas between lower and upper bounds are shaded with their respective color and indicate areas of possible streamflow. | 121 |
| C.3 | Flow Duration Curves of Historic and Rescaled Seasonal Variability Inflow Data of seven Catchments within the Zambezi River Basin. The areas between lower and upper bounds are shaded with their respective color and indicate areas of possible streamflow. | 122 |
| C.4 | Monthly Averages of Historical Streamflow Data with Fitted Fourier Series. Each Dot represents a monthly average value, one for each year (total of 20 years). The fitted Fourier series is displayed as a line. | 123 |

| | | |
|-----|--|-----|
| C.5 | Rescaled Seasonal Amplitude Catchment Inflows of seven Catchments within the Zambezi River Basin. Different line types indicate different applied factors. Dash-Dot line representing a lower seasonal amplitude factor. Dashed Lines higher seasonal amplitude factor and solid lines original synthetic seasonal average data. Panels (a) to (f) display the catchment areas of: Kariba, Kariba Lateral, Itthezi-Thezi, Cahora Bassa, Shire, Kafue Flats, and Bakota George. | 124 |
| C.6 | Rescaled Seasonal Phase Shift Catchment Inflows of seven Catchments within the Zambezi River Basin. Different line types indicate different applied factors. Dash-Dot line representing a lower seasonal phase-shift factor. Dashed Lines higher seasonal phase-shift factor and solid lines original synthetic seasonal average data. Panels (a) to (f) display the catchment areas of: Kariba, Kariba Lateral, Itthezi-Thezi, Cahora Bassa, Shire, Kafue Flats, and Bakota George. | 125 |
| D.1 | Scenarios of Interest (Hydropower Performance Failure). Dots represent objective values across 100,000 states of the world. Colors indicate policy specific scenario outcomes (25,000). Scenarios of interest describe worst 20 percent of hydropower outcomes highlighted in dark purple. | 128 |
| D.2 | Scenarios of Interest based on Environmental Performance Failure. Dots represent objective values across 100,000 states of the world. Colors indicate policy specific scenario outcomes (25,000). Scenarios of interest describe worst 20 percent of environmental outcomes highlighted in dark purple. | 128 |
| D.3 | Scenarios of Interest based on Irrigation Performance Failure. Dots represent objective values across 100,000 states of the world. Colors indicate policy specific scenario outcomes (25,000). Scenarios of interest describe worst 20 percent of irrigation outcome highlighted in dark purple. | 129 |
| D.4 | Scenarios of Interest based on Overall Performance Failure. Dots represent objective values across 100,000 states of the world. Colors indicate policy specific scenario outcomes (25,000). Scenarios of interest describe the scenarios that are in the worst 20 percent across all three objective (total number of 1134 scenarios) highlighted in dark purple. | 129 |
| D.5 | PRIM Density - Coverage Tradeoff Plot for the Best Hydropower Policy identifying hydropower deficit scenarios. Each scatter dot represents a scenario box. The color coding indicates the total number of uncertainty factors that are needed to describe the box. | 130 |
| D.6 | PRIM Density - Coverage Tradeoff Plot for the Best Hydropower Policy identifying environmental deficit scenarios. Each scatter dot represents a scenario box. The color coding indicates the total number of uncertainty factors that are needed to describe the box. | 130 |

| | | |
|------|---|-----|
| D.7 | PRIM Density - Coverage Tradeoff Plot for the Best Hydropower Policy identifying irrigation deficit scenarios. Each scatter dot represents a scenario box. The color coding indicates the total number of uncertainty factors that are needed to describe the box. | 131 |
| D.8 | PRIM Density - Coverage Tradeoff Plot for the Best Hydropower Policy identifying overall deficit scenarios. Each scatter dot represents a scenario box. The color coding indicates the total number of uncertainty factors that are needed to describe the box. | 131 |
| D.9 | PRIM Density - Coverage Tradeoff Plot for the Best Hydropower Policy identifying hydropower deficit scenarios. Each scatter dot represents a scenario box. The color coding indicates the total number of uncertainty factors that are needed to describe the box. | 132 |
| D.10 | PRIM Density - Coverage Tradeoff Plot for the Best Hydropower Policy identifying irrigation deficit scenarios. Each scatter dot represents a scenario box. The color coding indicates the total number of uncertainty factors that are needed to describe the box. | 132 |
| D.11 | PRIM Density - Coverage Tradeoff Plot for the Best Hydropower Policy identifying hydropower deficit scenarios. Each scatter dot represents a scenario box. The color coding indicates the total number of uncertainty factors that are needed to describe the box. | 133 |
| D.12 | PRIM Density - Coverage Tradeoff Plot for the Best Hydropower Policy identifying environmental deficit scenarios. Each scatter dot represents a scenario box. The color coding indicates the total number of uncertainty factors that are needed to describe the box. | 133 |
| D.13 | PRIM Density - Coverage Tradeoff Plot for the Best Hydropower Policy identifying hydropower deficit scenarios. Each scatter dot represents a scenario box. The color coding indicates the total number of uncertainty factors that are needed to describe the box. | 134 |
| D.14 | PRIM Density - Coverage Tradeoff Plot for the Best Hydropower Policy identifying environmental deficit scenarios. Each scatter dot represents a scenario box. The color coding indicates the total number of uncertainty factors that are needed to describe the box. | 134 |
| E.1 | Logistic Regression Contour Plots based on Signpost Condition Set 1. The plot displays the probability for the Best Hydropower policy to fail (Scenario of Interest is Hydropower Deficit). | 145 |
| E.2 | Logistic Regression Contour Plots based on Signpost Condition Set 1 (Best Hydropower Policy). The contour line color indicates failure probability, with lighter shades representing higher risks. Dark dots describe policy failure. | 150 |
| E.3 | Logistic Regression Contour Plots based on Signpost Condition Set 1 (Best Environment Policy). The contour line color indicates failure probability, with lighter shades representing higher risks. Dark dots describe policy failure. | 150 |

| | | |
|------|--|-----|
| E.4 | Logistic Regression Contour Plots based on Signpost Condition Set 1 (Best Irrigation Policy). The contour line color indicates failure probability, with lighter shades representing higher risks. Dark dots describe policy failure. | 151 |
| E.5 | Logistic Regression Contour Plots based on Signpost Condition Set 1 (Best Tradeoff Policy). The contour line color indicates failure probability, with lighter shades representing higher risks. Dark dots describe policy failure. | 151 |
| E.6 | Logistic Regression Contour Plots based on Signpost Condition Set 2 (Best Hydropower Policy). The contour line color indicates failure probability, with lighter shades representing higher risks. Dark dots describe policy failure. | 152 |
| E.7 | Logistic Regression Contour Plots based on Signpost Condition Set 2 (Best Environment Policy). The contour line color indicates failure probability, with lighter shades representing higher risks. Dark dots describe policy failure. | 152 |
| E.8 | Logistic Regression Contour Plots based on Signpost Condition Set 2 (Best Irrigation Policy). The contour line color indicates failure probability, with lighter shades representing higher risks. Dark dots describe policy failure. | 153 |
| E.9 | Logistic Regression Contour Plots based on Signpost Condition Set 2 (Best Tradeoff Policy). The contour line color indicates failure probability, with lighter shades representing higher risks. Dark dots describe policy failure. | 153 |
| E.10 | Logistic Regression Contour Plots based on Signpost Condition Set 3 (Best Hydropower Policy). The contour line color indicates failure probability, with lighter shades representing higher risks. Dark dots describe policy failure. | 154 |
| E.11 | Logistic Regression Contour Plots based on Signpost Condition Set 3 (Best Environment Policy). The contour line color indicates failure probability, with lighter shades representing higher risks. Dark dots describe policy failure. | 154 |
| E.12 | Logistic Regression Contour Plots based on Signpost Condition Set 3 (Best Irrigation Policy). The contour line color indicates failure probability, with lighter shades representing higher risks. Dark dots describe policy failure. | 155 |
| E.13 | Logistic Regression Contour Plots based on Signpost Condition Set 3 (Best Tradeoff Policy). The contour line color indicates failure probability, with lighter shades representing higher risks. Dark dots describe policy failure. | 155 |

- E.14 Streamflow Pattern of the Max ATP-Streamflow Condition. Comparison of historical monthly average streamflow data and Adaptation Tipping Point patterns based on the Adaptation Tipping Point Thresholds of a mean precipitation factor 0.965, and seasonal amplitudes of 1.05. . . . 156

List of tables

| | | |
|------|---|-----|
| 2.1 | Comparison of Robust and Dynamic Planning | 13 |
| 3.1 | Summary of Model Parameters | 27 |
| 3.2 | Summary of Model Policy Parameters | 28 |
| 5.1 | Summary of Uncertainty Factors | 50 |
| 5.2 | Best Hydropower Policy Analysis for Hydropower Deficit Scenario . . . | 56 |
| 5.3 | Monthly average streamflows for the KafueFlats catchment comparing historical data with monthly streamflow values that describe the Adaptation Tipping Point for Best Hydropower policy in regard to hydropower generation. | 60 |
| 6.1 | Summary of Deep Uncertainty Trends within the Zambezi River Basin | 65 |
| 6.2 | Summary of Uncertainty Factors' Influence Across Policies | 72 |
| 6.3 | Best Environment Policy Analysis for Hydropower and Irrigation Deficit Scenarios | 75 |
| 6.4 | Summary of Signpost Conditions for Each Policy Scenario | 79 |
| 6.5 | Summary of Model Accuracy Across Policy Sets | 80 |
| D.1 | Policy Distribution Across Different Scenarios of Interest | 127 |
| D.2 | Best Hydropower Policy Analysis for Hydropower Deficit Scenario . . . | 135 |
| D.3 | Best Hydropower Policy Analysis for Environment Deficit Scenario . . | 136 |
| D.4 | Best Hydropower Policy Analysis for Irrigation Deficit Scenario | 137 |
| D.5 | Best Hydropower Policy Analysis for Overall Deficit Scenario | 138 |
| D.6 | Best Environment Policy Analysis for Hydropower Deficit Scenario . . | 139 |
| D.7 | Best Environment Policy Analysis for Irrigation Deficit Scenario | 139 |
| D.8 | Best Irrigation Policy Analysis for Hydropower Deficit Scenario | 140 |
| D.9 | Best Irrigation Policy Analysis for Environmental Deficit Scenario . . . | 141 |
| D.10 | Best Tradeoff Policy Analysis for Hydropower Deficit Scenario | 142 |
| D.11 | Best Tradeoff Policy Analysis for Environmental Deficit Scenario | 143 |
| E.1 | Logistic Regression Model Parameters of Policy Failure for Best Hydropower Policy | 146 |

| | | |
|------|---|-----|
| E.2 | Logistic Regression Model Parameters of Policy Failure for Best Environmental Policy | 147 |
| E.3 | Logistic Regression Model Parameters of Policy Failure for Best Irrigation Policy | 148 |
| E.4 | Logistic Regression Model Parameters of Policy Failure for Best Tradeoff Policy | 149 |
| E.5 | Monthly streamflow patterns for the Itt catchment comparing historical data with ATP streamflow values. | 157 |
| E.6 | Monthly streamflow patterns for the Kafue Flats catchment comparing historical data with ATP streamflow values. | 157 |
| E.7 | Monthly streamflow patterns for the Kariba catchment comparing historical data with ATP streamflow values. | 158 |
| E.8 | Monthly streamflow patterns for the Cahora Bassa catchment comparing historical data with ATP streamflow values. | 158 |
| E.9 | Monthly streamflow patterns for the Shire catchment comparing historical data with ATP streamflow values. | 159 |
| E.10 | Monthly streamflow patterns for the Bakota George catchment comparing historical data with ATP streamflow values. | 159 |

Nomenclature

Acronyms / Abbreviations

ATP Adaptation Tipping Point

EMODPS Evolutionary Multi-Objective Direct Policy Search

PRIM Patient Rule Induction Algorithm

Executive Summary

The thesis aims to improve decision support for river basin management under Deep Uncertainty. A new framework is introduced and demonstrated using the transboundary Zambezi River Basin as a case study. Ultimately, it improves collaboration and cooperation in transboundary river basins, providing a decision-support tool for river basin management to improve Decision-making under Deep Uncertainty.

The thesis sets out to leverage Robustness Analysis to identify critical uncertainties and performance gaps that inform the definition of Signpost Conditions and Adaptation Tipping Points. Hence, this thesis asks:

How to leverage robustness analysis to improve the adaptive policy design in the context of river basin management under deep uncertainty?

Case Study Area

The Zambezi River Basin exemplifies a contextual situation that many transboundary river basins face globally. As one of the most affected by climate change, the basin is anticipated to struggle. Five water reservoirs along the Kafue and Zambezi rivers are used to generate hydropower and store and release water based on minimum environmental flows at three sides and eight water-demanding irrigation districts. Overall, it highlights the necessity for a detailed

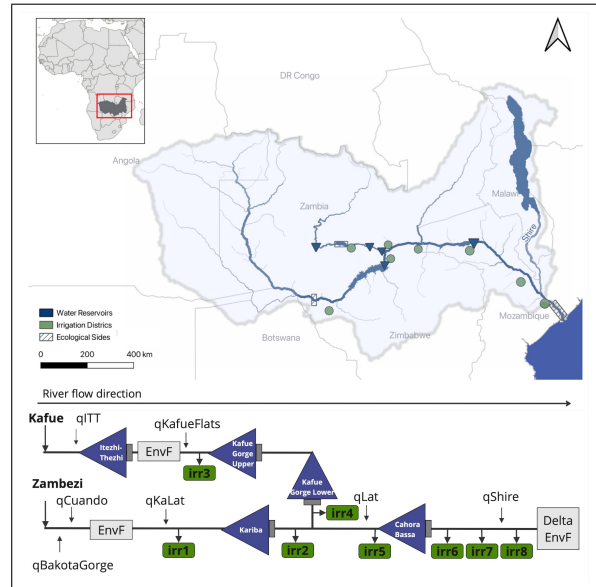


Fig. 1 The Zambezi River Basin.

analysis of tradeoffs while acknowledging Deep Uncertainty.

Methodology

The new methodology integrates the EMODPS decision support with a Robustness Analysis to identify system vulnerabilities and Adaptation Tipping Points. This includes:

- Uncertainty Analysis
- Open Exploration
- Scenario Discovery

First, a non-systematic literature review identifies the most critical uncertainties for the Zambezi River Basin.

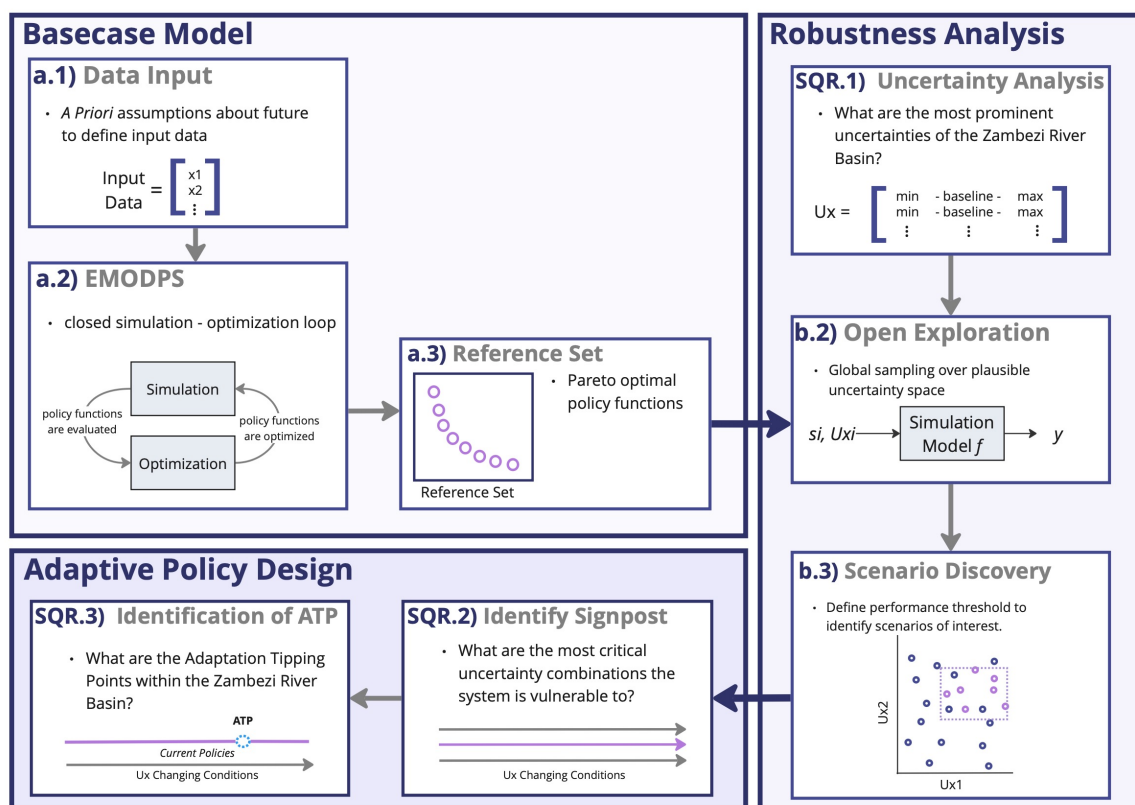


Fig. 2 Proposed Methodology.

Second, an Open Exploration experiment generates plausible future States of the World. This includes quantifying most critical uncertainties to explore system vulnerabilities. It is envisioned to hint at potential Signpost Conditions characterized by an interplay of uncertainties.

Third, Scenario Discovery utilizes Feature Scoring, PRIM and Logistic Regression Modeling to identify most critical uncertainty combinations. Altogether, this aids in identifying Signpost Conditions and quantifying Adaptation Tipping Points, both of which are critical for an adaptive policy design.

Results

Decreases in precipitation and lower seasonal amplitudes are linked to consistent policy failures, highlighting the basin's vulnerability to hydroclimatic shifts. A third condition is necessary to ensure an accurate and reliable definition of failure scenarios. Logistic regression models were able to accurately predict conditions under which the system fails to meet its objectives.

Thresholds were used to generate ATP streamflow conditions. These describe the contextual character of Adaptation Tipping Points for the Zambezi River Basin. It is recommended to choose the max ATP-condition as it describes a cautious approach that leads to early adaptation signals. Once the Zambezi River Basin expe-

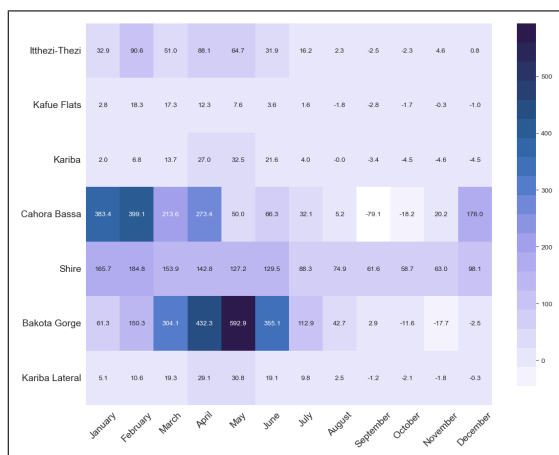


Fig. 3 ATP Streamflow Decrease.

periences similar decreases to Figure 3, operation strategies derived from historical data are not sufficient and will fail.

Implications

The framework enhances Dynamic Planning by integrating the EMODPS decision-support tool with Robustness Analysis. It offers workflow that overcomes the challenges surrounding the complex policy structure of Dynamic Adaptive Policy Plans. The framework allows policymakers to define contextual Adaptation Tipping Points, emphasizing the transition from *predict-then act* to *monitor-and-adapt* policy making. Stepping away from seeking fixed solutions towards promoting continuous dialogue and making responsive adjustments aligns with the goal of collaboration in transboundary river basin management, as policymakers can recognize the Deep Uncertain nature of river basins and stakeholder preferences.

Recommendations

To institutionalize the Dynamic Planning approach, establishing a cooperative monitoring system is recommended for the Zambezi River Basin. Given that mean precipitation and seasonal amplitudes are identified as primary drivers of system vulnerability, it is crucial to focus monitoring efforts on these variables.

Monitoring should focus on ATP-streamflow condition changes according to:

- Significant reductions in streamflow compared to historic data during the rainy season; particularly from January to June
- Special attention to the Cahora Bassa and Bakota Gorge catchments, where pronounced impacts are observed during rainy season streamflow, frequently exceeding 20 percent.
- Observing the comparatively milder decreases during the dry season, such as the 10.72 percent reduction in the same areas, which, while less severe, could still indicate adaptation needs.

Further, involved stakeholders including reservoir operators should be supported through training, advanced modeling tools, and demonstration projects to foster the transition towards monitoring river basins and adapting operating strategies accordingly.

Chapter 1

Introduction

River basins are under increasing pressure. Climate change, economic expansions, population growth, and the lack of transboundary management agreements are accelerating their degradation (Eckstein et al., 2021). In 2050, the number of people residing in water-stressed transboundary basins will double (Munia et al., 2016). Consequently, increasing water resource depletion and demand will intensify competition and conflicts (Nations, 2009; Watkins, 2006). With 60 percent of the world's freshwater resources flowing across political borders, inter-dependencies tied to transboundary river basins only grow more complex (Kecskes, 2020).

Effective river basin management is vital for human survival, ecosystem health, and advancing societies. The 1992 global Water Convention (WHO, 1999), Sustainable Development Goal 6 (United Nations, 2015), and regional strategies like the 2018-2030 African Ministers' Council on Water (AMCOW, 2018), and the 2021 EU Council Conclusions on Water, all actively emphasize this recognition. They promote multi-actor agreements for equitable water (re)allocation. It aims to resolve conflicts through cooperation, enhancing financial investments, benefit sharing, and social cohesion. For instance, Wheeler et al. (2016) state that a transboundary agreement for the Eastern Nile Basin could significantly minimize the risk of conflict.

Despite its benefits, reaching transboundary agreements takes time and effort. Distributing water between up- and downstream actors requires balancing diverse interests (Kedida and Arsano, 2024). Stakeholders' differing perceptions of a fair distribution of benefits and risks further complicate consensus (Turton and Ashton, 2008). Moreover, limited knowledge about hydroclimatic and socio-economic developments increases complexity (Zeitoun et al., 2013).

Effective river basin management must synthesize multiple timescales, ranging from short-term water needs to long-term sustainability goals. It requires decision-makers to make uncertain assumptions about the future (Dewar et al., 1993). These uncertainties are deep when probabilities are elusive or absent (Walker et al., 2003). Two approaches are prominent; Robust-and Dynamic Planning

Decision-makers account for uncertainties post-modeling, following a Robust Planning approach. Honing the principles of Exploratory Modeling Analysis, decision support eschews early commitment to a single scenario (Bankes, 1993). Instead, multiple alternative policies are evaluated across various future states of the world (Savage, 1972). Consequently, decision-makers can ensure policy effectiveness under Deep Uncertainty by prioritizing the least sensitive policies (Herman et al., 2015). However, the need to handle all scenarios equally may decrease performance due to their potential precautionary bias towards extreme scenarios. Moreover, the final policy selection depends on the chosen metric, raising the question of how robust robustness metrics are (Kwakkel et al., 2016).

In contrast, rather than prioritizing a robust policy post-modeling, policymakers emphasize an adaptive policy design. Adopting a proactive stance that anticipates future changes and necessary policy adaptations, Dynamic Planning embraces flexible policy plans to manage multiple states of the world (Kwakkel et al., 2010; Walker et al., 2001). Once changing conditions affect system performance significantly, policies adapt. Nevertheless, determining which conditions to monitor, called Signposts (Haasnoot et al., 2013), and when to adapt, called Adaptation Tipping Points (Kwadijk et al., 2010), is challenging.

To improve river basin management under Deep Uncertainty, policymakers must account for the multiplicity of future outcomes. While robust and dynamic approaches have limitations and are often viewed contrary to others, this thesis aims to integrate them into a comprehensive framework. Groves et al. (2015) argue that exploratory analysis could highlight conditions under which policies fail. This thesis utilizes computational modeling, specifically Robustness Analysis within the framework of Exploratory Modeling Analysis, to identify critical performance gaps. These gaps are expected to reveal critical combinations of uncertainties, informing the definition of Signposts and quantifying Adaptation Tipping Points. Understanding what to monitor and when to adapt will reduce reliance on robust measures and improve the adaptive policy design. However, while the potential benefits are clear, practical implementation in river basin management remains largely theoretical and has yet to be realized.

Conclusively, all the above reveal a significant research gap in the practical application of a modeling framework that utilizes Robustness Analysis to enhance adaptive policy design for river basin management under deep uncertainties, and hence, this thesis asks:

How to leverage robustness analysis to improve the adaptive policy design in the context of river basin management under deep uncertainty?

The thesis aims to improve decision support for river basin management under Deep Uncertainty. A new framework is introduced and demonstrated using the transboundary Zambezi River Basin as a case study. First, a non-systematic literature review identifies relevant uncertainties. Second, an Open Exploration experiment generates

plausible future States of the World. The following Scenario Discovery explores critical combinations of uncertainty factors. This aids in identifying Signpost Conditions and quantifying Adaptation Tipping Points, both of which are critical for an adaptive policy design. Ultimately, it improves collaboration and cooperation in transboundary river basins, providing a decision-support tool for river basin management to improve Decision-making under Deep Uncertainty.

The thesis is structured as follows: Succeeding the introduction, a background chapter introduces relevant concepts. It further discusses Robust-and Adaptive planning and motivates the research gap. Next, the Zambezi River Basin case study area is presented before the methodology, methods, and experimental setup are outlined. Subsequently, the proposed workflow is demonstrated in the analysis section. Finally, the thesis concludes with results, discussion, and recommendations.

Chapter 2

Theoretical Background

This chapter contextualizes river basin management. First, problem context highlights system complexity. Next, the decision context introduces the fundamentals of river basin management. Deep uncertainty is introduced before Robust-and Dynamic Planning is discussed. Afterward, computational models are pictured as decision-support tools. Subsequently, the basics of modeling river basin management are detailed, followed by the introduction of Evolutionary Multi-objective Direct Policy Search. The chapter concludes by specifying the persisting knowledge gap, which informs three sub-research questions.

2.1 River Basin Management

This section introduces river basin management. First, it details river basin complexities. Afterward, the decision arena of river basin management is introduced, laying the foundations for the decision context of river basin management.

2.1.1 Problem Context

River basin management describes a Wicked Problem (Ackoff, 1979). Complexities become particularly pronounced in the decision arena, where ambiguity about performance metrics leads to problem interpretations. These differences in viewpoints reflect the diverse values and objectives each actor brings to the table. It complicates consensus on what constitutes a *good* solution. For example, industrial stakeholders may argue from a utilitarian perspective for more significant water allocations based on economic output. At the same time, environmental groups may adopt a prioritarian approach, emphasizing the needs of endangered ecosystems. Such ambiguity challenges the decision-making process and exemplifies its wicked nature. Solutions cannot be simply categorized as true or false but are evaluated as good or bad based on the perspectives of each stakeholder (Rittel and Webber, 1973).

Furthermore, the problem formulation in river basin management is continually evolving. As new information emerges or environmental conditions change, the understanding of the problem adjusts, influencing stakeholder preferences and necessitating adjustments in strategies. Consequently, allocating water within river basins requires extensive negotiation and ongoing renegotiation to reconcile the shifting interests of diverse stakeholders. Each implemented decision affects the system and typically spawns new conditions, illustrating that every wicked problem is unique and often a symptom of another problem. Consequently, policy levers can not be easily transferred from one context to another without significant adjustments, as they must be tailored to the specific external factors of each basin. This situation continuously reshapes the decision context, making decisions inherently contentious and perpetually unresolved, emphasizing that no *final solution* is ever attainable in river basin management.

2.1.2 Decision Context

River basins are socio-technical ecological systems characterized by multi-level interactions among hydrological, ecological, and socio-economic dimensions. These interactions are inherent to deep uncertainties and create complex and intertwined relationships, positioning the problem context for river basin management into the domain of wicked problems, see Section 2.1.

Policy Lever

In general, river basin management employs a control-volume approach, focusing on the capacity to manage water storage within the basin. Water reservoirs, often created through damming, serve as crucial storage volumes, where decision-makers can determine how much water to store and release based on current and anticipated needs. This control is essential for effectively managing water distribution across the river basin.

The primary decision challenge is to find the best operating policies (L), also called control strategies, under varying external factors beyond the decision-maker's control (X). Thus, policymakers must find release decisions that achieve superior performance across multiple objectives and external conditions. Performance is determined by performance metrics (M).

Deep Uncertainty

River basins are subject to Deep Uncertainty. Building on Knight (1921), who made a foundational distinction between calculable risks and incalculable uncertainties, (Walker et al., 2003) defined a spectrum of uncertainty from deterministic systems with well-defined parameters to total ignorance, known as "unknown unknowns." River basin management typically encounters uncertainty beyond Level 3. Here, future events are unpredictable due to the complex interactions and limited understanding of the processes involved. Despite this, the extensive body of research based on historical

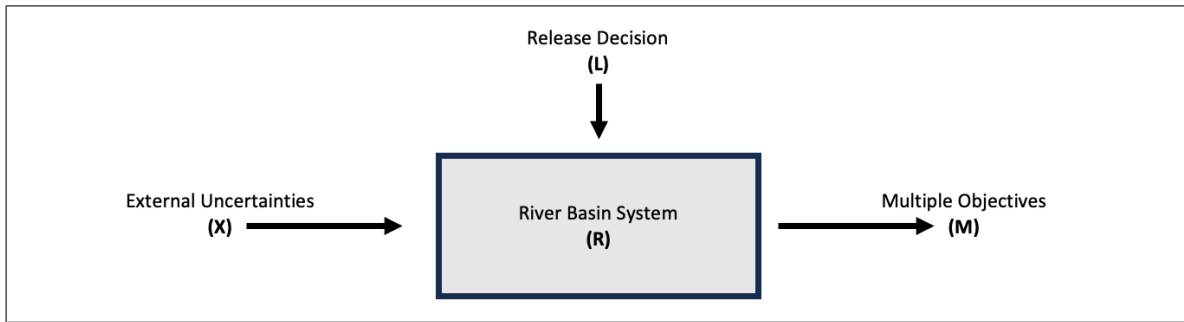


Fig. 2.1 XLRM Framework Diagram for River Basin Management. Policy levers (L) describe reservoir release decisions to improve the system (R) under varying external conditions (X) captured by performance metrics (M).

data provides insights into potential changes in precipitation patterns, water flows, temperature fluctuations, and hydroclimatic extremes.

This existing knowledge positions river basin management within Level 4a uncertainty, as described in (Marchau et al., 2019). Unlike Level 4b, which entails total ignorance about future states, Level 4a acknowledges the presence of many plausible future states of the world. These futures are still deeply uncertain, but the systematic study of past trends and variable conditions provides a structured basis for predicting potential outcomes, allowing for more informed decision-making despite the inherent uncertainties.

2.2 Deep Uncertain River Basins

This section introduces two key concepts of Decision-making under Deep Uncertainty. Subsequently, advantages and limitations are discussed. Finally, computational models are presented as potential decision-support tools to handle deep uncertain river basins.

2.2.1 Decision-making Under Deep Uncertainty

River basin management falls under Decision-making under Deep Uncertainty. Conventional *predict-then-act* approaches fall short when decision contexts are subject to deep uncertainty. Methods grounded in expected value utility theory require exact probabilities, especially. For instance, cost-benefit analysis predicts and evaluates utility values against a cost function given one specific scenario. However, deeply uncertain systems challenge these approaches. Popper et al. (2009) points out it is the "inability to grapple with the long-term's multiplicity of plausible futures" [p.50] that demonstrates the inadequacy of traditional approaches (Dessai et al., 2009; Lempert, 2003). Consequentially, new frameworks have emerged. According to Herman et al. (2020), the main two concepts are Robust Planning, which focuses on identifying policy alternatives that perform well across a broad spectrum of future conditions, and

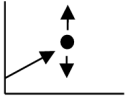

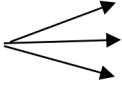
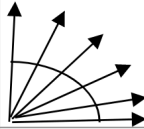
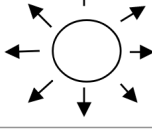
| Complete determinism | Level 1 | Level 2 | Level 3 | Level 4 (deep uncertainty) | | Total ignorance |
|----------------------|--|---|--|--|---|-----------------|
| | | | | Level 4a | Level 4b | |
| | A clear enough future  | Alternate futures (with probabilities)  | A few plausible futures  | Many plausible futures  | Unknown future  | |
| | A single (deterministic) system model | A single (stochastic) system model | A few alternative system models | Many alternative system models | Unknown system model; know we don't know | |
| | A point estimate for each outcome | A confidence interval for each outcome | A limited range of outcomes | A wide range of outcomes | Unknown outcomes; know we don't know | |
| | A single set of weights | Several sets of weights, with a probability attached to each set | A limited range of weights | A wide range of weights | Unknown weights; know we don't know | |

Fig. 2.2 Progressive Transition Table of Levels of Uncertainty from (Marchau et al., 2019). Levels range from deterministic systems to total ignorance, with four different levels in between. The main criteria are context, system model, system outcomes, and weights.

Dynamic Planning, which seeks to develop adaptive policies that adjust in response to evolving conditions.

2.2.2 Robust Planning

Robust Planning prioritizes a policies' ability to handle diverse conditions rather than optimal performance in specific scenarios. Thus, it aims to minimize the policies sensitivity to changing conditions (Herman et al., 2020).

Decision support for Robust Planning follows a *generate-first-choose-later* approach (Hwang and Masud, 2012). In contrast to traditional decision support, which typically integrates stakeholder preferences from the beginning through a Priori aggregation of costs and benefits, Robust Planning adopts decision support a Posteriori through Robustness Analysis (Tsoukiàs, 2008). Identifying and evaluating a broad spectrum of potential scenarios to pinpoint system vulnerabilities before imposing stakeholder preferences ensures that policy plans are both satisfactory to stakeholders and robust. According to Herman et al. (2015), it follows a four-step approach. Their insights are summarised below.

Identification of Alternative Policies

First, policy alternatives are identified. The identification method depends on the characterization of the system's uncertainties. With well-defined scenarios, decision-makers can pre-specify policy alternatives according to Decision Scaling (Brown and

Wilby, 2012) or Robust Decision Making (Hine and Hall, 2010; ?). With somewhat characterized uncertainties¹ frameworks like Many-Objective Robust Decision Making (Kasprzyk et al., 2013) integrate simulation and optimization approaches to refine decisions. Conversely, Robust Optimization (Watkins Jr and McKinney, 1997) is necessary when scenarios are deeply uncertain. This allows decision-makers to select multiple potential policies to evaluate within the next steps.

Generation of States of the World

Second, a set of uncertain states of the world is generated. While Decision Scaling, Robust Decision Making, and Multi-objective Robust Decision Making employ global exploratory sampling (Bryant and Lempert, 2010), Info-Gap frameworks sample outward from an expected initial state until encountering failure (Hipel and Ben-Haim, 1999). This step provides a meaningful representation of the multiplicity of future states against which policy alternatives can be evaluated.

Quantifying Robustness Metrics

Third, identified policy alternatives are evaluated across previously generated future states of the world. It quantifies the robustness of decision alternatives against various states of the world. Robustness metrics fall into two categories: regret and satisficing measures (Lempert and Collins, 2007). Regret measures focus on the cost of deviating from optimal or expected outcomes. In contrast, satisficing measures assess the extent to which solutions meet predefined performance thresholds across uncertain conditions. It equips decision-makers with metrics to compare solutions, thereby facilitating informed decision-making under Deep Uncertainty.

Identifying Critical Uncertainties

Finally, critical uncertainty factors are identified. This follows a consequence-oriented sensitivity analysis to isolate key uncertainty factors. Robust Decision-Making and Multi-objective Robust Decision-Making approaches utilize methods like the Patient Rule Induction Method (PRIM) to pinpoint sensitive ranges within the uncertainty space. This step allows decision-makers to identify specific uncertain factors that require attention.

2.2.3 Dynamic Planning

Dynamic Planning focuses on flexible and adaptive policy structures. It aims to promote policies that can adjust in response to changes and new insights (Haasnoot et al., 2013; Pahl-Wostl, 2007). It does not seek permanent robust policy solutions but promotes dynamic policy plans that can evolve in response to deep uncertainties

¹Deep uncertain relations are assumed to follow an underlying distributions that can be approximated

(Herman et al., 2020). Dynamic Planning includes four main components. According to Herman et al. (2020), these are policy structure, uncertainty characterization, solution method, and robustness testing. The following outlines each of them based on the review from Herman et al. (2020) about dynamic water resources planning under deep uncertainty.

Defining Policy Structures

In Dynamic Planning, overall policy structures include the policy action, Signposts (Haasnoot et al., 2013), and Adaptation Tipping Points (Kwadijk et al., 2010). Policy actions can be infrastructure (hard) and operation (soft) policies (Bertoni et al., 2019). Signposts determine indicator variables that provide information about whether the foundational assumptions of the current policy remain valid. Monitoring these Signposts is essential for the adaptive policy design (Kwakkel et al., 2010; Walker et al., 2001). It ensures that the implementation is on track and that necessary adjustments are timely and effective. Adaptation Tipping Points represent crucial thresholds within the system where the existing policy fails to achieve its objectives, signaling that the system's conditions are nearing or have reached a point of unacceptable performance (Marchau et al., 2019).

Characterization of Uncertainties

Once policy structures are established, the system's uncertainties must be characterized. This involves utilizing models and scenarios to identify and quantify uncertainties, often represented by ensembles of synthetic scenarios. These scenarios are typically developed either through parameterizing a stationary stochastic process with historical observations (Haasnoot et al., 2015) or by employing General Circulation Models to establish a non-stationary stochastic process (Fletcher et al., 2019; Hui et al., 2018). To comprehensively characterize uncertainties, three main approaches are employed: sampling uncertainty, which deals with natural variability and limited data (Quinn et al., 2018); exogenous uncertainty, arising from external climatic factors; and endogenous uncertainty, which focuses on the unpredictable internal dynamics of the system (Haddeland et al., 2014).

Solution Method

Different methods are used to synthesize policy structure and characterize uncertainties. Selecting the appropriate solution method is problem-specific. Stochastic Dynamic Programming (Hui et al., 2018) offers high accuracy with well-defined variables but faces computational limits; see Section 2.3.3. Open Loop methods (Borgomeo et al., 2016) provide efficiency but risk overfitting. Policy Search allows flexible adaptation to changing conditions but demands careful function and parameter selection to avoid fitting errors (Giuliani et al., 2017).

Validation

Towards the end, the adaptive policy structure is tested using more realizations from the same uncertainties characterized and used within the simulation method or by introducing new variables or distributions. While the first checks for overfitting to specific scenarios, the second evaluates adaptability to broader uncertainties. The goal is to confirm the policy's effectiveness under varying conditions (Lempert and Collins, 2007).

Dynamic Adaptive Policy Pathways

The Dynamic Adaptive Policy Pathway exemplifies the rationale of Dynamic Planning (Haasnoot et al., 2013). Its adaptation pathway map visually represents the complex policy structure, including multiple policy actions and adaptation points (derived from Signposts and Adaptation Tipping Points); see Figure 2.3.

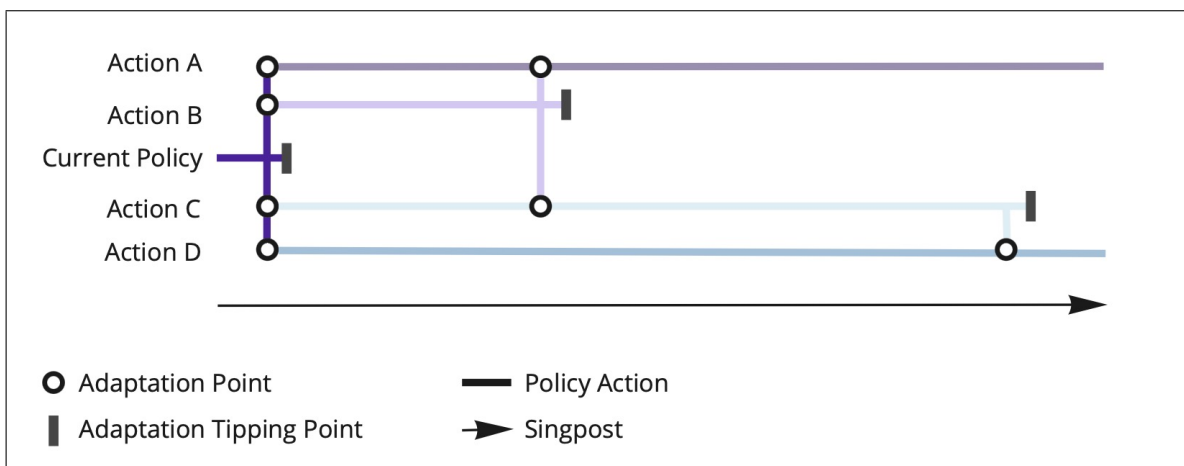


Fig. 2.3 Dynamic Adaptive Policy Pathway Map. It illustrates a metro map commonly used for Dynamic Adaptive Policy Pathway planning. It depicts various policy actions over time, starting from the current policy. It outlines potential future paths, each representing a response to changing conditions captured by the Signpost. Policies adapt when current policy actions reach adaptation tipping points.

Starting from the current situation, if current policy targets are missed, decision-makers have several paths to maintain or enhance policy performance. Actions A and D are viable for achieving long-term goals across all scenarios but could be costly. Thus, policymakers might first implement Action B or C and monitor performance. If Action B is chosen, once it reaches an Adaptation Tipping Point, a transition to Action A or C may be necessary, leading to adaptation points. This flexibility allows adjustments to be made in response to new data or unexpected conditions and postpone costly policy implementations into the future. The adaptation pathways map shows the effectiveness of each action over time.

2.2.4 Comparing Robust and Dynamic Planning Approaches

Robust and Dynamic Planning excels in Decision-making under Deep Uncertainty differently. Each approach has specific benefits and challenges, which are discussed below. A summary is presented in Table 2.1.

Robust Planning results in dependable policy outcomes with strategies that ensure effectiveness across a wide range of future states of the world. It is particularly beneficial for deep uncertain river basins, providing a stable framework that withstands system variability (Herman et al., 2015). However, the inherent rigidity of Robust Planning hinders timely adaptations to new information. In the continuous context of river basin management, this may result in operational policies that fail to respond to environmental or social changes. Consequently, Robust Planning could constrain flexibility, potentially leading to performance loss if underlying assumptions about the system change.

Furthermore, Robust Planning often favors static near-term solutions, which can lead to costly over-design. Moreover, adopting more conservative strategies for robustness might increase costs (Borgomeo et al., 2018). In contrast, Dynamic Planning solutions are more fluid, which allows policymakers to postpone costly infrastructure policies, first applying soft policy actions to avoid lock-ins (Haasnoot et al., 2013).

In contrast to Robust Planning, Dynamic Planning supports precise responses to emerging information. This could potentially enhance policy performance (Dias et al., 2020). For instance, the Dutch Delta Program utilizes Dynamic Planning to adjust flood risk management strategies based on real-time sea level rise monitoring and socio-economic shifts. Its flexible structure ensures that safety measures are adapted to changing conditions (Bloemen et al., 2019; Marchau et al., 2019; van Buuren, 2019).

Despite its advantages, Dynamic Planning is not without complexities. Its policy plan does not only consist of a single policy action but includes identifying critical Signposts and quantifying Adaptation Tipping Points, both particularly challenging tasks (Adger et al., 2009; Kwakkel and Pruyt, 2013; Schipper and Burton, 2009). Additionally, once Signposts are established, monitoring systems must be put in place and regularly assessed, which adds complexity and costs. Therefore, implementing a single robust policy appears more straightforward than managing a complex policy structure.

The more straightforward policy structure allows for multi-objective optimization approaches in Robust Planning. It provides clear decision paths that allow the balance between cost, reliability, and environmental impact. However, it requires initial consensus on objectives, which is challenging to achieve and may lead to over-designed solutions, adding to the inflexibility of Robust Planning. Conversely, dynamic Planning engages stakeholders continuously, which enhances adaptability but requires more complex management and coordination efforts (Cohen and Herman, 2021). It further complicates multi-objective optimization attempts.

Table 2.1 Comparison of Robust and Dynamic Planning

| Robust Planning | Dynamic Planning |
|---|---|
| <p>Advantages:</p> <ul style="list-style-type: none"> • Results in dependable outcomes, effective across various future states. • Simple policy structure that provides clear decision paths. • Provides a stable framework for decision-making. <p>Limitations:</p> <ul style="list-style-type: none"> • Rigidity hinders adaptations to new information. • May result in policies that fail to respond to changes. • Often favors static solutions, leading to costly over-design. • Requires initial consensus on objectives, which is difficult to achieve. • Depends on methodological choices that lead to inconsistent applications. | <p>Advantages:</p> <ul style="list-style-type: none"> • Supports precise responses to emerging information. • Allows postponing costly policies, prioritizing smaller policy actions first. • Engages stakeholders continuously, enhancing adaptability. <p>Limitations:</p> <ul style="list-style-type: none"> • Complexity in managing dynamic policy structures. • Requires identifying critical Signposts and quantifying Adaptation Tipping Points. • Regular assessment of monitoring systems adds complexity and costs. • Complicates multi-objective optimization due to timing and sequencing of actions. |

The ambiguity in defining robustness through a wide array of metrics can lead to inconsistent applications across projects (Herman et al., 2015). The reliance on a detailed Robustness Analysis involves multiple methodological choices, from how decision alternatives are generated to how uncertainties are quantified. Consequentially, these choices influence outcomes and the overall robustness of the planning process, ultimately raising questions about the robustness of these methodological choices themselves (Kwakkel et al., 2016).

In summary, while providing stable and dependable outcomes, Robust Planning often suffers from rigidity, leading to over-design and inflexibility in the face of changing assumptions. Dynamic Planning, conversely, offers adaptability and responsiveness, yet it is complicated by the need to identify clear Signposts and quantify Adaptation Tipping Points accurately.

2.2.5 Decision Support Tools for Deep Uncertainty

In Robust-and Dynamic Planning, computational models have become indispensable decision-support tools for policymakers. They help them better understand the relationships between river basin systems, external factors, and policy levers.

Furthermore, computational models are leveraged for optimization in Robust Planning (Kasprzyk et al., 2013). It aims to find the best operating policies by systematically exploring the decision space to maximize or minimize specific objectives. However, the process often relies on predefined input assumptions about external conditions.

Simulation models help test and evaluate the optimized policy levers under different conditions to reduce input dependency. They help assess how well policies perform when subjected to change. Here, simulation often follows an Exploratory Modeling Analysis approach. It assesses a fixed set of policies to gain insights into their robustness under changing external factors.

Essentially, computational optimization-and simulation models support decision-makers in developing and validating policies that achieve optimal objectives and remain effective under varying and uncertain future conditions. Three key areas are presented.

Rival Framing

Computational modeling is used to explore different problem formulations. This approach directly confronts the wicked nature of decision-making, where the intricacies of physical water management intertwine with conflicting socio-economic interests and ethical considerations of equity and justice. For instance, Quinn et al. (2017) discuss how these models can be used to uncover how problem formulation uncertainties influence environmental management decisions. Here, simulation models helped to visualize how differing assumptions and starting points affect policy outcomes. This not only aids in reconciling conflicting views but also enhances transparency, fostering a more profound understanding among stakeholders and guiding them toward a consensus.

Multi-tradeoff Analysis

Computational models are used to analyze and optimize various objectives. For instance, the Many-Objective Robust Decision-Making approach (Kasprzyk et al., 2013) allows for the dis-aggregation, optimization, and analysis of policies across diverse objectives. It helps policymakers identify solutions that maintain efficacy across various possible futures, circumventing the common multi-objective challenge where no single policy optimally satisfies every criterion. In another study, Owusu et al. (2022) used computational models to highlight tradeoffs between anthropogenic water demands for hydropower, irrigation, and recreation and the needs of river ecosystems and services in the Volta River.

Exploratory Modeling

Deep uncertainty necessitates exploratory policy analysis to ensure policies remain effective across various future conditions Kwakkel and Pruyt (2013). Computational models are integral to this process, as they allow the testing of policy performance under multiple scenarios. For instance, Zatarain Salazar et al. (2022) illustrate the application of Robust Decision-making in environments characterized by Deep Uncertainty. Their analysis focuses on developing policies that maintain effectiveness across various future scenarios.

2.3 Modeling River Basin Management

The previous sections emphasized decision challenges in river basin management, particularly under conditions of Deep Uncertainty. This section introduces the fundamental approaches and methods for modeling river basin management.

2.3.1 Mass-Balance Approach

The mass balance approach is fundamental in modeling river basin systems. Grounded in the principle of continuity, it ensures that all water entering, exiting, and being stored within the system is accounted for. This provides a clear picture of water availability and distribution. Key components of the mass balance equation are inflow, outflow, and changes in storage.

The most basic representation of the mass balance for a water reservoir is:

$$S_{t+1} = S_t + I_{t+1} - Q_{t+1} \quad (2.1)$$

where S_t is the storage at time t , I_{t+1} is the inflow, and Q_{t+1} is the outflow at the next time step $t + 1$.

The equation sums overall inflows and outflows for systems with multiple inflows and outflows. $\sum I_{t+1}$ represents the total inflows and includes factors like precipitation, upstream releases, and runoff, while $\sum Q_{t+1}$ represents the total outflows, including water releases, or evaporation.

$$S_{t+1} = S_t + \sum I_{t+1} - \sum Q_{t+1} \quad (2.2)$$

Utilizing the mass balance approach, policy analysts can model the current state of a river basin comprising multiple water reservoirs. This provides a comprehensive understanding of the water distribution and storage dynamics within the basin. Each reservoir's state is defined by its storage levels, which are continually updated based on the balance of incoming and outgoing water.

2.3.2 Decision Problem

The aim is to find the optimal operating policies for each reservoir. This involves specifying the appropriate amount of water to release at any given time to meet current demands. This can be illustrated using a single reservoir example with three water demanding downstream actors at time step t .

To account for the demands of Actors A, B, and C, we can define the release R_t to meet the demands of all three actors. Let $D_{A,t}$, $D_{B,t}$, and $D_{C,t}$ represent the demand values for Actor A, B, and C, respectively. The total demand at time t is $D_t = D_{A,t} + D_{B,t} + D_{C,t}$. The release R_t can then be defined as:

$$R_t = \begin{cases} D_t, & \text{if } S_t + I_t > D_t \\ S_t + I_t, & \text{if } S_t + I_t \leq D_t \end{cases} \quad (2.3)$$

If the total available water exceeds the demand D_t , then the release R_t equals the demand D_t . This ensures that the demand is fully met. If the total available water is less than or equal to the demand, then the release R_t equals the total available water. However, in practice, conflicting interests among different actors mean it is often impossible to fully satisfy all demands simultaneously.

In addition, given the background of Arrow's paradox, premature aggregation of objectives is problematic. It implies that any aggregation of preferences results in a subset of preferences dominating the aggregate preference. This essentially leads to a form of dictatorship where one preference set dominates.

Therefore, it is crucial to disaggregate the objectives early in the modeling process and frame the optimization problem as a multi-objective problem to optimize multiple objectives simultaneously. The general formulation is expressed as:

$$\begin{aligned} & f_m(\mathbf{u}_t), \quad m = 1, 2, \dots, M; \\ & \text{subject to} \\ & g_j(\mathbf{u}_t) \geq 0, \quad j = 1, 2, \dots, J; \\ & h_k(\mathbf{u}_t) = 0, \quad k = 1, 2, \dots, K; \\ & u_{ti}^{(L)} \leq u_{ti} \leq u_{ti}^{(U)}, \quad i = 1, 2, \dots, n; \end{aligned} \quad (2.4)$$

Where:

- $f_m(\mathbf{u}_t)$ is the vector function of M objective functions. Each objective function represents a different goal, such as maximizing water supply for hydropower generation, irrigation demand, or drinking water. These objectives often conflict, necessitating solutions that balance tradeoffs.

- \mathbf{u}_t is the vector of n decision variables. These are the controllable levers for the system, namely an operation strategy that consists of a sequence of release decisions.
- $g_j(\mathbf{u}_t)$ and $h_k(\mathbf{u}_t)$ represent J inequality and K equality constraints, respectively. They ensure conditions are met without exceeding limits, such as maximum pollutant levels or minimum environmental flow requirements.
- $u_{t_i}^{(L)}$ and $u_{t_i}^{(U)}$ are the lower and upper bounds of the decision variables. It ensures that solutions remain feasible and practical, respecting physical constraints and regulatory requirements.

With increasing reservoirs and longer time horizons, finding optimal operation strategies becomes a complex problem. This complexity arises because each release decision impacts subsequent decisions, necessitating a strategy that addresses immediate demands and anticipates future conditions and requirements across multiple reservoirs.

2.3.3 The Three Curses of Modeling

Giuliani et al. (2016) identified three curses for optimizing river basin management. They argued that traditional approaches are severely limited because they frame the decision problem as a sequential decision-making process and rely on value functions over a discrete state-decision space. They framed it as the three curses of modeling, which are explained below.

Curse of Dimensionality

Computational cost increases exponentially with the dimensionality of the state space. As the number of reservoirs and other system components grows, the number of potential states and decisions increases significantly. This makes it challenging to explore all possible states and identify optimal solutions within a reasonable time frame and computational effort.

Curse of Multi-Objectives

River basin management involves multiple conflicting objectives. Balancing these objectives requires sophisticated multi-objective optimization techniques. In a sequential decision-making context, these tradeoffs must be evaluated and balanced at each decision point, complicating the optimization process.

Curse of Modeling

River basin management requires detailed modeling of various socio-technical ecological dimensions. In sequential decision problems, precise modeling is even more critical, as inaccuracies can propagate through the decision-making process, leading to suboptimal

outcomes. However, the more detailed the model, the more computationally intensive it becomes to simulate and optimize.

2.4 Evolutionary Multi-Objective Direct Policy Search

Previous sections positioned computational modeling as a decision-support tool for river basin management; see Section 2.2.5). However, the modeling process faces significant challenges outlined by Giuliani et al. (2016); see Section 2.3.3.

This section presents Evolutionary Multi-Objective Direct Policy Search (EMODPS) as today's gold standard decision-support tool. Its main components, Direct Policy Search and Multi-Objective Evolutionary Algorithms, are introduced. Afterward, the approach is discussed in the context of Decision-making under Deep Uncertainty.

2.4.1 Direct Policy Search

The Direct Policy Search framework addresses the challenges of high-dimensional state spaces and deep uncertainty in water reservoir management. Instead of discretizing release decisions, Direct Policy Search uses global approximators to describe an underlying optimal state-to-action relationship. This reduces the number of decision variables, making it more computationally efficient by focusing on parameters that describe a policy function. To ensure flexibility, two nonlinear approximating networks, namely Artificial Neural Networks and Radial Basis Functions, are commonly used (Giuliani et al., 2014).

Between global approximators, Radial Basis Functions have the upper hand. Giuliani et al. (2014) found that they demonstrated superior performance in approximating the Pareto front, achieving better coverage and dominance compared to Artificial Neural Networks. Between Radial Basis Functions, Zatarain Salazar et al. (2024) demonstrated that the choice of its activation functions, such as Gaussian, inverse quadratic, and exponential, significantly impacts the quality of Pareto optimal solutions and overall model performance. It showed that the modified squared exponential and squared exponential Radial Basis Functions often provide superior results, enhancing solution quality and diversity.

2.4.2 Multi-Objective Evolutionary Algorithms

EMODPS leverages Multi-Objective Evolutionary Algorithms to tackle the curse of multi-objectives. It is a class of heuristic search algorithms based on the principles of natural selection and genetics (Coello, 2007). They play a crucial role in addressing the curse of multi-objectives through their ability to navigate complex objective functions and circumvent local optima. This allows the efficient exploration of tradeoffs between conflicting goals (Giuliani et al., 2014).

Algorithms such as NSGAI (Deb et al., 2002), ϵ -MOEA (Deb et al., 2003), ϵ -NSGAI (Kollat, 2005), and Borg MOEA (Hadka and Reed, 2013) have demonstrated superior performance in estimating Pareto fronts. ϵ -MOEA, Borg MOEA, and ϵ -NSGAI are particularly notable for their advanced features like epsilon-dominance archiving, adaptive population sizing, and time continuation, which enhance search diversity and convergence (Zatarain Salazar et al., 2016).

2.4.3 EMODPS and Deep Uncertainty

In synthesizing Direct Direct Policy Search and Multi-Objective Evolutionary Algorithms, EMODPS enables policymakers to handle complex, high-dimensional data. Therefore, unlike traditional methods, EMODPS can seamlessly integrate exogenous variables into the policy search process, allowing for the consideration of scenarios (Giuliani et al., 2016). It allows policymakers to find and assess policy alternatives over a wide range of plausible futures, thereby excelling the principles of Robust Planning.

However, the closed simulation-optimization loop of EMODPS introduces data dependencies that might decrease the robustness of optimized policy functions. Global approximators tend to overfit policy parameters to data inputs. Conclusively, policy robustness may solely depend on the quality and range of input data. In addition to previously discussed limitations in Section 2.2.4, this is problematic when models rely on historical data or specifically defined scenarios.

2.5 Research Questions

Ultimately, the issue of overfitting policy functions to input patterns could compromise robust performance when actual conditions deviate from those assumed. Consequently, the robustness of EMODPS outputs is tied to the specific assumptions fed into the framework. Once these assumptions change, policies will lose performance, a prominent limitation of Robust Planning; see Section 2.2.4.

Therefore, to improve Decision-making under Deep Uncertainty for river basin management, this thesis does not follow a Robust Planning approach but instead explores opportunities to improve the Dynamic Planning Principle. EMODPS's ability to integrate exogenous variables into the simulation-optimization loop is consequently utilized to improve the adaptive policy design. In particular, the thesis sets out to leverage Robustness Analysis to improve the definition of the dynamic policy structure for river basin management. This addresses challenges related to the definition of Signposts and the quantification of Adaptation Tipping Points.

Conclusively, the thesis explores a new methodology for applying Robustness Analysis to identify critical uncertainties and performance gaps that inform the definition of Signpost conditions and Adaptation Tipping Points. Hence, this thesis asks:

RQ1) *How to leverage robustness analysis to improve the adaptive policy design in the context of river basin management under deep uncertainty?*

To answer the main research question, a new methodology is proposed in Section 4.1 and demonstrated using the Zambezi River Basin as a case study in Section 5.1. This methodology includes three main parts.

First, the characterization of critical uncertainties within the Zambezi River Basin aims to understand the external system factors providing the basis for the generation of states of the world. Hence, it is asked:

SRQ1) *What are the most prominent uncertainties of the Zambezi River Basin?*

Second, the Robustness Analysis focuses on the generation of states of the world. This includes quantifying uncertainties to explore system vulnerabilities. It is envisioned to hint at potential signpost conditions characterized by an interplay of uncertainties. Thus, this thesis asks:

SRQ2) *What are the most critical uncertainty combinations the system is vulnerable to?*

Third, the most critical uncertainty combinations are further explored and used to define Adaptation Tipping Points. Therefore, this thesis asks:

SRQ3) *What are the adaptation tipping points within the Zambezi River Basin?*

Summary

River basin management utilizes a control-volume approach. The goal is to find optimal operating policies for water reservoirs to manage water distribution within the basin effectively. This describes an entwined decision matrix in which complexities are amplified by deep uncertainty about values and external conditions, thus leading to a decision space categorized under Level 4a uncertainty. Here, the future presents multiple plausible states, demanding Robust-and Dynamic Planning beyond traditional *predict-then-act* models.

Robust Planning, while providing stable and dependable outcomes, often suffers from rigidity, leading to over-design and inflexibility in the face of changing assumptions. Dynamic Planning, conversely, offers adaptability and responsiveness yet is complicated by the need to identify clear Signposts and quantify Adaptation Tipping Points.

Computational models have proven to play a pivotal role in the decision process. As decision-support tools, they allow to simulate and optimize river basin management policies across different problem formulations, multiple objectives, and various external conditions. However, modeling river basin management is challenging due to the three curses of dimensionality, multi-objectives, and modeling.

EMODPS, addressing all three, has emerged as today's golden standard for modeling river basin management. Leveraging Direct Policy Search and its reliance on global approximators decreased dimensionality and allowed for flexible input data handling. In addition, Multi-objective Evolutionary Algorithms offer a more detailed analysis of multi-objective tradeoffs.

Currently, EMODPS allows policymakers to include and test diverse scenarios, enabling robustness analysis post-modeling. Furthermore, by approximating a policy function rather than determining static release decisions, EMODPS provides an overarching strategy that describes the state-to-action relationship.

However, the policy function depends on the input data. This dependency decreases the robustness, leading to lower performance once system conditions change. Thus, rather than following a Robust Planning approach, this thesis aims to utilize Robustness Analysis to improve Dynamic Planning for river basin management through:

- The identification of Signposts.
- The quantification of Adaptation Tipping Points.

Chapter 3

Case Study Area

This Section introduces the Zambezi River Basin as this thesis case study. First, the study area is introduced, and its main characteristics are described. Afterward, the focus shifts to the computational model. The main conceptual components, structure, and objectives are highlighted, underlining why the Zambezi River Basin is a suitable case study for this thesis.

3.1 Zambezi River System

The Zambezi River Basin illustrates the intricate complexities many transboundary river basins face. It is Africa's fourth largest river basin, spanning over 1.37 million km² across eight countries. The basin provides for around 40 million people and is pivotal for regional survival, economic growth, and poverty reduction (Lautze et al., 2017; O'Leary et al., 1998; World Bank, 2010). At the same time, its pluvial character makes the basin vulnerable to climate variability, causing it to be one of the most affected river basins by climate change (Kling et al., 2015). Establishing the Zambezi Watercourse Commission and its ratification in 2014 have been critical steps towards fostering collaborative management. The commission exemplifies an effort in strategic planning and policy development necessary for accommodating the multifaceted needs of eight sovereign nations sharing the basin's resources.

Two rivers dominate the study area: the Zambezi and Kafue River (Figure 3.1). The Zambezi River originates in the uplands of northwestern Zambia. It passes through Angola and re-enters Zambia, flowing southeast. In south Zambia, the Zambezi turns eastward, forming the border with Namibia. It passes by Botswana and traverses the border between Zambia and Zimbabwe before cutting across Mozambique to the Indian Ocean. The Kafue River, entirely within Zambia, originates from the Copperbelt and joins the Zambezi downstream of Lake Kariba.

The rivers supply water to three main sectors. Hydropower is a dominant water use with a capacity estimated at 20,000 megawatts (MW) (Tumbare and Authority,

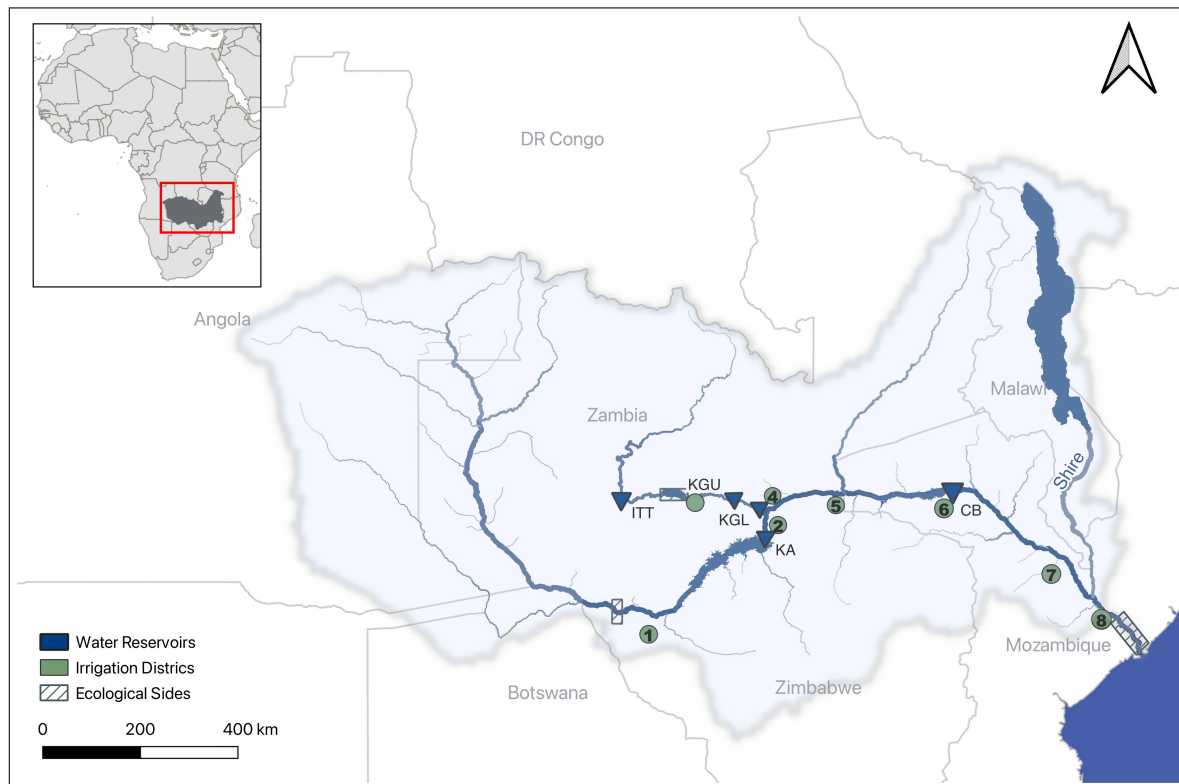


Fig. 3.1 Map of the Zambezi River Basin. The map highlights eight irrigation districts, three main ecological sides, and five water reservoirs. The basin spans across eight riparian countries - Angola, Botswana, Malawi, Mozambique, Namibia, Tanzania, Zambia, and Zimbabwe.

2004). Today, the Cahora Bassa (2,075 MW) and Kariba (1,320 MW) reservoirs at the Zambezi River, and the Itzhi-Tezhi (150 MW) and Upper and Lower Kafue Gorge (900 MW, 750 MW) dams at the Kafue River generate most of it (World Bank, 2010). Agriculture is another important economic sector in the Zambezi River Basin, with an annual irrigated area of around 260,000 hectares (World Bank, 2010). Additionally, the basin comprises ecological attractions protected by minimal environmental flow requirements. Victoria Falls, Kafue Flats, and its river Delta are the three most critical ecological sites.

3.2 Zambezi Model

The thesis focuses on developing a methodology that improves the adaptive policy design within the EMODPS framework. Thus, no new model is implemented; instead, an existing EMODPS decision-support tool is utilized. The Zambezi model was developed by Arnold et al. (2023) to inform the optimal sequencing strategy for planning and operation policies and later transferred from C++ to Python by Yasin Sari.

The Zambezi River Basin follows the control volume approach and describes the dynamic interaction between water reservoirs, catchment areas, and irrigation districts. The main model components follow the structure of Figure 3.2. Comprehensive UMLs of the model classes can be found in Appendix A.

Central to the model are five reservoirs. Its release strategies determine the amount allocated to hydropower generation, agricultural irrigation, and the maintenance of environmental flows. Each reservoir is represented by a **Reservoir** class. It provides critical functions that transform storage levels to water surface levels, compute storage volumes from water heights, and calculate surface areas, which are essential for evaporation. Furthermore, the class simulates the release decisions via the integration and daily integration functions at time-step t to compute the reservoir states at time-step $t + 1$.

The **Catchment** class represents the seven main inflow points of the Zambezi River Basin. They are essential to managing hydrological data within the river basin model, which focuses mainly on inflow dynamics. The class handles monthly streamflow data to simulate water movements throughout the river system. Data is exogenous based on inflow vectors from 1986 to 2005, with a monthly resolution for each catchment. The spatial character and flow patterns are implemented via flow delays. For instance, water released from the Itezhi-Thezhi Reservoir takes two months to reach the Kafue Gorge Upper Reservoir.

Irrigation areas are aggregated into eight central districts and are defined by a 12-month demand vector repeating the same demand pattern every year, again defined as exogenous. The amount of water allocated to each irrigation district is determined by an irrigation policy function following a logic similar to that of the reservoir release decisions.

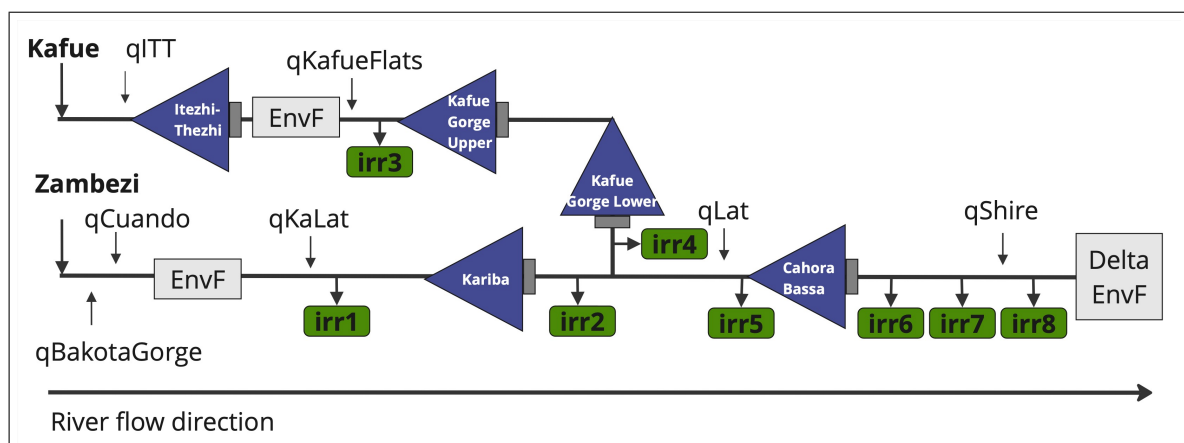


Fig. 3.2 Conceptual Diagram of the Zambezi River Basin Model. The model has three main components: five water reservoirs, three ecological sides, and eight irrigation districts. The main rivers are the Kafue and Zambezi Rivers, with additional inflows from seven catchment areas.

3.2.1 Model Structure

Building on the conceptual model, the implementation follows the traditional EMODPS architecture utilizing a closed simulation-optimization loop, explained in Section 2.4. With a 20-year time horizon and daily resolution, it simulates the current policy functions, evaluates their performance, and optimizes promising solutions described by policy parameters in a continuous cycle. Table 3.1 summarizes the main model settings.

The governing equation for each reservoir k in the basin follows the fundamental laws of mass balance:

$$S_{k,t+1} = S_{k,t} + I_{k,t} - R_{k,t} - E_{k,t} \quad (3.1)$$

In this equation, $S_{k,t}$ and $S_{k,t+1}$ represent the storage volumes at the start and end of each day, respectively. $I_{k,t}$ is the total inflow, encompassing both direct tributary inputs from catchments and delayed contributions from upstream reservoirs, $R_{k,t}$ denotes the water released, and $E_{k,t}$ accounts for evaporation losses. The Kariba reservoir can be represented as:

$$I_{Kariba,t} = q_{KaLat} + q_{Bg} + q_{Cuando} + \sum_j q_{j,t} \quad (3.2)$$

It captures inflows from key tributaries such as q_{KaLat} , q_{Bg} , and q_{Cuando} , as well as from additional tributaries $\sum_j q_{j,t}$ feeding into the Kariba reservoir.

Control over water releases $R_{k,t}$ is executed through a policy function, which dynamically adjusts the volume of water released based on the reservoir's current storage $S_{k,t}$, downstream demand $D_{k,t}$, and operational constraints encoded within the policy:

$$R_{k,t} = f(Policy_k, S_{k,t}, D_{k,t}) \quad (3.3)$$

3.2.2 Policy Functions

The Zambezi model encompasses operating policies for five water reservoirs and water allocation to eight irrigation districts. Operating strategies are derived using global approximators. Specifically, the model employs non-convex Gaussian Radial Basis Function networks to approximate the state-to-action relationship. Table 3.2 provides a more detailed summary of the model's policy function setting.

The k -th release decision within the policy-vector u_t is defined as:

Table 3.1 Summary of Model Parameters

| Parameter | Value | Type | Description |
|------------|-------|------|---|
| Simulation | 1 | int | The number of consecutive simulation runs performed. |
| Neurons | 1 | int | Number of neurons (or nodes) in a neural network. |
| T | 12 | int | Period of seasonality (per year), referring to monthly data. |
| H | 240 | int | Total simulation duration in months. |
| Objectives | 3 | int | Number of objective variables to be optimized during the simulation. |
| Variables | 230 | int | Number of variables in the model, encompassing state, input, and control variables. |

$$u_k = \delta_k + \sum_{i=1}^N w_{i,k} \phi_i(I_t) \quad (3.4)$$

where N is the number of Radial Basis Functions, δ_k is a constant parameter, and $w_{i,k}$ is the weight of the i -th Radial Basis Function. This implementation varies from a general Radial Basis Function by adding the constant δ_k , which allows for a specific target release.

Each Radial Basis Function $\phi_i(I_t)$ is defined as:

$$\phi_i(I_t) = \exp \left(- \sum_{j=1}^M \left(\frac{(I_t)_j - c_{j,i}}{b_{j,i}} \right)^2 \right) \quad (3.5)$$

where M is the number of inputs, and c and b are the center and radius vectors. The centers c must lie within $[-1, 1]$ and the radii b within $(0, 1]$.

In addition to the reservoir operating policy parameters, an irrigation policy $\theta_\omega(\kappa)$ defines the amount of water for the i -th irrigation district (ω_i), according to this non-linear hedging rule (Celeste and Billib, 2009):

$$\omega_{t+1}^{id} = \begin{cases} \min \left(q_{t+1}, \nu_t^{id} \cdot \left(\frac{q_{t+1}}{h^{id}} \right)^{m^{id}} \right) & \text{if } q_{t+1} \leq h^{id} \\ \min(q_{t+1}, \nu_t^{id}) & \text{else} \end{cases} \quad (3.6)$$

Here, q_{t+1} represents the volume of water available in the river channel at the diversion point, $\nu_{id,t}$ denotes the monthly water demand, and h_{id} and m_{id} are parameters that regulate the diversion channel.

The policy functions within this model are parameterized with 230 parameters and described through eleven Radial Basis Functions.

Table 3.2 Summary of Model Policy Parameters

| Attribute | Value | Type | Description |
|---------------|-------|------|--|
| Function | 4 | int | Type of the general function approximator: 1-RBF, 2-ANN, 3-Piecewise linear, 4- Non-convex RBF |
| Input | 7 | int | Number of inputs to the policy function. |
| Output | 5 | int | Number of outputs of the policy function. |
| RBFs | 11 | int | Number of structures in an RBF network, specific to RBF. |
| Irr-Districts | 8 | int | Number of irrigation districts required for the irrigation policy. |

3.2.3 Objectives

Following EMODPS, parameterized policy levers are described by global approximators, here non-convex Gaussian Radial Basis Functions. Parameters are optimized using the Generational Borg MOEA. Optimization seeks to minimize the three objectives via the release and irrigation policies.

Objectives are implemented using deficits across the domains of hydropower, irrigation, and environmental flow requirements. It allows policymakers to evaluate how well the system meets the needs of different sectors and highlights any shortfalls ¹. Environmental minimum flows are set as monthly constraints, while irrigation targets are also defined on a monthly demand basis. Hydropower targets are calculated daily to reflect the continuous nature of energy production needs.

Hydropower

Hydropower deficits are calculated based on the difference between the five water hydropower dams' targets and actual electricity generation. This is crucial for energy security and economic development in the region. The model calculates hydropower production daily, with the actual production being defined as:

$$P_{actual} = \eta g \gamma \bar{h} q \quad (3.7)$$

where η describes turbine efficiency, g gravitational acceleration (9.81 m/s²), γ water density (1000kg/m³), \bar{h} net hydraulic head, and q turbinated flow.

¹For this study, target values are taken from the base model and assumed to be agreed upon by all stakeholders.

The annual average hydropower production deficit is then measured to evaluate performance where T_{hydro} is the target hydropower production, and P_{actual} is the actual production. It is defined as:

$$J_{HPP} = \frac{1}{N} \sum_{t=0}^H |T_{hydro} - P_{actual}| \quad (3.8)$$

Environmental Minimal Flows

Environmental flow deficits assess the failure to meet minimum flow requirements across the three ecological sides. Minimal flows are vital for biodiversity, fisheries, and providing ecosystem services that local communities depend on. The model evaluates environmental flow requirements every month, using the sum of squared flow deficits where T_{target} is the target flow, and r_{actual} is the actual flow from reservoir releases and irrigation diversions. Specifically, the deficit for the delta environment is calculated by comparing the actual flow with the target flow for the delta. It is defined as:

$$J_{EFT} = \frac{1}{H} \sum_{t=0}^H (\max(T_{target} - r_{actual}, 0))^2 \quad (3.9)$$

Irrigation

Irrigation deficits measure the shortfalls in water supply for agriculture across the eight central irrigation districts. It is essential for food security and sustaining livelihoods. The model normalizes irrigation deficits to ensure equal weighting across different irrigation districts. Irrigation targets are defined monthly to reflect the seasonal nature of water needs. The deficits are calculated as the squared differences where $T_{irrigation}$ is the water demand and ω_{actual} is the actual abstraction for the i -th irrigation district. This formulation ensures equal weighting of irrigation deficits across districts. It is described as:

$$J_{ID} = \frac{1}{H} \sum_{t=0}^H \left(\frac{\max(T_{irrigation} - \omega_{actual}, 0)}{T_{irrigation}} \right)^2 \quad (3.10)$$

Summary

In conclusion, the Zambezi River Basin exemplifies a contextual situation that many transboundary river basins face globally. As one of the most affected by climate change, the basin is anticipated to struggle. Five water reservoirs along the Kafue and Zambezi rivers are used to generate hydropower and store and release water based on minimum environmental flows at three sides and eight water-demanding irrigation districts. Further, the basin's transboundary character and the establishment of the Zambezi

Watercourse Commission underline the importance of cooperative management. It highlights the necessity for a detailed analysis of tradeoffs and deep uncertainties.

The EMODPS model is used as a decision-support tool to navigate the competing objectives of hydropower, agriculture, and environmental conservation. It allows the optimization of the operation strategies for the basin's five significant reservoirs, facilitating an analysis of trade-offs.

Chapter 4

Method

This section introduces the proposed methodology for leveraging Robustness Analysis to enhance the adaptive policy design in river basin management. Subsequently, the methods are illustrated, with a focus on the assessment methods and experimental settings.

4.1 Methodology

Figure 4.1 shows the framework's three main components. It builds upon an existing EMODPS model, thus omitting steps related to problem framing and model implementation. First, the conventional EMODPS framework is leveraged to identify policy alternatives. This results in a reference set. Subsequently, the generation of future states of the world follows a bottom-up Exploratory Modeling Analysis principle. Finally, identifying critical uncertainties follows a detailed Scenario Discovery that informs the dynamic policy structure.

4.1.1 Identification of Policy Alternatives

The base case Zambezi model is utilized to generate a range of policy alternatives. For a detailed model discussion; see Section 3.2. The output delivers Pareto-optimal solutions, forming a Pareto front across three objectives. Post-processing leads to a reference set that serves as a baseline for subsequent analyses. Pareto sets are explored using established quality metrics alongside visual analysis; see Section 4.3. The whole application is demonstrated in Section 5.1.

4.1.2 Robustness Analysis

Robustness Analysis, subsequent to the generation of policy alternatives, begins with characterizing critical uncertainties. A non-systematic literature review is employed.

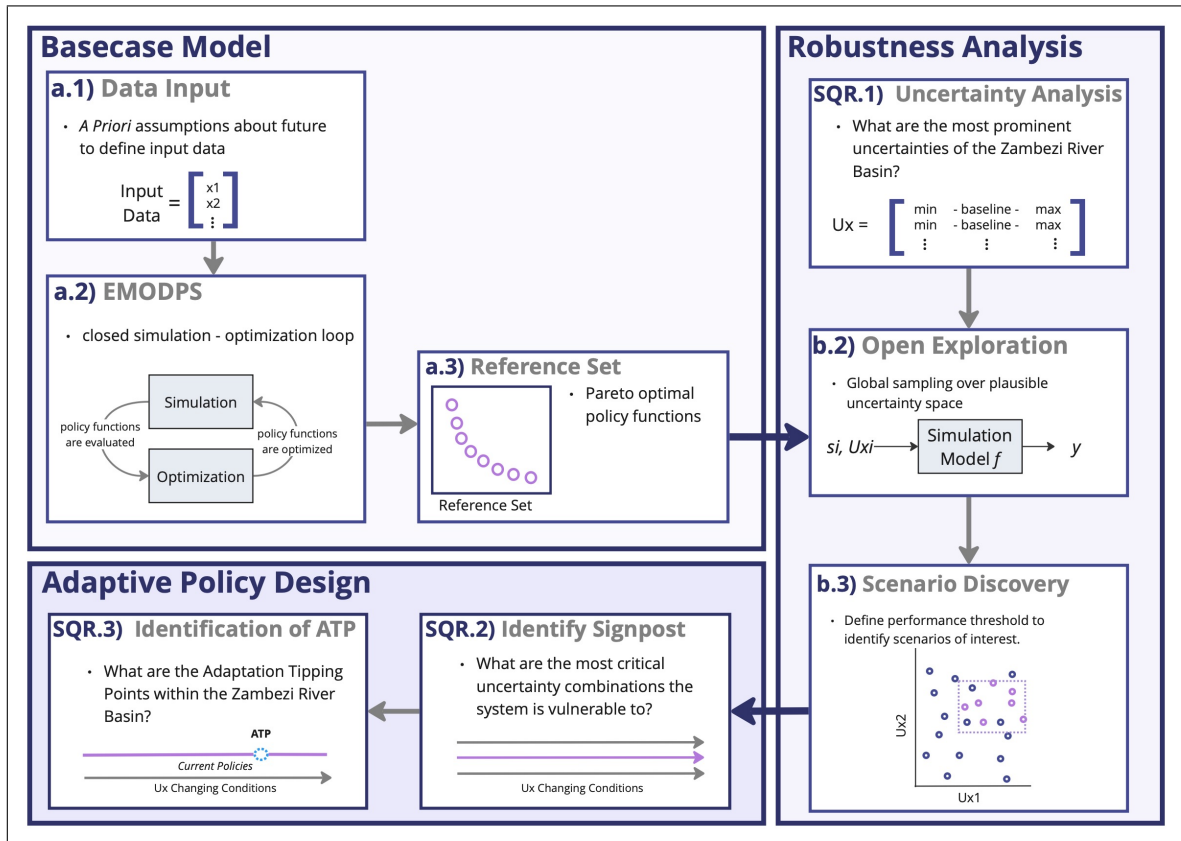


Fig. 4.1 Conceptualized Methodology Workflow. The workflow is structured into three main components. **a)** Conventional EMODPS describes the Zambezi model, resulting in Pareto-optimal policies. **b)** Robustness Analysis includes the identification of key uncertainties through Open Exploration and Scenario Discovery. **c)** Improving the Adaptive Policy Design focuses on the identification of Signpost and Adaptation Tipping Points

The results will answer the first sub-research question about key uncertainties. Afterward, the results are translated into quantifiable uncertainty factors and integrated into the Zambezi model.

Subsequently, the generation of future states of the world follows an Exploratory Modeling approach sampling over the quantified uncertainty factors and four selected policy functions. The definition of performance thresholds determines failure states, which are analyzed using a Scenario Discovery approach.

4.1.3 Improvement of Adaptive Policy Design

Results from the Scenario Discovery will identify single and combinations of uncertainties regarding which policies are most vulnerable. These will inform the definition of Signpost Conditions. The thesis introduces a Signpost Condition as a critical

uncertainty factor that is necessary to reliably and accurately describe system failure states. This way system performance can be understood as the systems Signpost which is described through a set of Signpost Conditions. Performance gaps determine the contextual character of Adaptation Tipping Points. The specific values defining the boundaries of the uncertainty space under which the system fails inform Adaptation Tipping Point Thresholds. In the final step, these thresholds translate into new streamflow patterns that describe the quantified Adaptation Tipping Points.

4.2 Method

The following Section introduces methods for uncertainty characterization, Open Exploration, and Scenario Discovery.

4.2.1 Uncertainty Characterization

Uncertainty characterization describes a critical step within the Dynamic Planning approach; see Section 2.2.3. It is context-dependent and much relies on the modeler's ability to:

- Identify key Uncertainty Drivers.
- Translate Uncertainty Drivers into Uncertainty Factors.
- Integrate Uncertainty Factors into the model structure.

Identification of Uncertainties

A non-systematic search strategy across the Scopus online library is employed¹. The analysis focuses primarily on synthesizing scientific literature to establish a comprehensive list of Uncertainty Drivers.

The search is limited to English-language peer-reviewed articles that contribute to modeling river basin management under consideration of Deep Uncertainty. Search criteria tailor a query string to extract articles on the Zambezi River Basin. Urban issues and short-term studies are deliberately excluded only to identify trends that align with the spatial and temporal scale of the model.

The following query is used: "Zambezi River Basin" AND (uncertainty OR "critical uncertainties" OR "drivers of uncertainty" OR "deep uncertainty") AND (modeling OR modelling OR "scenario analysis" OR "water management") AND NOT (urban OR "Short term" OR "water quality") AND (LIMIT-TO (LANGUAGE, "English")).

¹Future studies could benefit from expert interviews to deepen insights into regional trends and projections.

Quantifying Uncertainty Drivers

Uncertainty Drivers are quantified using a statistical rescaling method introduced by (Quinn et al., 2018). Lower and upper bounds are defined to set the stage for the Exploratory Modeling Analysis. The specific range parameter builds upon the insights gained from the initial uncertainty analysis. It involves careful consideration of a conservative safety margin for each factor to ensure a meaningful representation of deep uncertainties².

4.2.2 Open Exploration

Open Exploration is employed to understand and identify system vulnerabilities across many futures. The `ema_workbench`, a python library for Exploratory Modeling Analysis, is leveraged to generate a wide range of plausible futures following the methodology of Bryant and Lempert (2010).

Running simulations with the Zambezi model over four different Pareto-optimal solutions across a broad spectrum of plausible future scenarios generates many scenarios. Scenarios y are defined through policy levers s and combinations of uncertainty factors U_{x_i} as:

$$y = f(s, U_{x_i}) \quad (4.1)$$

A performance threshold is defined to identify outcomes of interest. With this thesis focusing on policy vulnerabilities, scenarios of interest aim to capture conditions that display policy failure. Thus, a performance threshold Y^I is set to focus on the worst 25 percent of outcomes. This leads to the final set of interesting scenarios I_s , being defined as:

$$I_s = \{x_I \mid f(s, x_I) \leq Y^I\} \quad (4.2)$$

The uncertainty space is sampled, using Latin Hypercube Sampling (Saltelli and Chan, 2000). The uncertainty space is spanned by lower and upper boundaries of uncertainty factors previously defined.

Four policy levers are selected from the Zambezi model reference set: three optimal policies, one for each objective, and a tradeoff policy. The Best Tradeoff policy was selected based on the variability between objective values. Selecting the policy with the lowest variability between normalized objective values ensured a balanced policy approach.

²It should be noted that this step depends on the case area. Thus, rather than prescribing a specific method for representing deep uncertainties, the thesis's approach is specific to the characteristic uncertainties of the Zambezi River Basin. Results are assumed to characterize a meaningful representation of the future states of the world.

4.2.3 Scenario Discovery

Building upon the Open Exploration, exploratory modeling results are first analyzed using Feature Scoring and PRIM. Feature scoring ranks uncertainty factors by their impact on outcomes. Thus, it provides a first overview of critical Signpost Conditions. Its main advantage to PRIM is that it does not depend on threshold settings or peeling factors. Afterward, PRIM is utilized to better understand the combinatorial effects of Signpost Conditions. Together, their ability to analyze the impact of uncertainty factors on policy failure is leveraged to inform the definition of multiple sets of Signpost Conditions.

Identified sets of Signpost Conditions provide input for the following Logistic Regression Modeling. Different sets are evaluated on their ability to predict policy failure. Results describe the boundaries delineating failure from success states and inform Adaptation Tipping Point Thresholds.

Feature Scoring

The main objective is to determine which uncertainty factors have the most significant impact on the likelihood of policy failure. Factors with the highest importance score are used to inform the definition of Signpost Conditions. The importance score for each feature can be mathematically represented as follows:

$$\text{Score}(X_j) = \frac{\Delta\text{Loss}(X_j)}{\sum_{k=1}^p \Delta\text{Loss}(X_k)} \quad (4.3)$$

Where:

- $\text{Score}(X_j)$ is the importance score of the j -th feature,
- $\Delta\text{Loss}(X_j)$ is the change in the loss function when the j -th feature is removed from the model.
- p is the total number of features.

Patient Rule Induction Algorithm

PRIM is leveraged to identify scenario boxes based on the binary indicator of policy failure or success. The goal is to detect combinations of Signpost Conditions that best describe policy failure outcomes.

It works by iteratively peeling and pasting operations to find the scenario boxes. The peeling operation removes the portion of the data with the worst outcomes, while the pasting operation refines the subgroup to maximize the outcome of interest.

The following steps characterize the algorithm:

1. **Peeling Away**

- Identify a box in the covariate space that includes all observations.
- Sequentially remove the regions with the worst outcomes from this box.

2. Pasting In

- Refine the box by adding back some observations that were removed during peeling to improve the homogeneity of the box.

3. Stopping Criterion

- Continue peeling and pasting until the improvement in the outcome is marginal or a predefined stopping criterion is met.

Logistic Regression Modeling

The logistic regression modeling approach is based on Quinn et al. (2018), which applied a regression model for Scenario Discovery. In particular, it was applied to identify factors that most significantly affect the ability of reservoir operation policies to provide protection against 100-year floods.

The regression model is defined as:

$$\ln \left(\frac{p_i}{1 - p_i} \right) = \mathbf{X}_i^T \beta \quad (4.4)$$

Where p_i is the probability of failure in the i^{th} scenario, \mathbf{X}_i represents the vector of covariates, including previously identified signpost conditions, and β are the coefficients estimated through Maximum Likelihood Estimation.

In particular, different sets of Signpost Conditions as model predictors are evaluated using McFadden pseudo-R squared values. It is a metric used to evaluate the goodness-of-fit for logistic regression models. It is defined as:

$$R_{\text{McFadden}}^2 = 1 - \frac{\ln \hat{L}(M_{\text{Full}})}{\ln \hat{L}(M_{\text{Intercept}})} \quad (4.5)$$

Where:

- $\ln \hat{L}(M_{\text{Full}})$ is the log-likelihood of the full model, including all covariates,
- $\ln \hat{L}(M_{\text{Intercept}})$ is the log-likelihood of the intercept-only model, which predicts the mean probability of success across all scenarios.

This metric measures the improvement of the entire model over the intercept model, with higher values indicating better model performance. In practice, covariates are added incrementally to the model, prioritizing those that significantly increase R_{McFadden}^2 .

This iterative process continues until the addition of new covariates yields minimal improvement. The Python library `statsmodels` is used for implementation.

Afterward, the most accurate regression model is leveraged to differentiate system outcomes into areas of failure and success. Results provide the means to identify boundary conditions that differentiate system outcomes into areas of failure and success. This informs the quantification of Adaptation Tipping Point Thresholds, which are translated into Adaptation Tipping Points using the methods defined when quantifying uncertainty drivers. Results present the quantified Adaptation Tipping Points as new streamflow patterns of the seven Zambezi River Basin's catchment areas.

4.3 Assessment Metrics

A combination of established quality indicators and visual analysis techniques is utilized to evaluate EMODPS optimization results. Quality indicators provide a comprehensive assessment of solution convergence. In parallel, visual analysis is utilized to interpret the shapes of Pareto fronts, explore multi-objective tradeoffs, and analyze the distribution of failure and success spaces within the uncertainty space.

4.3.1 Quality Indicators

Established quality indicators in multi-objective optimization are Generational Distance, Hypervolume, Additive-Epsilon Indicator, and Epsilon Progress.

Generational Distance

Generational Distance measures how close solutions from an approximation set are to the reference set (Van Veldhuizen and Lamont, 1998). It calculates the average Euclidean distance between each solution in the approximation set and the nearest solution in the reference set. The formula for Generational Distance is:

$$GD = \left(\frac{1}{n} \sum_{i=1}^n d_i^2 \right)^{\frac{1}{2}} \quad (4.6)$$

Where n is the number of solutions in the approximation set, and d_i is the Euclidean distance between the i -th solution in the approximation set and the nearest solution in the reference set. A smaller Generational Distance indicates improved convergence.

Hypervolume

The Hypervolume indicator assesses both the diversity and proximity of the solutions by quantifying the volume of the objective space dominated by the approximation set. The hypervolume is normalized against the reference set, with values closer to one

indicating that the approximation set covers the same volume as the reference set, thus reflecting good diversity and convergence (Zitzler and Thiele, 1999).

Additive Epsilon Indicator

The Additive-Epsilon Indicator evaluates the consistency of the solutions. It determines the maximum distance an approximation set needs to be shifted to dominate the reference set. Thus, it is defined as:

$$\epsilon = \min\{\epsilon' \mid \forall \mathbf{y} \in R, \exists \mathbf{x} \in A : \mathbf{f}(\mathbf{x}) + \epsilon' \geq \mathbf{f}(\mathbf{y})\} \quad (4.7)$$

where R is the reference set, A is the approximation set, $\mathbf{f}(\mathbf{x})$ and $\mathbf{f}(\mathbf{y})$ are the objective vectors of solutions \mathbf{x} and \mathbf{y} , respectively, and ϵ' is the additive epsilon value.

Epsilon Progress

Epsilon Progress tracks the progress of the optimization process. It measures the solution set's incremental improvement compared to the previous iteration. Specifically, the Epsilon Progress calculates the additive epsilon value. This value represents the minimum amount that needs to be added to each objective in the current approximation set to make it weakly dominated by the reference set (Zitzler et al., 2003). Decreasing Epsilon Progress values indicate better convergence and tradeoff coverage.

4.3.2 Visual Analysis

The visual analysis focuses on three main plotting types: pair plots, parallel coordinate plots, and contour plots.

Pair Plots

Pair plots facilitate understanding of the shape of Pareto fronts. They can visualize both the distribution of individual objectives and their pairwise relationships. The diagonal of the matrix displays density distribution plots for each objective. It allows to investigate their distributions and variability. The off-diagonal matrix is envisioned to display scatter plots and kernel density estimates. This provides insights into the tradeoffs between pairs of objectives and to discern the shape of the Pareto fronts.

Parallel Coordinate Plots

Parallel coordinate plots display Pareto-policy interactions and visualize the tradeoffs among specific policies within the multi-objective context. By aligning the objectives on parallel axes and plotting their values, these plots provide a comprehensive view of how various policies perform across objectives.

Contour Plots

Contour plots visualize the uncertainty space between pairwise uncertainty factors segmented into policy success and failure areas. Contourlines illustrate the boundaries between successful and unsuccessful policy outcomes.

Other Visualizations Approaches

In addition, the following graphs are used to communicate insights:

- **Flow Duration Curves** summarize streamflow data against its exceedance probability. They are leveraged to illustrate insights about the frequency and magnitude of different streamflow ensembles that describe different states of the world.
- **Yearly Streamflow Averages** display the average streamflow for each year, providing a clear view of long-term trends and annual variations.
- **Heatmaps** are used to visualize insights into Feature Scoring and Adaptation Tipping Point streamflow differences.
- **Density-Coverage Tradeoff Plots** for PRIM show the balance between the density of policy failures and the coverage of the identified subgroups. They are leveraged to highlight insights into the effectiveness of the PRIM in isolating scenarios of interest, helping to identify Signpost Conditions.

4.4 Experimental Settings

The base case optimization utilizes the Zambezi model, introduced in Section 3.2, and optimizes the policy functions over 200,000 function evaluations. Five different seeds are used to manage variability. Epsilon values of 0.2, 0.5, and 0.3 are selected to balance convergence speed and solution diversity. Computations are performed on Delft Blue, the high-performance computing environment from TU Delft (Delft High Performance Computing Centre , DHPC). The optimization is set up for multi-node processing. In total, it utilizes 64 nodes. Each node has access to 48 CPUs and 1GB of memory per CPU.

The main experiment describes an Open Exploration simulation. The Zambezi model is used for simulation. The Zambezi model simulates four policies, each against 25,000 uncertainty conditions, creating a total of 100,000 scenarios. Results detailing scenario settings and objective values are stored in two files for subsequent analysis. Again, the simulation utilizes Delft Blue with the same settings.

Summary

This section detailed the proposed methodology for enhancing adaptive policy design in river basin management through a Robustness Analysis. It includes identifying policy alternatives using the EMODPS framework. Robustness Analysis follows, characterizing uncertainties, Open Exploration, and Scenario Discovery.

This approach is expected to improve the adaptive policy design by identifying scenarios that reveal critical system performances. It includes the definition of Signpost Conditions, different sets of Signpost Conditions, Adaptation Tipping Point Thresholds, and the quantification of Adaptation Tipping Points. Tools such as the EMA Workbench facilitate Exploratory Modeling Analysis, while Logistic Regression aids in evaluating accurate sets of Signpost Conditions and identifying Adaptation Tipping Point Thresholds.

Assessment metrics, including Generational Distance and Hypervolume and visual analysis like pair plots, evaluate the effectiveness of the optimization process. The experimental settings are defined, utilizing Delft Blue's high-performance computing capabilities.

Chapter 5

Analysis

This Section demonstrates the practical application of the proposed methodology. First, it exemplifies how to establish the reference set. Next, the uncertainty characterization is outlined, detailing how to convert Uncertainty Drivers into Uncertainty Factors. Afterward, it illustrates the Exploratory Modeling Analysis. Finally, Scenario Discovery is performed to identify Signpost Conditions and Adaptation Tipping Point Thresholds to quantify Adaptation Tipping Points¹.

5.1 Zambezi Base Case Run

The results of the base case run produced five distinct Pareto sets. Each reveals a different set of solutions, as displayed in Appendix B. Outcomes vary slightly across different seeds: the first run yielded 185 Pareto optimal solutions, while the fourth produced 190 solutions. The total number of solutions ranged from 185 in the first run to 279 in the third, illustrating some variability in optimization performance.

5.1.1 Reference Set

Results from the five different Pareto sets are post-processed to build a reference set. It leverages an epsilon-non-dominated sorting algorithm, using the `pareto.py` script based on the method from Woodruff and Herman (2013). This approach involves ranking solutions with an epsilon threshold set to 0.05. Therefore, solutions with lower differences are treated as equivalent. It filters out minor variations and thus only includes distinctly non-dominated solutions.

The outcome is an epsilon-non-dominated Pareto solution set comprising 364 distinct solutions. Each solution in Figure 5.1 represents an optimal Pareto epsilon non-dominated policy function across the three objectives.

¹The respective notebooks for each analysis steps can be found in the open GitHub repository here: [Visit GitHub Repository](#)

Pair plots and density plots illustrate the complex interactions and tradeoffs between objectives. Density plots on the diagonal show the distribution of each objective, indicating where policy outcomes are concentrated. For instance, hydropower displays a bimodal distribution, suggesting two primary modes of operation among optimal solutions. In contrast, the environmental objective is leaning towards higher values, indicating higher deficits and lower prioritization of environmental considerations in many of the optimal solutions.

The off-diagonal scatter plots reveal the tradeoffs between pairs of objectives. In particular, the plot between hydropower and the environment shows a clear negative correlation, highlighting the typical tradeoff between energy production and environmental preservation. The denser regions of these plots indicate areas where compromises between objectives are most common.

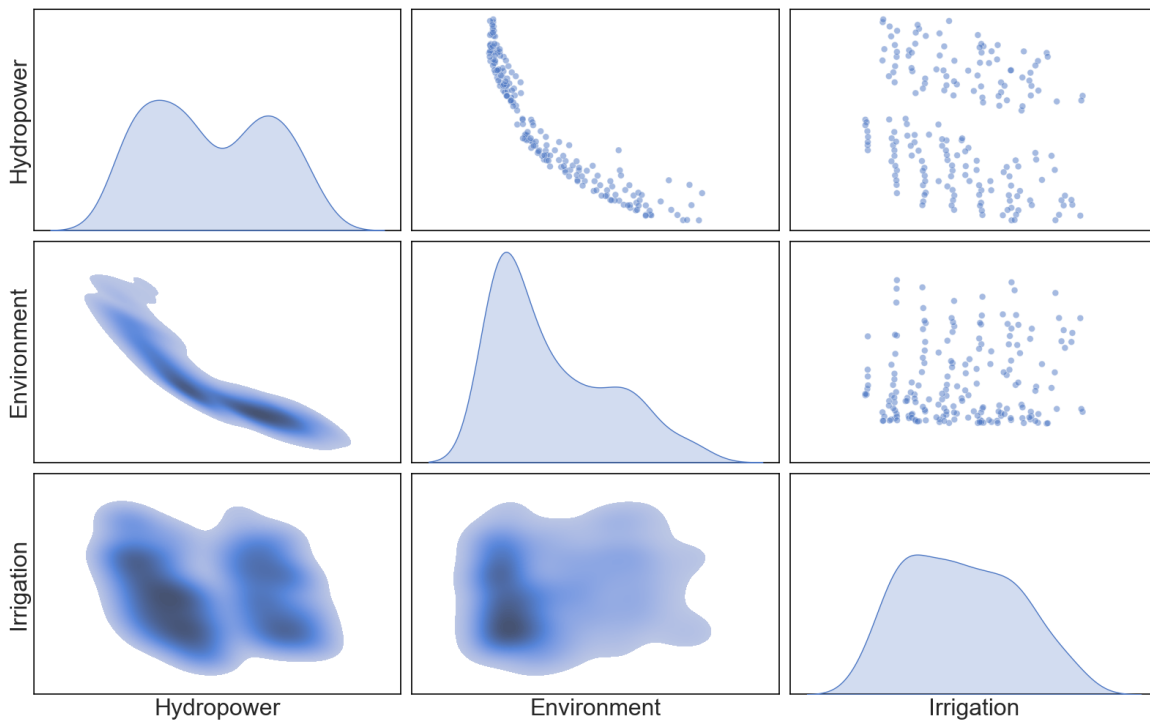


Fig. 5.1 Pair Plot and Density Distribution of Reference Set. A comprehensive visualization of MinMax normalized Pareto-optimal solutions across three objectives derived from five seeds. Diagonal panels display density plots for each objective, with lower values indicating better performance. Off-diagonal scatter plots illustrate pairwise tradeoffs between the objectives.

5.1.2 Convergence

To evaluate the optimization performance, quality metrics from the `ema_workbench` library are utilized; see Section 4.3.

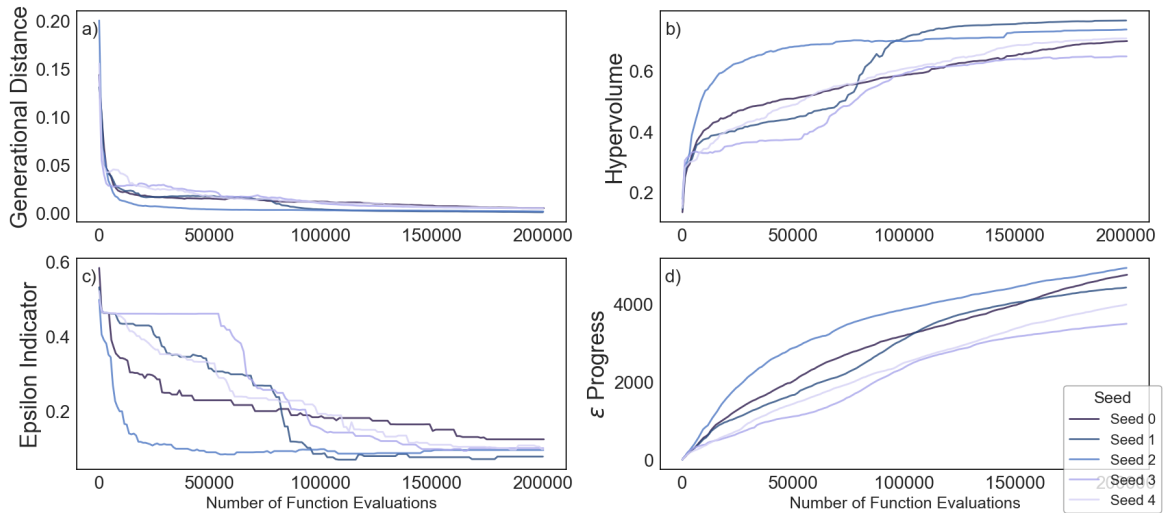


Fig. 5.2 Quality Indicators for Basecase Run. The figure illustrates four key performance metrics across five seeds over 200,000 NFEs. a) Generational Distance measures convergence towards the Pareto front. b) Hypervolume highlights the quality and diversity of solution space. c) Additive Epsilon Indicator reflects solution accuracy. d) Epsilon Progress displays epsilon improvements, indicating convergence.

Generational Distance

Using `GenerationalDistance`, the distances between population iterations and the reference set are computed. Data is retrieved from the optimization archives that store data at 1000 function evaluation intervals. Results show that all seeds initially exhibit a high generational distance, indicating a significant gap between the initial populations and the reference set. There is a rapid decline in generational distance across all seeds, stabilizing after approximately 50,000 evaluations, suggesting effective convergence near the Pareto front.

Hypervolume

The volume covered by the Pareto sets is measured using the `Hypervolume` method. It highlights an initial increase in Hypervolume across all seeds. This indicates an expansion in the volume covered by the Pareto sets. Following this initial surge, a slower yet steady improvement continues until around 150,000 function evaluations. At this point, the Hypervolume stabilizes, indicating that solutions are approaching maximum coverage of the objective space in relation to the reference set.

Additive Epsilon Indicator:

The `AdditiveEpsilonIndicator` function is utilized to monitor convergence rates. The decrease in this metric across all seeds suggested swift convergence, which stabilized after about 100,000 function evaluations.

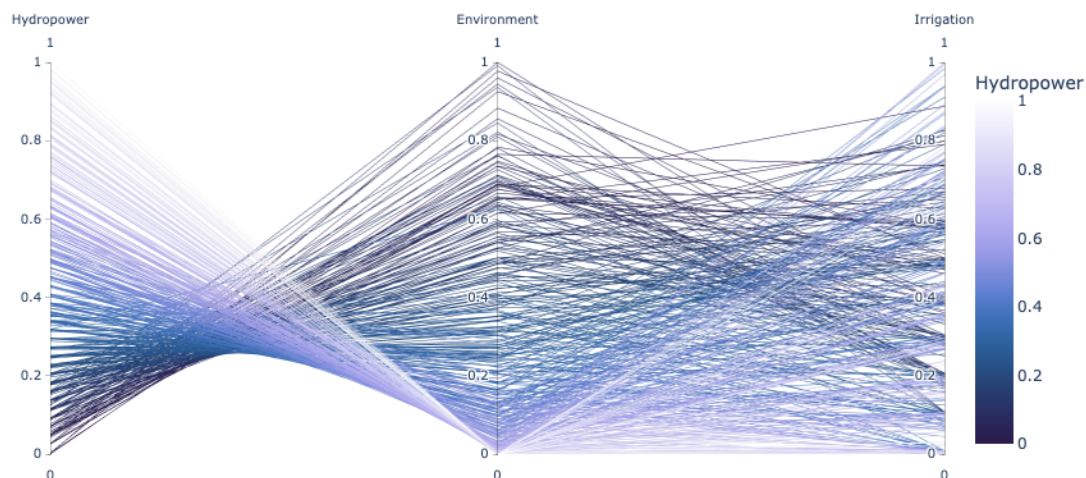


Fig. 5.3 Parallel Coordinate Plot. It displays Tradeoffs among Hydropower, Environment, and Irrigation. Each line represents a different solution from the reference set, with the vertical position on each axis indicating the MinMax normalized performance score. Lower values are preferred. The color gradient from light purple to dark blue represents the hydropower objective value; the darker, the better.

Epsilon Progress

The optimization progress during the optimization is tracked with the help of the `MultiprocessingEvaluator` class from the `ema_workbench`. The `EpsilonProgress` function allows consistent recording of the algorithm's convergence during the optimization phase. Post-optimization, data is retrieved from a CSV file for a detailed analysis. Results show an upward trend in Epsilon Progress across all seeds. The rate of increase began to slow around 150,000 evaluations. It suggests that the algorithm is near convergence.

Results indicate that the algorithm performs well for the base case across different seeds. All metrics indicate a consistent convergence towards the reference set. The rapid initial improvements in the Generational Distance and Additive-Epsilon Indicator suggest that the model quickly narrows the search space and identifies promising regions. Furthermore, the continued improvement in Hypervolume and Epsilon Progress reflects the algorithm's ability to maintain diversity and enhance solution quality over time.

5.1.3 Multi-objective Tradeoffs

For the multi-objective tradeoff analysis, a Parallel Coordinate Plot visualizes the objective values extracted from the reference set. The policy lines' shades are based on the hydropower deficit, with darker shades indicating superior performance.

Figure C.3 indicates that policies that excel in one objective tend to perform poorly in others. This hints at tradeoffs among the objectives. For instance, purple shading suggests that most policies with a high Hydropower deficit yield better results across the Environment and Irrigation objective. Similarly, policies that prefer hydropower perform worse, especially regarding the environmental objective.

5.2 Uncertainty Characterization

First, deep uncertainties within the system are identified. A non-systematic literature review is leveraged to identify the main Uncertainty Drivers within the Zambezi River Basin. It should be noted that critical uncertainties differ and are case-specific. Hydroclimatic uncertainties of mean precipitation, inter-annual variability, and seasonal shifts are critical for the Zambezi River Basin. Socio-economically, irrigation demand is considered the most relevant. Results are presented in Section 6.1 with greater detail.

An aspect that determines the translation of identified trends into factors is the model structure. The Zambezi model sets most of them as exogenous; see Section ???. To allow for Open Exploration, the model structure is edited to account for crucial Uncertainty Drivers within the simulation process. The following Section details the approach.

5.2.1 Manipulation of Streamflow Data

A statistical rescaling method developed by Quinn et al. (2018) is applied for streamflow manipulation. It informs the implementation of a `StreamflowRescaler` class, which, during the model initialization, takes the historical streamflow data and manipulates it according to the approach outlined below. Conclusively, it allows the adjustment of monthly streamflow data in regard to inter-annual variability, mean precipitation change, and seasonal shifts using just six parameters. This is beneficial given the computational demands of exploring multiple uncertain factors.

Synthetic Streamflow Generation

First, synthetic streamflow ensembles are generated by leveraging the synthetic streamflow generator from (Kirsch et al., 2013; Nowak et al., 2010). It is based on historical data from 1986 to 2005. Every step is performed across all catchment areas².

Second, ensembles: historical Y_H and synthetic Y_S are log-transformed. It ensures that subsequent analyses are based on data approximating normal distributions. This facilitates better statistical treatment. Appendix C.2 displays the resulting flow duration curves.

²Data vector for the Cuando catchment is omitted because it is empty and only considered with infinite small inflow values for the base case model

Mean Precipitation and Variability

The synthetic streamflow ensembles Y_s are standardized to generate synthetic standard normal monthly flows Z_s given the monthly mean μ_j and standard deviation σ_j of the log normal historical monthly flows with:

$$Z_{s,ij} = \frac{Y_{s,ij} - \mu_j}{\sigma_j} \quad (5.1)$$

For illustration, Figure 5.4 illustrates rescaled inflow data using a constant mean precipitation M_μ and inter-annual variability M_σ multiplier to backtransform $Z_{s,ij}$ into new inflow data sets $Q'_{S,ij}$. The backtransformation is outlined in Equation 5.4. Appendix 5.4 displays more comprehensive figures across all catchment areas.

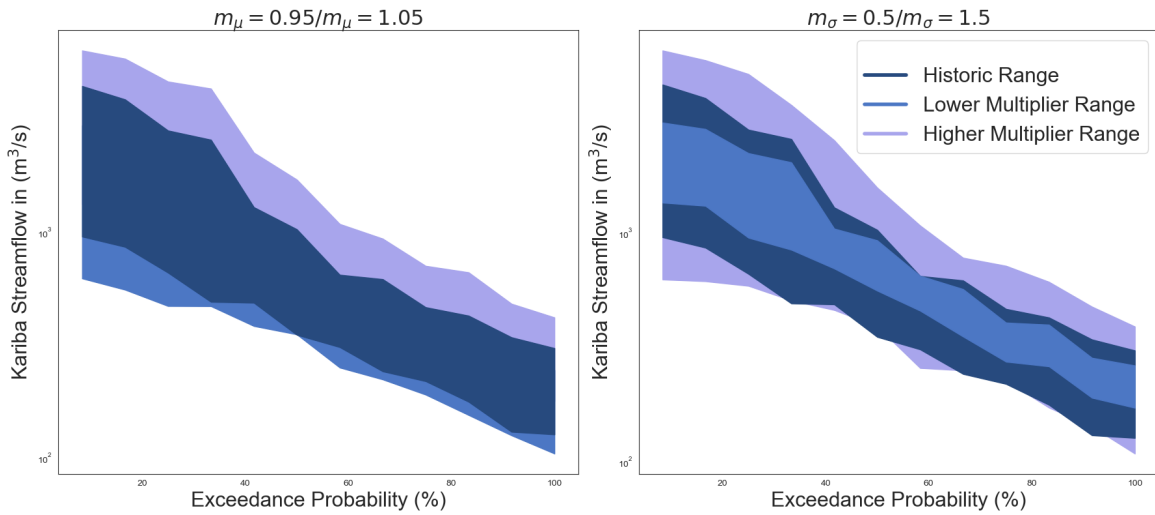


Fig. 5.4 Kariba Catchment Exceedance Probability Under Different Scenarios. The left panel displays the effect of different mean precipitation multiplier values (m_μ). The right panel shows the effect of different interannual variability multiplier values (m_σ).

Seasonal Shift

Changes in the seasonal distribution of flows utilize a second-order Fourier series fitted to the historical log-space monthly means. This process captures the essential characteristics of the wet and dry seasons with minimal parameters. The Fourier series is described as:

$$\hat{y}_1(i) = y + C_1 \cos\left(\frac{2\pi i}{12} - \phi_1\right) + C_2 \cos\left(\frac{4\pi i}{12} - \phi_2\right) \quad (5.2)$$

Where i the month index, y the mean of the historical series, C_1 and C_2 the amplitudes, as well as ϕ_1 and ϕ_2 the phase shifts are fitted based on the historical log-space monthly means. Appendix C.4 displays the Fourier series for each catchment.

Afterward, seasonal patterns can be adjusted to simulate potential shifts in the timing and amplitude of the wet and dry seasons. Amplitude multipliers (mC_1 for the primary, mC_2 for the secondary seasonal pattern) and phase shift deltas ($d\phi_1$ and $d\phi_2$) are used to manipulate the fitted Fourier series parameters as follows:

$$y_2(i) = \hat{y} + m_{C_1}C_1 \cos\left(\frac{2\pi i}{12} - (\phi_1 + d\phi_1)\right) + m_{C_2}C_2 \cos\left(\frac{4\pi i}{12} - (\phi_2 + d\phi_2)\right) \quad (5.3)$$

These adjustments allow the generation of scenarios that vary in the onset and intensity of the wet and dry seasons. Figure 5.5 illustrates these adjustments. Appendix C.5 and Appendix C.6 provide comprehensive information about other catchments.

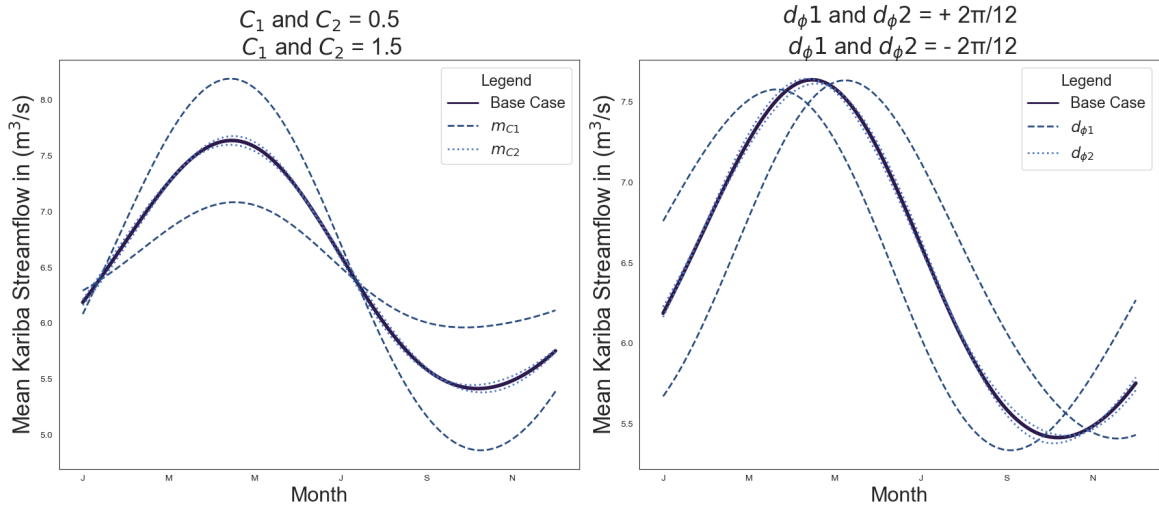


Fig. 5.5 Kariba Catchment Seasonal Variability. The left panel displays different seasonal amplitude values of m_{C_1} and m_{C_2} . The right panel shows the effect of different seasonal phase shift values of $d\phi_1$ and $d\phi_2$.

Adjusted Streamflow Scenarios

Following the definition of $\hat{y}_1(i)$ and $y_2(i)$, the synthetic inflow ensembles Y_s are standardized as described in Equation 5.1. Afterward, these standardized synthetic streamflows are back-transformed into new adjusted streamflow ensembles as follows:

$$Q'_{S,ij} = \exp(M_\mu \hat{\mu}_j + M_\sigma \hat{\sigma}_j Z_{S,ij}) \quad (5.4)$$

Here, M_μ is a monthly varying multiplier while M_σ is a constant multiplier. This again follows Quinn et al. (2018). The monthly varying mean multiplier $M_{\mu,j}$ is defined through:

$$M_{i,j} = \left[m_j \frac{y_2(i)}{y_1(i)} \right], \quad (5.5)$$

This method enables the manipulation of monthly streamflow data with six factors. Preliminary analysis shows that second order amplitudes m_{C2} and phase shifts $d\phi_2$) exhibit minimal changes; see Figure 5.5. Thus, they are set to a constant multiplier of one, reducing the number of uncertainty factors that must be sampled. It increases computational efficiency within the Open Exploration.

In conclusion, hydroclimatic uncertainty trends of mean precipitation changes, inter-annual variability and seasonal shifts are represented through factors of a Log-space mean multiplier m_μ , log-space standard deviation multiplier m_σ , log-space multipliers m_1 , as well as log-space delta shifts $d\phi_1$.

5.2.2 Temperature

Deep uncertainties surrounding temperature increase are represented through an adjustment of the evaporation rate. In contrast to streamflow data, temperature is not directly part of the model. However, associated evaporation rates, influenced by temperature, are considered and significantly affect the storage volumes of reservoirs. The Zambezi model sets evaporation rates in an exogenous manner. They vary by reservoir and exhibit a repeating 12-month pattern.

Rising temperatures during the simulation period of 20 years are captured by implementing a delta shift for each reservoir. This shift is calculated in relation to the base evaporation rate. While Quinn et al. (2018) used an absolute value, here, a shift in relation to the base case evaporation is leveraged. It allows the change of all evaporation rates equally with only one parameter.

The `Reservoir` class of the Zambezi model, which manages the evaporation rates, is adjusted according to the sampled evaporation rate.

5.2.3 Irrigation Demand

Initially, three demand multipliers were used to adjust the monthly demand values of all irrigation districts annually. The base case model defines eight exogenous demand vectors, one for each district. While monthly differences in demand recognize seasonality, the values are static for 20 years and do not account for changing demand patterns.

Population growth is assumed to be the primary driver of irrigation demand. Thus, population growth data from the United Nations World Population Prospect Report

from 2022 (United Nations, Department of Economic and Social Affairs, Population Division, 2022) was analyzed. Here, the country's population growth projections are based on ten scenarios. They differ due to different considerations of variables like fertility rates or migration patterns. The highest projection from these scenarios is selected to align with the principles of Deep Uncertainty. In addition, a conservative margin of ten percent is added to the multiplier. The original base case values are set as the lower bound.

The demand multipliers are collapsed into one. It assumes that the population growth of one country and its irrigation districts affect the demand of the others. Hence, the demand multiplier with the highest upper range is taken as the general demand multiplier.

5.3 Exploratory Modeling

This Section demonstrates how Open exploration builds the foundation for identifying Signpost Conditions and Adaptation Tipping Point Thresholds. It follows the Exploratory Modeling Analysis paradigm and systematically explores the impacts of four policy decisions across 25,000 uncertainty conditions, leading to a total of 100,000 states of the world.

5.3.1 Selection of Policy Levers

Numerous scenarios define plausible futures, each described by a combination of policy levers and uncertainty factors.

Four optimal policies from the reference set are selected. The early commitment to specific policies contradicts the conventional Robustness Analysis approach. However, this thesis argues that this is valid for the following reasons. Robustness Analysis aims to identify policy alternatives that are least sensitive to changing conditions. In contrast, an adaptive policy plan can deviate from this approach by focusing on the ability to adapt once conditions change. However, the adaptive policy design is primarily not based on choosing a robust policy but addresses Deep Uncertainty through continuous policy adjustment. Hence, selecting any Pareto optimal policy, identifying its signposts, and quantifying Adaptation Tipping Points aligns with the Dynamic Planning principle. Therefore, the thesis focuses only on improving the adaptive policy design for four policies, according to the policy selection described in Section 4.2.2.

5.3.2 Sampling the Uncertainty Space

The uncertainty space is defined through ranges of identified uncertainty factors. Lower and upper bounds span the entire space. Table 5.1 comprehensively summarizes relevant uncertainty factors and their ranges.

The following uncertainty boundaries were chosen for the streamflow multipliers based on iterative adjustments. Decreasing evaporation seems unrealistic. However, the lower bound is set to -10 percent to account for Deep Uncertainty. The upper bound is defined with an evaporation increase of 40 percent.

For the subsequent analysis, these factors are assumed to capture the identified uncertainty trends effectively.

Table 5.1 Summary of Uncertainty Factors

| Uncertainty Factor | Range | Description |
|---------------------------|-------------------------------------|---------------------------------------|
| m_μ | 0.9 to 1.05 | Mean Precipitation Changes |
| m_σ | 0.95 to 1.2 | Inter-annual Variability |
| m_{C1} | 0.8 to 1.2 | Seasonal Amplitude (Main coefficient) |
| $d_{\phi 1}$ | $-\frac{\pi}{6}$ to $\frac{\pi}{6}$ | Seasonal Phase shift (Main shift) |
| m_demand | 1.0 to 1.031 | Irrigation Demand Multiplier |
| δ_{evap} | -10 to 40 | Change in evaporation rate |

5.3.3 Open Exploration

The Zambezi model is utilized to simulate the four specific policies selected from the reference set under a range of uncertainty conditions. In Section 5.1.1, a total of 364 Pareto-optimal policy alternatives is generated. This is scoped down to four policy levers in Section 5.3.1. Furthermore, the uncertainty space is defined through uncertainty factors determined in Section 5.3.2, and established ranges are summarized in Table 5.1.

The `ema_workbench` is leveraged to generate the broad spectrum of plausible future states of the world. It allows multiple instances of the Zambezi model to be run and retrieves outcomes across different policies and uncertainty settings. The experimental settings are detailed in Section 4.4. Results are displayed in Figure 5.6.

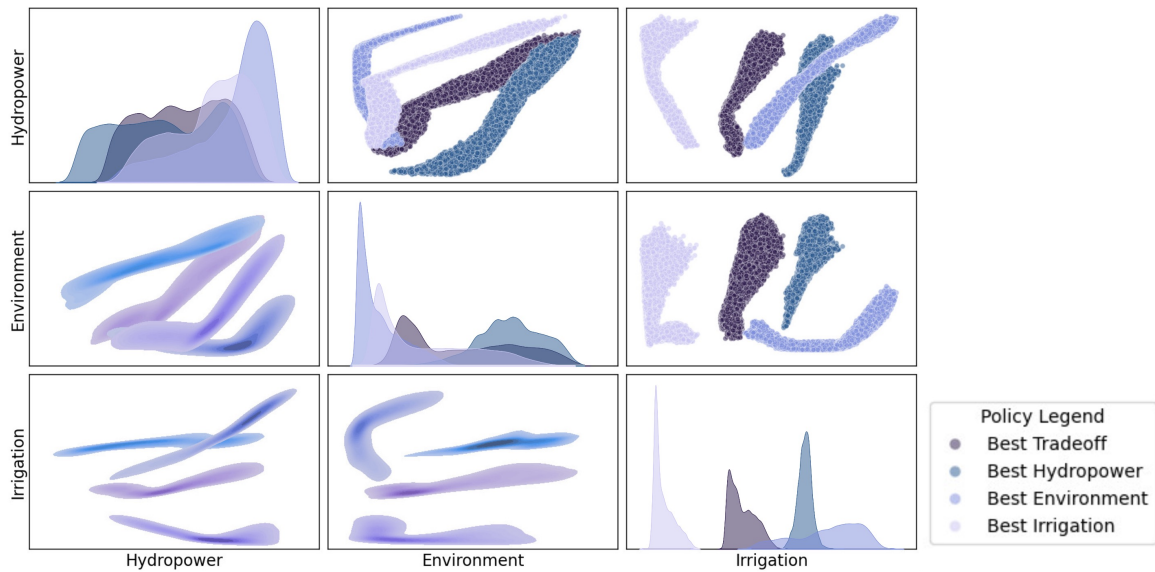


Fig. 5.6 Open Exploration Scenario Outcomes. The figure illustrates the distribution and tradeoffs of objective values for hydropower, environment, and irrigation under 25,000 uncertainty conditions. Diagonal panels show frequency distributions of objective deficits, with color intensity indicating occurrence frequency: darker shades for more common outcomes and lighter for rarer ones. The upper panels depict scatter plots comparing two objectives. The color coding differentiates four policies.

Distribution plots on the diagonal display the frequency of objective values across the generated states of the world. Narrow distributions suggest that policies often yield similar outcomes despite uncertainties. Conversely, broader distributions hint at condition-dependent policies. The consistency of policy outcomes also relates to the tightness or spread of the scatter plot clusters. Tight clusters indicate similar policy outcomes across various scenarios, suggesting robustness against varying conditions. Conversely, wider spreads highlight more significant variability.

The location of clusters along the axes indicates policy tradeoffs. Clusters positioned towards the lower regions suggest scenarios where objective deficits are low and, hence, system performance is high. In contrast, clusters towards the upper regions indicate higher deficits, reflecting compromised performance.

Hydropower:

- The Best Environment and Irrigation policies frequently result in higher hydropower deficits. Aligns with previously identified tradeoffs.
- Best Hydropower policy, despite its focus, exhibits significant deficits under challenging conditions, indicating its vulnerability to certain uncertainty conditions.
- Both Best Hydropower and Best Tradeoff policies display similar distribution tails in high deficit scenarios.

Environment:

- Best Environment policy features a sharp peak at lower deficit values, suggesting it effectively minimizes environmental deficits across scenarios.
- Best Irrigation policy shows similar characteristics but displays a broad tail that extends into higher deficit outcomes.
- Both Best Hydropower and Best Tradeoff policies demonstrate broader distributions with tendencies toward higher deficits, indicating inconsistent environmental conservation across many scenarios.
- Best Tradeoff occasionally reaches moderate outcomes, though it generally shows suboptimal results.
- Overall shape of Best Tradeoff policy scenario clusters is similar to Best Environment and Irrigation, but high deficit scenarios are prominent. It also reflects the challenges of managing hydropower deficits.

Irrigation:

- objective distributions for Irrigation are narrow, emphasizing that system performance is tightly linked to the policy implemented.
- Best Irrigation policy exhibits robust performance, consistently achieving low irrigation deficits across all scenarios.
- Best Tradeoff policy results in higher deficit scenario outcomes. No overlaps in scenario outcomes suggest that worst-case scenarios under the Best Irrigation policy still outperform the best scenarios under the other policy options.
- Best Hydropower policy also has a narrow distribution but generally shows higher deficits.
- The Best Environment policy presents a broader range of outcomes with no distinct peak, generally leaning towards higher deficits, indicating a focus on optimizing environmental flows that may adversely affect irrigation efficiency.

A preliminary analysis of Open Exploration indicates that no single policy consistently excels across all generated states of the world. This aligns with the initial selection criteria of optimal performance in the base case rather than their robustness. This distinction is crucial, as this thesis focuses not on excelling robustness analysis to select inherently robust policies but on enhancing adaptive planning capabilities. Therefore, instead of identifying policy alternatives, this thesis demonstrates how to leverage Robustness Analysis to identify Signpost Conditions and Adaptation Tipping Point Thresholds to quantify Adaptation Tipping Points. It is demonstrated in the subsequent Section.

5.4 Scenario Discovery

Scenario Discovery investigates high deficit scenarios retrieved from the Open Exploration simulation. For demonstration purposes, the best hydropower policy is analyzed across the 25,000 different plausible future scenarios.

Identification of Scenarios of Interest

A performance threshold differentiates between scenarios of interest and those of lesser importance. For the Zambezi River Basin, defining the threshold at the 75th percentile is assumed to capture the most critical scenarios in terms of performance for each objective value. Additionally, scenarios that cause the system to fail across all three objectives are defined as overall failure scenarios.

The focus on system failure is imagined to uncover conditions under which the system exhibits suboptimal performance, thereby identifying potential system vulnerabilities and conditions that require adaptation. For instance, under the Best Hydropower policy, a clear difference in performance outcomes between scenarios deemed successes and failures is observed. Specifically, the mean sum of annual hydropower deficit in terawatt hours for failed scenarios is approximately 21.80 TWh, compared to 14.37 TWh for successful ones. Moreover, environmental and irrigation objectives similarly reflect differential impacts. In terms of environmental flow, failed scenarios show a squared flow deficit between target and actual flows of about 4.56 million m^3/s , which reduces to approximately 3.18 million m^3/s in successful scenarios. For irrigation, the squared differences between targeted and actual values are 2.16 in failures versus 2.02 in successes. Scenarios of interest are visualized in Appendix D.1.

5.4.1 Defining Signpost Conditions

System vulnerabilities are identified using Feature Scoring and PRIM. Feature Scoring is used to identify the most critical uncertainty factors. Afterward, PRIM is used to assess which uncertainty combinations the system is most vulnerable to. Together, this hints at Signpost Conditions that cause system performance gaps.

Feature Scoring

Feature scoring allows us to determine the influence of uncertainty factors on model outcomes. High-importance values highlight factors that significantly impact outcomes of interest. Scores were determined for each objective across all four selected policies.

Results are captured in Figure 5.7. Preliminary analysis for the Best Hydropower policy suggests:

- The mean precipitation multiplier displays high influence across all objectives. It indicates a critical role for hydropower, environmental, and irrigation objectives.

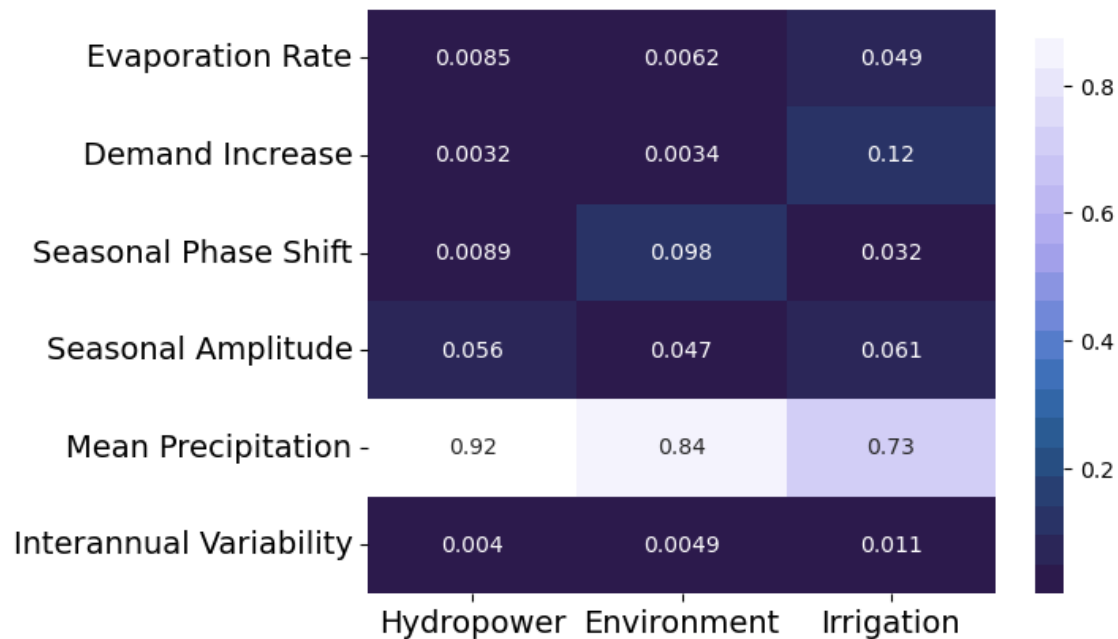


Fig. 5.7 Feature Scoring Heatmap for Best Hydropower Policy. The heatmap displays the importance of uncertainty factors in relation to the objective outcomes, with lighter colors indicating higher importance.

- The Second most influential uncertainty factors are objective dependent, with seasonal amplitudes significant for hydropower generation, shifting seasonality for environmental minimum flows, and uncertainties capturing irrigation demand for irrigation.

Overall, changes in precipitation is consistently the most important factor across all objectives. It indicates its critical role in the pluvial Zambezi River Basin. Other uncertainties, like demand multipliers, seasonal amplitudes, and phase shifts, exhibit variability in their importance depending on the specific objective.

PRIM

The PRIM analysis serves as a critical subsequent step to feature scoring, which identified changes in precipitation as the most dominant factor. The PRIM analysis dives deeper into the system's complexities, exploring how combinations of uncertainty factors contribute to defining critical scenarios. This allows for identifying more accurate and reliable conditions that describe scenarios where single factors alone do not fully capture the dynamics leading to system failure.

PRIM is employed to identify precise combinations of signpost conditions for each policy across the different sets of interest. Several scenario boxes are highlighted in Figure 5.8. Each box, represented by a scatter dot, can be understood as a narrative that describes scenarios characterized by certain uncertainty factors that lead to high

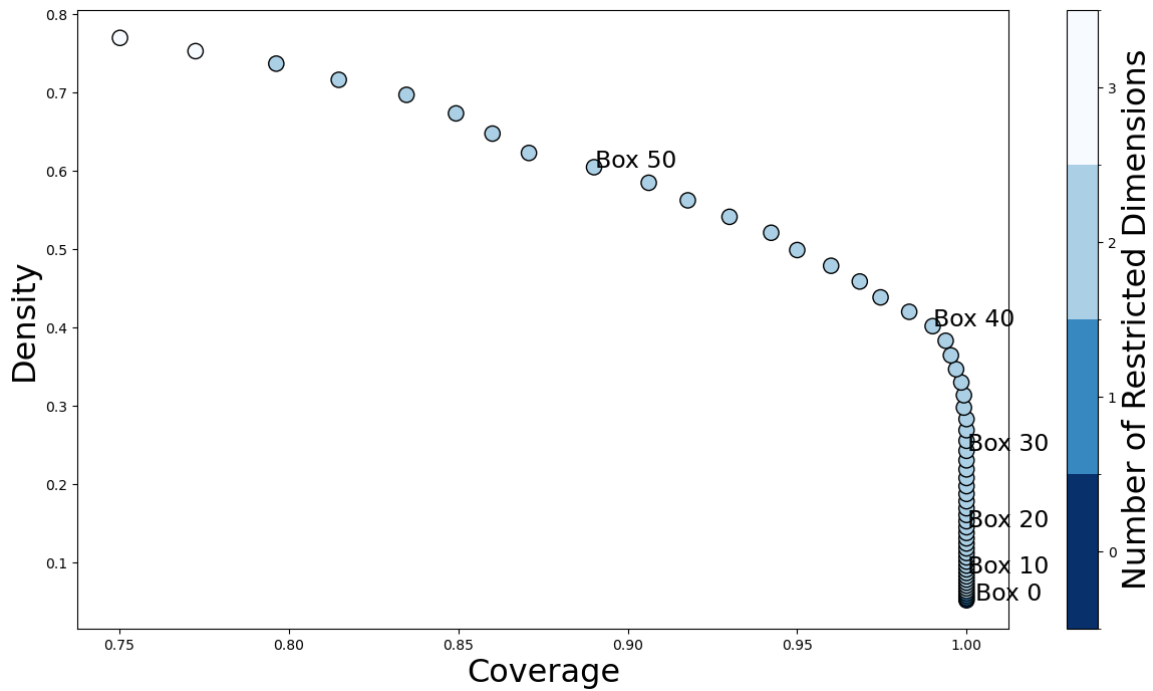


Fig. 5.8 PRIM Density - Coverage Tradeoff Plot. Each scatter dot represents a scenario box described by uncertainty factors. The color coding indicates the total number. Density displays how accurate the box is in identifying failure scenarios. Coverage indicates how reliable the scenario box is in covering all failure scenarios.

hydropower deficits. A box with high coverage and high density should be selected to infer appropriate signpost conditions. This ensures that signpost conditions effectively describe a wide range of scenarios of interest while being mainly exclusive to those scenarios.

For instance, Figure 5.8 shows that as the plot progresses from Box 50 toward Box 30, there is an increase in coverage but a decrease in density. This suggests a broader but less accurate scenario identification. Factors that describe these boxes are analyzed according to their density coverage tradeoff.

The focus is placed on high-coverage, high-density boxes to identify sets of Signpost Conditions. These represent scenarios where specific, narrowly defined conditions influence a wide range of outcomes of interest. This is valuable since it highlights critical conditions, pinpoints general vulnerabilities within the system, and thus informs accurate and reliable signpost conditions.

Scenario boxes are analyzed for their density-coverage tradeoff to identify Signpost Conditions that can describe system failure accurately and reliably. Table 5.2 summarizes information about several scenario boxes. The tradeoff is depicted by the Coverage and Density column. The subsequent three columns display combinations of

Table 5.2 Best Hydropower Policy Analysis for Hydropower Deficit Scenario

| Box ID | Coverage | Density | Uncertainty Factor | Min | Max |
|--------|----------|---------|--|-----------------------|-----------------------|
| 1 | 1.00 | 0.05 | m_{C1} | 0.80 | 1.18 |
| 5 | 1.00 | 0.07 | m_{C1} | 0.80 | 1.14 |
| 10 | 1.00 | 0.09 | m_{μ} m_{C1} | 0.90 0.80 | 1.04 1.00 |
| 20 | 1.00 | 0.15 | m_{C1} m_{μ} | 0.90 0.80 | 0.96 1.14 |
| 40 | 1.00 | 0.40 | m_{C1} m_{μ} | 0.90 0.80 | 0.93 1.10 |
| 58 | 0.75 | 0.77 | m_{C1} m_{μ} δ_{evap} | 0.90 0.80 -5.09 | 0.92 1.01 40.00 |

critical uncertainties and their value ranges. Min and Max's values are not considered but included for completeness³ but displayed for completeness.

- The seasonal amplitude is, as a baseline signpost condition, necessary to achieve high coverage values. This adds more insights into the critical influence of the mean precipitation; see Section 5.4.1.
- However, seasonal amplitude alone is not sufficient to accurately identify scenarios of high hydropower deficit.
- Only in addition to mean precipitation and evaporation rate, higher density values are achieved; see box 58 in Table 5.2.

Seasonal amplitude, mean precipitation, and evaporation rates should be considered signpost conditions. Together, these uncertainty factors are sufficient to describe 75 percent of scenarios where hydropower generation results in high deficits with an accuracy of 77 percent.

5.4.2 Quantification of Adaptation Tipping Points

Adaptation Tipping Point Thresholds are quantified using a logistic regression model. This model predicts system failure or success based on the previously defined set of Signpost Conditions. The critical boundary condition established by this model defines the policy's Adaptation Tipping Point Thresholds, delineating the uncertain conditions

³PRIM focus is to identify combinations of signpost conditions. These combinations do not include parameter ranges. Those are determined in the subsequent step using a logistic regression model

under which the system will likely fail or succeed. Finally, thresholds are quantified into an Adaptation Tipping Point, which results in new streamflow patterns that describe conditions necessitating the policy to change.

Logistic Regression

The logistic regression model takes the three Signpost Conditions of the mean precipitation change, seasonal amplitude, and evaporation as predictors. It allows policymakers to pinpoint boundary conditions at which the probability of system failure changes promptly. This boundary is interpreted as an Adaptation Tipping Point Threshold. It signifies areas in the uncertainty space where minor variations could disproportionately affect system performance.

The analysis used the `statsmodels` library in Python for model building. It added an intercept to the Open Exploration dataset, selected Signpost Conditions, and fitted the logistic regression model. The model fitness is examined using McFadden's pseudo- R^2 . Results display an unusually high Pseudo R-squared value for logistic regression of 0.8711. This indicates that chosen Signpost Conditions perfectly or nearly perfectly predict the outcomes of hydropower failure or success.

- Mean precipitation multiplier has the strongest negative coefficient. It suggests that a decrease in precipitation increases the probability of hydropower outcomes displaying high deficits. The substantial magnitude of the coefficient points to its critical impact.
- Similarly, an increase in seasonal amplitude leads to a higher risk of high hydropower deficit values. Its impact is less pronounced than that of mean precipitation.
- Increase in delta evaporation correlates with a higher likelihood of high hydropower deficit outcomes.
- The model can perfectly predict 0.86 of observations. This might indicate complete quasi-separation, indicating the model being overfitted to the Best Hydropower policy.

Identification of Adaptation Tipping Point Thresholds

The regression model identifies boundary conditions within the uncertainty space that differentiate success and failure scenarios. Figure 5.9 focuses on the three primary Signpost Conditions, displaying the relationship between two, with the third held at its mean value as a base condition. Plotted scenario data is scoped down to mean precipitation scenarios ranging from 0.9 to 0.95, deliberately focusing on critical regions where hydropower deficits become increasingly likely. It allows a more thorough analysis of the boundary conditions. A contour plot across the whole uncertainty space can be found in Appendix E.1.

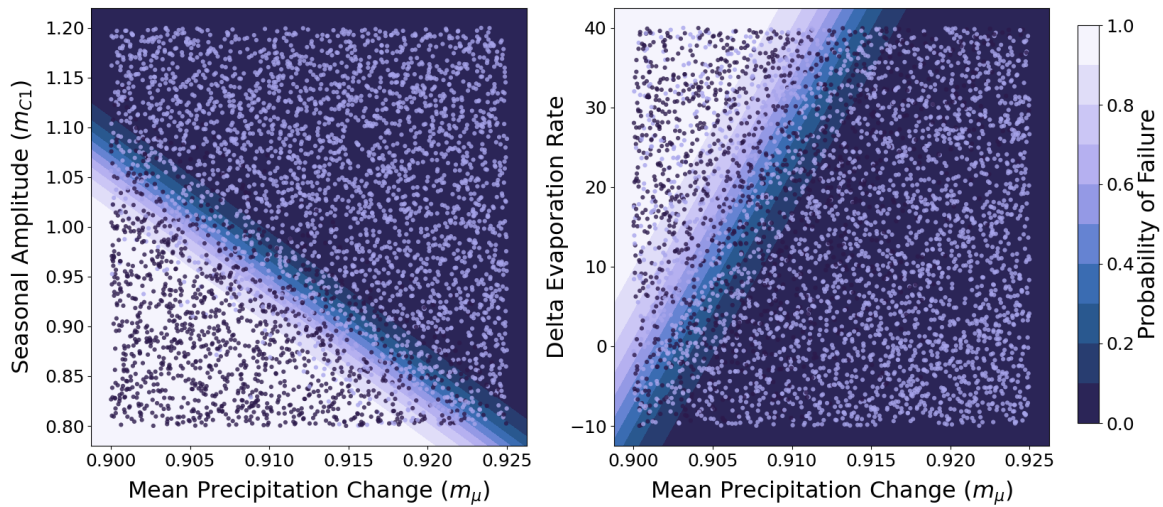


Fig. 5.9 Logistic Regression Contour Plot for Best Hydropower Policy. The probability of policy failure is shown across three signpost conditions. The contour line color indicates failure probability, with lighter shades representing higher risks. Dark dots describe policy failure.

The contour plots in Figure 5.9 display the scenario outcomes as dots, with colors indicating success or failure states. The logistic regression model defines the probability of success across varying levels of Mean Precipitation Change and Seasonal Amplitude in a) and of Mean Precipitation Change and Evaporation rate in subplot b). The following points detail the analysis:

- Most significant transitions from lower to higher probabilities of failure occur as the mean precipitation factor decreases below 0.92. Specifically, the region between values of 0.90 to 0.92 marks a critical decrease in hydropower reliability.

Adaptation Tipping Point Thresholds:

- For m_{μ} values above 0.925, failure probability remains below 20 percent.
- When m_{μ} falls below 0.925, failure probability sharply increases to over 60 percent, especially when Seasonal Amplitude is low ($m_{C1} < 0.90$).
- Higher Seasonal Amplitudes ($m_{C1} > 1.05$) significantly mitigate risks, reducing failure probabilities to below 40 percent even at the lowest precipitation levels.
- Lower Evaporation Rates below 0 decrease the failure probability to about 60 percent with m_{μ} at 0.9, showing less impact than Seasonal Amplitude.
- Evaporation Rates above zero show a clear gradient of increased failure probability, highlighting heightened sensitivity to these conditions.

Quantification of Adaptation Tipping Points

Visual analysis has delineated Adaptation Tipping Point Thresholds likely to result in high performance deficits. These thresholds are translated into actionable system variables. Using the statistical manipulation of streamflow data, introduced in Section 5.2.1, thresholds are converted into actual streamflow patterns ⁴.

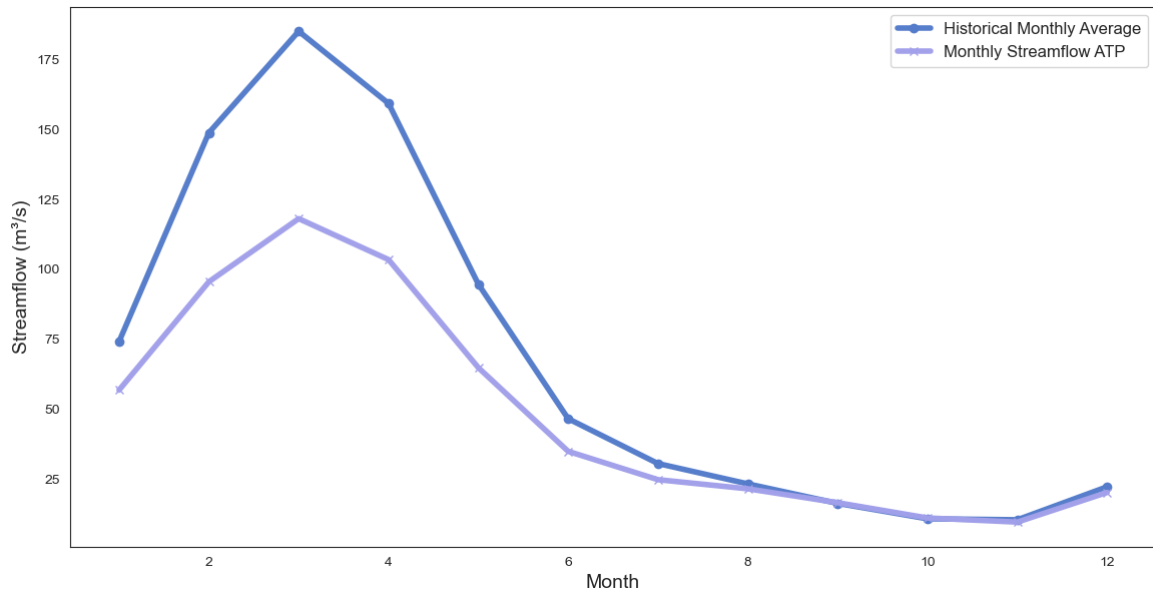


Fig. 5.10 Comparison of Monthly Average Streamflow and Adaptation Tipping Point for the Kafue Flats catchment. The monthly streamflow Adaptation Tipping Point indicates the upper limit of the generated streamflow patterns. Once actual streamflow data falls below this graph, the Best Hydropower policy should adapt.

For illustrating purposes, the generated streamflow patterns for the Kafue Flats are analyzed to understand the system's Adaptation Tipping Point. As shown in Figure 5.10, the identified Adaptation Tipping Point manifests a decrease, averaging an annual decrease of 199 m³/s from historical levels. It translates to an overall reduction of 24,2 percent annually. These reductions are particularly severe during the wet season. For instance, March, a month with historically high flows, records an absolute decrease of 67.11 m³/s or 36.24 percent. Table 5.3 provides detailed changes per month.

Key observations include:

- Pronounced streamflow reductions from February to April, exceeding 35 percent, signal crucial months that traditionally contribute to reservoir replenishment and peak power generation.

⁴Changes in evaporation rate are not considered, as translating these into direct temperature changes is challenging and extends the scope of this thesis. Thus, while recognized as a Signpost Condition, evaporation is not leveraged to describe an Adaptation Tipping Point

- The identified streamflow pattern indicates a critical flow reduction, which, if realized, would necessitate policy adaptation measures.

Table 5.3 Monthly average streamflows for the KafueFlats catchment comparing historical data with monthly streamflow values that describe the Adaptation Tipping Point for Best Hydropower policy in regard to hydropower generation.

| Month | Historical | ATP Condition | Abs. Decrease | Pct. Decrease |
|-----------|------------|---------------|---------------|---------------|
| January | 74.03 | 56.67 | 17.35 | 23.44 |
| February | 148.84 | 95.47 | 53.37 | 35.86 |
| March | 185.19 | 118.08 | 67.11 | 36.24 |
| April | 159.36 | 103.41 | 55.95 | 35.11 |
| May | 94.61 | 64.71 | 29.91 | 31.61 |
| June | 46.43 | 34.74 | 11.68 | 25.17 |
| July | 30.37 | 24.59 | 5.78 | 19.02 |
| August | 23.10 | 21.33 | 1.77 | 7.65 |
| September | 16.11 | 16.35 | -0.24 | -1.47 |
| October | 10.59 | 10.89 | -0.30 | -2.83 |
| November | 10.23 | 9.40 | 0.82 | 8.06 |
| December | 22.05 | 20.03 | 2.02 | 9.17 |

Once Signpost Conditions are identified and Adaptation Tipping Points quantified, resulting streamflow patterns provide a clear metric for policymakers to effectively communicate policy vulnerabilities and critical thresholds to stakeholders, facilitating informed decision-making under deep uncertainty.

Additionally, resulting streamflow patterns could enhance the development of new adaptive policies. By incorporating these patterns as input data, a subsequent EMODPS run could uncover optimal operational strategies tailored to adaptation tipping points. This process hinges on the global approximators' tendency to overfit, which, in this context, ensures that the derived policy functions are closely aligned with the newly identified streamflow scenarios.

Summary

The Section demonstrated Robustness Analysis to enhance adaptive policy design for the Zambezi River Basin.

Initially, the Zambezi EMODPS model identified epsilon non-dominated Pareto-optimal operation strategies. Quality assessments confirmed optimization's convergence, ensuring optimal results. Subsequent analyses highlighted tradeoffs, particularly between hydropower and environmental goals. Furthermore, clustered policy outcomes indicate preferences for either hydropower or irrigation objectives.

Afterward, key uncertainties were characterized, including the identification of Uncertainty Drivers. Those were effectively translated into quantifiable model factors of mean precipitation change, interannual variability, seasonal amplitudes, seasonal shifts, evaporation rates, and irrigation demand.

Next, multiple states of the world were generated. Based on their optimal performance and tradeoff capabilities in the base case, four policies were simulated across 25,000 uncertainty conditions, resulting in 100,000 scenarios. Results showcased substantial tradeoffs with policies showing varying degrees of robustness and vulnerability. Notably, no single policy excelled across all scenarios and objectives.

The following Scenario Discovery identified Signpost Conditions under which the Best Hydropower policy fails. Critical conditions were isolated using a combination of performance thresholds, Feature Scoring, and PRIM. A logistic regression model was established. The regression model helped identify Adaptation Tipping Point Thresholds by highlighting the probabilities of system failure, thereby defining the system's boundary conditions. Thresholds were translated into streamflow patterns that describe the Adaptation Tipping Point for the Best Hydropower policy in the Zambezi River Basin. Ultimately, this allows for better communication and subsequent development of new better suited policies.

Key insights concerning the Best Hydropower policy are:

Signpost Conditions:

- Mean precipitation change (m_μ)
- Seasonal amplitude (m_{C1})
- Evaporation rate (δ_{evap})

Adaptation Tipping Point Thresholds:

- Mean Precipitation $m_\mu < 0.925$.
- Seasonal Amplitude $m_{C1} < 1.05$.
- Evaporation Rate $\delta_{evap} > 15$.

Adaptation Tipping Point:

- Annual streamflow reduction of 24.2 percent.
- Absolute streamflow decrease of 199 m³/s.
- February, March, and April are critical months with over 35 percent of streamflow decrease.

Chapter 6

Results

This Section presents results according to the sub-research questions. First, the main uncertainties in the Zambezi River Basin are presented. Second, critical system vulnerabilities across four policies are analyzed to identify Signpost Conditions. Subsequently, the results linked to the identified Adaptation Tipping Points are displayed.

6.1 Key Uncertainties in the Zambezi River Basin

The non-systematic literature review concluded with 263 papers. Additional keywords filtered these, focusing on papers that directly relate to the spatial and temporal scope of the Zambezi region. Afterward, the total number was distilled to a manageable amount, assessing relevance. With a subsequent forward and backward citation search, 26 key peer-reviewed articles formed the foundation of the qualitative uncertainty characterization.

The reviewed literature consistently highlights river basins as complex systems marked by Deep Uncertainty. Mainly, hydroclimatic and socio-economic factors emerged as pivotal due to their profound impact on system performance.

6.1.1 Hydroclimatic Uncertainties

Climate change introduces significant uncertainties into hydrological assumptions critical for river basin management. The impacts on Africa's hydrology create unpredictable effects for river basins. Studies by Maharjan and Issahaku (2014) and Kusangaya et al. (2014) highlight challenges posed by climate change. They emphasize altered ecological and hydrological dynamics across river basins. The work of Beilfuss et al. (2012) and Kling et al. (2015) further validate these concerns, highlighting the vulnerability of the Zambezi River Basin as one of the hardest hit by climate change.

Further, Desanker and Justice (2001) projects a temperature rise of 1.5-3°C by mid-century, with precipitation patterns potentially decreasing by 10-30 percent (Desanker

and Justice, 2001; Kling et al., 2015; Kusangaya et al., 2014). Hulme et al. (2001) and Shongwe et al. (2009) report increased inter-annual variability, with precipitation during the wet season decreasing by 31-35 percent and the dry season by one percent. Beilfuss et al. (2012) anticipates a 15-25 percent increase in extreme flooding events.

Conclusively, the most critical hydroclimatic uncertainties are altered precipitation patterns, interannual variability, seasonal shifts, and temperature increases.

6.1.2 Socio-economic Uncertainties

Socio-economic uncertainties in the Zambezi River Basin primarily stem from unpredictable water demand factors. Fluctuating development trajectories, population growth, and macroeconomic policies are key drivers. Hughes and Farinosi (2020) and Hughes et al. (2020) have observed that these factors significantly complicate strategic planning. For instance, they expect the population to increase by up to 50 percent by 2050. Additionally, they estimated that irrigation water demand could increase by 30-50 percent because of enhanced food security.

Furthermore, the literature highlights the increasing conflict between surging demand and decreasing supply. Hulme et al. (2001) project the Zambezi River Basin to face decreasing water availability by up to 15 percent. For instance, Beilfuss et al. (2012) and Kling et al. (2015) project 10-25 percent reductions in hydropower generation due to decreased river flows and increased evaporation rates. Additionally, Maharjan and Issahaku (2014) anticipates irrigation declines despite the projected increase in demand.

Given these dynamics, uncertainties surrounding the development of irrigation water demand in the Zambezi River Basin are seen as the most relevant socio-economic uncertainty.

It is concluded that the most prominent uncertainties within the Zambezi River Basin are precipitation changes that might decrease by up to 30 percent. Interannual variability is expected to affect the wet season mainly. Additionally, seasons are expected to shift up to a month. Moreover, temperature increase and irrigation demand are additional uncertainties relevant to the Zambezi River Basin. Table 6.1 summarizes the six identified Uncertainty Drivers.

Table 6.1 Summary of Deep Uncertainty Trends within the Zambezi River Basin

| Uncertainty | Estimations | Source |
|---------------------------------|---|--|
| Precipitation Changes | Mean Decrease 10-30% by 2050 | Kusangaya et al. (2014) |
| | Mean Decrease 15-25% | Desanker and Justice (2001) |
| | Mean Decrease 10-20% | Kling et al. (2015) |
| | Decrease by 20% | Hulme et al. (2001) |
| | Decrease by 10-15% | Hulme (2005) |
| | Decrease by up to 10% | Shongwe et al. (2009) |
| Inter-annual Variability | Precipitation Decrease: | |
| | Wet Season (31-35%) | Shongwe et al. (2009) |
| | Dry Season (1%) | Shongwe et al. (2009) |
| | Increased precipitation extremes | New et al. (2006), Tadross et al. (2005), Beilfuss et al. (2012) |
| Seasonality Shift | Increased variability by $\pm 25\%$ | Hulme et al. (2001) |
| | One month shift | Shongwe et al. (2009) |
| | Seasonal rainfall shift 15 days earlier | Hulme et al. (2001) |
| Temperature Increase | 1.5-3°C rise by mid-century | Desanker and Justice (2001) |
| | Increase of 1.5-3°C | Desanker and Justice (2001) |
| Population Growth | Increase by 50% by 2050 | Hughes and Farinosi (2020) |
| | Increase by 30-50% by 2050 | Hughes et al. (2020) |
| Irrigation Demand | 25% increase in water withdrawals | Kusangaya et al. (2014) |

6.2 Critical Signpost Conditions for the Zambezi River Basin

To improve the adaptive policy structure, it is critical to identify system vulnerabilities and define adaptation tipping points the policy under consideration. It necessitates a thorough understanding of how various uncertainty factors impact the operational viability of specific policies. Robustness analysis is applied to analyze these influences. Critical uncertainty factors that describe conditions under which policymakers should consider adapting to new operational strategies to optimize performance are identified as signpost conditions. Results evaluate four distinct policies: Best Hydropower, Best Environment, Best Irrigation, and Best Tradeoff. It begins with the outcomes from feature scoring, followed by the findings from the PRIM analysis.

6.2.1 Feature Scoring

Feature Scoring results are summarized in a comprehensive heatmap in Figure 6.1. It categorizes the impact of various uncertainty factors across the specific policies, each aimed at optimizing system performance. Heatmap's color gradient—dark to light—illustrates the importance of uncertainty factors, with lighter colors indicating higher importance.

Uncertainty Factor Influence Across Policies

A comparative analysis of how each uncertainty factor impacts the different policy objectives across all policies shows that the mean precipitation multiplier is the most influential and dominant uncertainty factor. Other factors, such as phase shifts, demand multipliers, and seasonal amplitude, show a minor influence on objectives.

- **Mean Precipitation** is dominant across all policies, with importance scores typically above 0.65, highlighting its critical role in managing hydropower generation, environmental flows, and irrigation needs. It shows slightly more consistent influence in the Best Environment and Best Tradeoff policies than Best Hydropower and Best Irrigation, suggesting its pivotal role across varying policy focuses.
- **Seasonal Phase Shift** shows variable influence, with relatively high impacts on irrigation objectives (up to 0.15 in Best Irrigation). It suggests that current irrigation practices are highly dependent on seasonal patterns—lesser but notable effects in environmental management, suggesting impacts on ecological processes and flow timings.
- **Seasonal Amplitude**: Moderately influential, especially in Hydropower and Irrigation, with scores indicating its role in managing seasonal water availability, which seems crucial for power generation and agricultural cycles. Less pronounced in Environmental policies, indicating a more minor role in affecting ecosystem-dependent water levels.

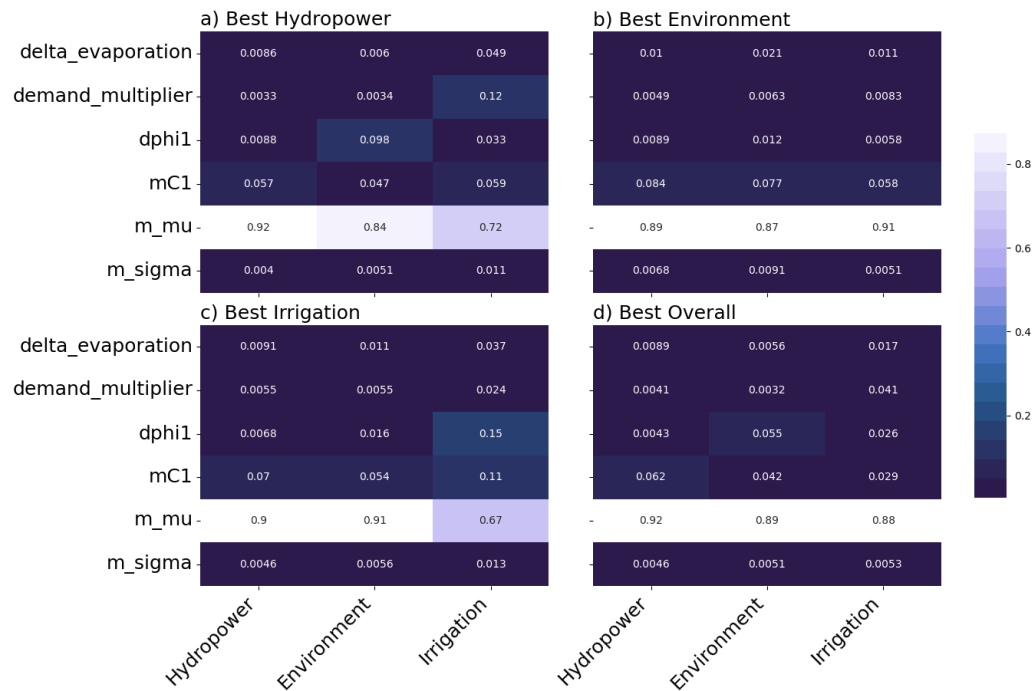


Fig. 6.1 Feature Scoring Summary across Four Policies. The heatmap displays the importance of uncertainty factors in relation to the objective outcomes, with lighter colors indicating higher importance.

- **Evaporation Rate** has lower influence across all policies. Notably, it mostly affects the irrigation outcomes, with scores up to 0.049 under the Best Hydropower policy. Given the Best Environment policy, evaporation rates also indicate a higher influence on environmental minimum flows.
- **Demand Multiplier** shows the highest impact in irrigation (up to 0.041), where changes in water demand directly influence agricultural water use. Minimal influence on hydropower and environmental objectives, indicating that fluctuations in water demand do not heavily alter outcomes in these areas.
- **Interannual Variability**: Consistently low influence across all policies, with scores typically below 0.01, suggesting that year-to-year variability has a minimal direct impact on the immediate operational decisions in hydropower, environment, and irrigation.

Uncertainty Factor Influence Under Specific Policy

The adaptive policy structure depends on the chosen policy. Thus, the following presents a more specific analysis of the four policies.

Best Hydropower Policy: The mean precipitation multiplier seems to be the most influential and dominant uncertainty factor. While other factors such as phase shifts,

demand multiplier, and seasonal amplitude show minor influence on objectives, the change in mean precipitation emerges as the critical Signpost Condition.

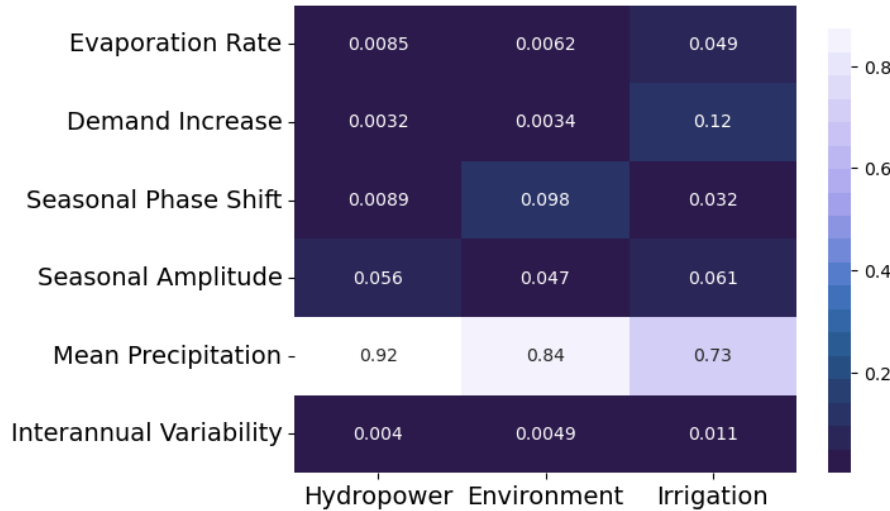


Fig. 6.2 Feature Scoring Heatmap for Best Hydropower policy. The heatmap displays the importance of uncertainty factors in relation to the objective outcomes, with lighter colors indicating higher importance.

- **Predominance of mean precipitation**

- Mean precipitation shows dominant influence across all objectives, scoring 0.92 for Hydropower, 0.84 for Environment, and 0.73 for irrigation.
- It indicates that changes in precipitation significantly affect the policy outcome, making it a critical Signpost Condition for policy adaptation.

- **Small influence of seasonal phase-shift and demand multipliers**

- Seasonal phase shifts show the highest importance for the environmental objective, with a score of 0.098. It emphasizes the challenges of meeting current minimum flow requirements under shifting seasonality.
- The demand multiplier notably affects the Irrigation objective with a score of 0.12, indicating its influence in adjusting to changes in water demand for agricultural use.

- **Minor impact of other uncertainty factors**

- Seasonal amplitudes exhibit a slightly more pronounced impact on hydropower (0.057) and Irrigation (0.059) objectives compared to the environment (0.047).
- Despite some impact, most factors like evaporation and interannual variability play minimal roles compared to mean precipitation changes, with low influence scores across the board.

Best Environment Policy: The mean precipitation continues to be of the highest influence across all objectives. In particular, its influence is more consistent across the three objectives. In contrast, other factors like seasonal phase shifts and demand multipliers show reduced influence, highlighting their lesser importance in shaping environmental outcomes than hydropower or irrigation policies.

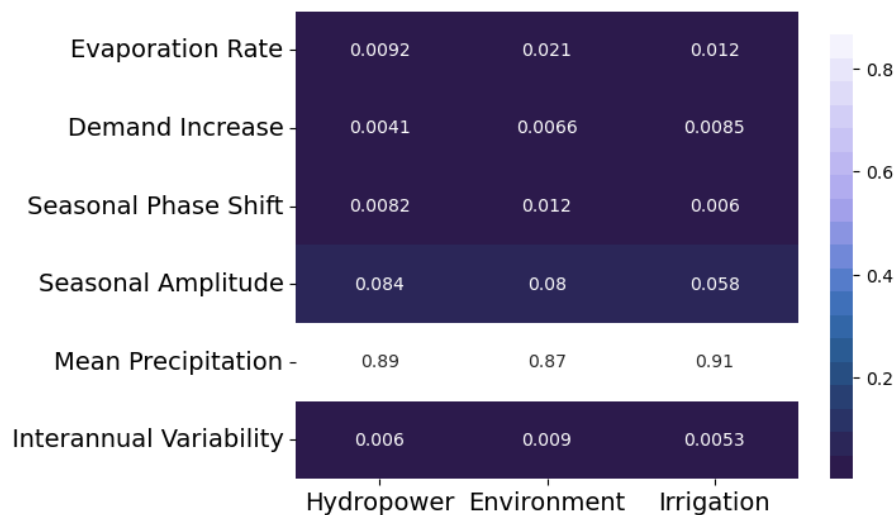


Fig. 6.3 Feature Scoring Heatmap for Best Environment policy. The heatmap displays the importance of uncertainty factors in relation to the objective outcomes, with lighter colors indicating higher importance.

- **Mean precipitation consistently dominant**
 - Mean precipitation shows more consistent influence across all objectives, scoring 0.89 for Hydropower, 0.87 for Environment, and 0.91 for irrigation.
 - It indicates that under the Best Environment policy, objectives depend even more on changes in precipitation compared to Best Hydropower.
- **Increased influence of the seasonal amplitude**
 - While not as dominant as precipitation, seasonal amplitude changes show increased significance with relatively high scores of 0.084 for hydropower and 0.077 for environment.
 - This factor’s heightened relevance in the environmental policy suggests its effect on seasonal water availability and flow.
- **Other factors have low influence**
 - Despite their roles, other factors such as demand multipliers and delta evaporation score lower, indicating a lesser impact on the policy’s outcomes.
 - In particular, seasonal phase shift and demand increase loss influence respective to environmental and irrigation objectives.

Best Irrigation Policy: The feature scoring for the Best Irrigation policy shows a pattern where mean precipitation remains a dominant factor, much like in the Best Hydropower policy, but with an increased influence from seasonal amplitudes and phase shifts.

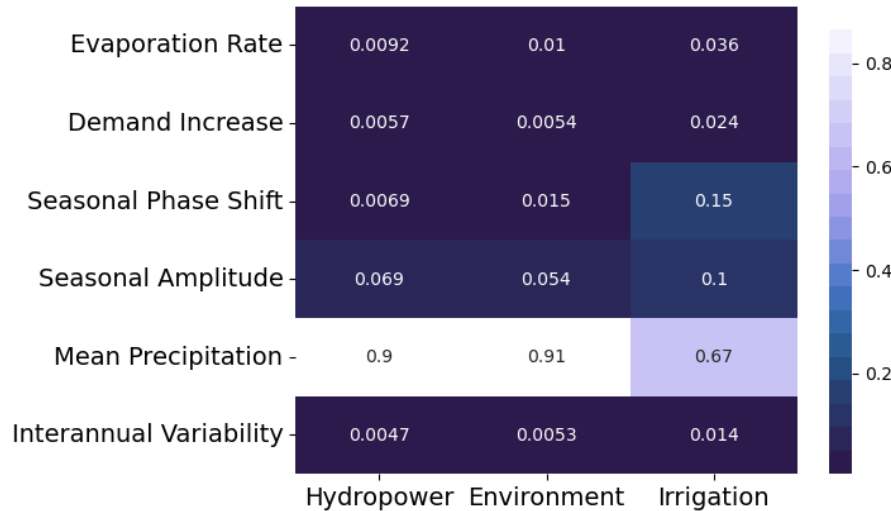


Fig. 6.4 Feature Scoring Heatmap for Best Irrigation policy. The heatmap displays the importance of uncertainty factors in relation to the objective outcomes, with lighter colors indicating higher importance.

- **Mean precipitation dominant but variable**

- Similar to the Best Hydropower policy, mean precipitation is crucial, with scores of 0.90 for hydropower, slightly higher at 0.91 for environment, and lower at 0.67 for irrigation.
- While still highly influential, variability across these scores indicates a less consistent impact compared to its role in the Best Environment policy. It suggests that other factors play an important role in irrigation management.

- **More diverse influence on irrigation deficits**

- Seasonal amplitudes show a more pronounced effect in irrigation, with a relatively high score of 0.11 compared to 0.07 in hydropower and 0.054 in environment.
- Seasonal phase shift also emerges as more important for irrigation objectives, scoring 0.15, compared to its influence under the Best Hydropower (0.033) and Environment (0.0058) policies.

Best Tradeoff Policy: The mean precipitation is the most influential factor, indicating a consistently high influence across all objectives, similar to the Best Environment policy. Other factors have more objective specific influence.

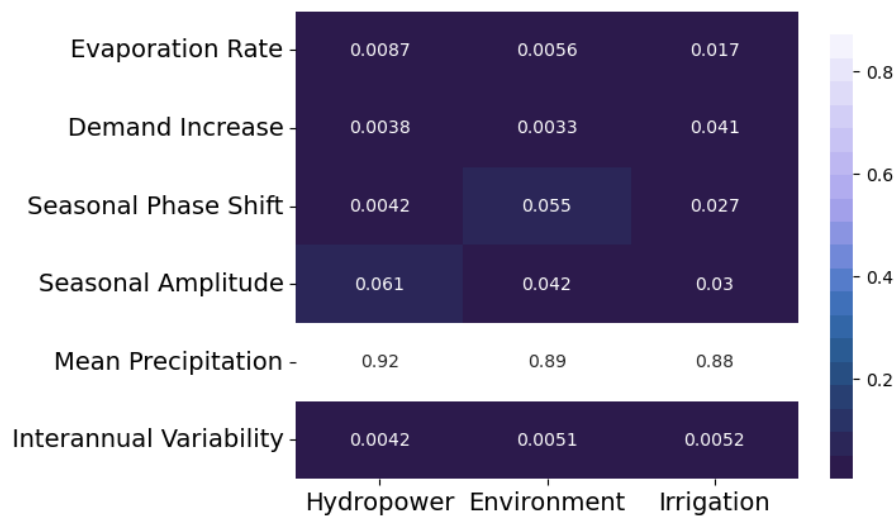


Fig. 6.5 Feature Scoring Heatmap for Best Tradeoff policy. The heatmap displays the importance of uncertainty factors in relation to the objective outcomes, with lighter colors indicating higher importance.

- **Mean precipitation consistently dominant**

- Mean precipitation shows similar influence under the Best Environment policy across all objectives, scoring 0.92 for Hydropower, 0.89 for Environment, and 0.88 for irrigation.
- It indicates that under the Best Tradeoff and Best Environment policy, objectives depend even more on changes in precipitation compared to the Best Hydropower and Best Irrigation policies.

- **Seasonal amplitudes and phase shifts with targeted impacts.**

- Seasonal amplitude impacts are moderate across all sectors, with its effects slightly more pronounced in Hydropower (0.062) and Environment (0.042).
- Seasonal phase shift shows the impact on the environment objective with a score of 0.055. It is lower than the Best Hydropower policy but much higher compared to the Best Environment and Best Irrigation policy, indicating that a seasonal phase shift is more critical for ensuring environmental minimum flows, especially under the influence of meeting hydropower demands.

Mean precipitation is the most dominant factor, and thus is considered a baseline Signpost Condition. In contrast, other factors like seasonal phase shifts and seasonal amplitudes show a relative variable moderate influence. Interannual variability consistently shows minimal impact across all policies, similar to the evaporation rate with minor influence under the Best Hydropower policy.

Table 6.2 Summary of Uncertainty Factors' Influence Across Policies

| Uncertainty Factor | Best Hydropower | Best Environment | Best Irrigation | Best Tradeoff |
|---------------------------|------------------------|-------------------------|------------------------|----------------------|
| Mean Precipitation | Variable High | Constant High | Variable High | Constant High |
| Seasonal Phase Shift | Moderate | Low | Moderate | Minor |
| Seasonal Amplitude | Minor | Minor | Moderate | Minor |
| Demand Increase | Moderate | Very Low | Low | Minor |
| Interannual Variability | Low | Very Low | Low | Very Low |
| Delta Evaporation | Minor | Low | Low | Low |

6.2.2 PRIM

This Section presents the results of the PRIM analysis conducted for the Zambezi River Basin, focusing on four key policies. The analysis aimed to identify critical combinations of Signpost Conditions under different scenarios of interest as outlined in Section 5.4. By employing PRIM, the study complements previous insights from feature scoring by focusing on critical combinations of uncertainty factors that render the basin vulnerable within these specific policy contexts.

Critical Signpost Conditions are defined based on their density-coverage tradeoff. Detailed tables can be found in the Appendix D.6. Conditions that describe high density-high coverage scenario boxes are taken as critical Signpost Conditions because:

High Density Box

- Ensures accurate identification of scenarios of interest.
- Scenarios within a box predominantly lead to system failures.
- Reduce the risk of false positives, guaranteeing that identified Signpost Conditions are precise and specifically target the failure scenarios.
- High-density Signpost Conditions prompt adaptation responses that are highly specific to system failures, crucial to avoid unnecessary adaptations.

High Coverage Box

- Ensures reliable identification of scenarios of interest.
- Signpost Conditions manage to capture all relevant combinations of uncertainty factors that lead to system failure.
- Reduce the risk of being unprepared for scenario conditions the system cannot handle without adaptation.
- High-coverage Signpost Conditions guarantee reliable insights important for effective adaptation.

Best Hydropower Policy

Under the Best Hydropower policy, performance gaps across all three objectives are apparent. Thus, critical uncertainty combinations are assessed across four scenarios: Hydropower, Environmental, Irrigation, and Overall deficit. Figure 6.8 displays the identified scenario boxes and reveals distinct density-coverage tradeoffs across the four scenario sets of interest. They differ in shape and the number of factors required to define these scenarios.

- **Hydropower Deficit:** As coverage increases from low to high, there is a noticeable and gradual decrease in density. This trend suggests that while broader Signpost Conditions can capture a larger array of scenarios, they also tend to include many that do not lead to system failure, diluting the accuracy of predictions.
 - Combinations of seasonal amplitude and precipitation changes are important to cover scenarios under which the Zambezi River Basin exhibits high hydropower deficits. They offer a good balance, with Box 50 covering 89 percent of scenarios and a density of 60 percent.
 - A More precise description is required, including evaporation rates. This leads to a coverage value of 0.75 with a density of 77 percent.
 - The combination of seasonal amplitude, precipitation changes, and evaporation rates is identified as the critical set of Signpost Conditions.
- **Environmental Deficit:** The density remains high and stable across a wide range of coverage until sharply dropping near full coverage. This pattern suggests that environmental deficit scenarios can be effectively captured with a simple set of uncertainty factors without significant loss of specificity until very broad conditions are considered.
 - Mean precipitation plays a single important role in defining scenarios of interest, identifying high-density, high-coverage scenario boxes with 92 percent coverage and 93 percent density.

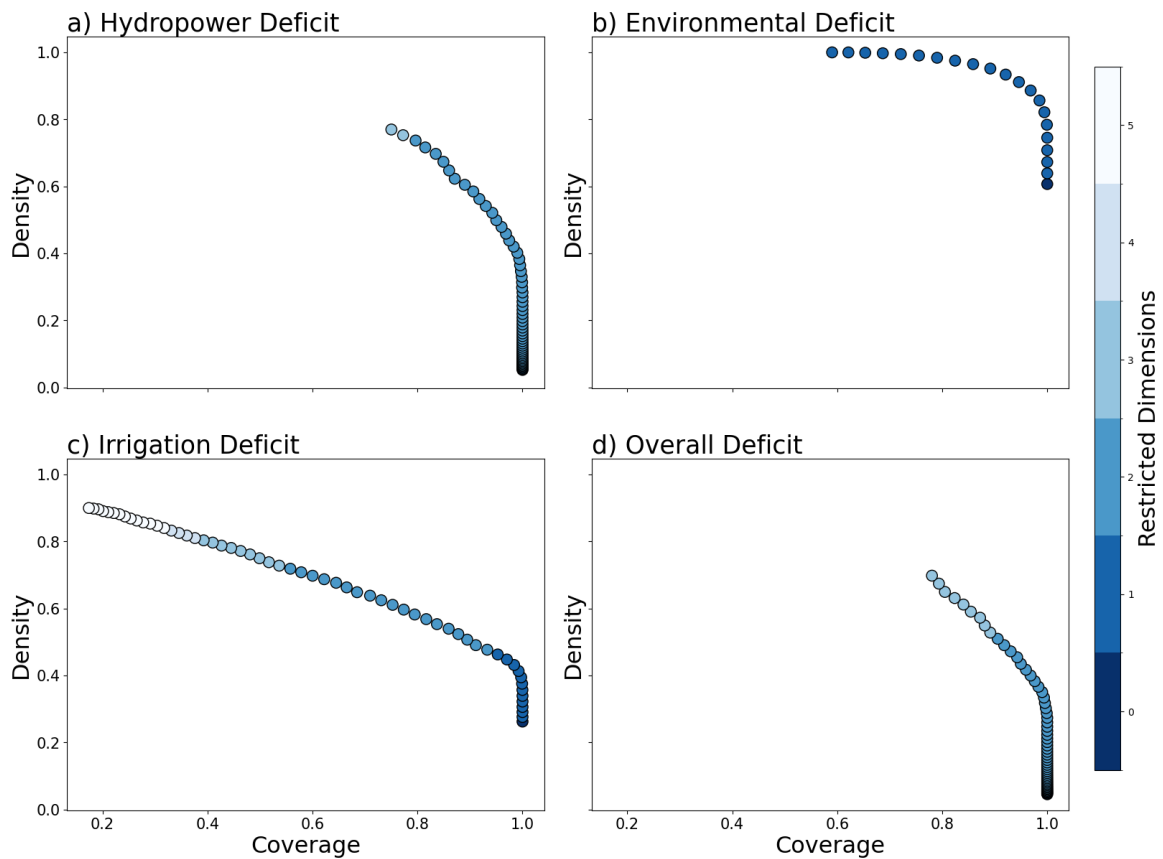


Fig. 6.6 Summary of PRIM Density - Coverage Tradeoff Plots for Best Hydropower Policy. Subplots describe the scenario of interest, which PRIM tries to describe under the Best Hydropower policy.

- It suggests that mean precipitation changes predominantly influence environmental deficits. Thus, it is identified as a Signpost Condition.
- **Irrigation Deficit:** The plot shows a consistent, linear decline in density as coverage increases. This suggests a more straightforward tradeoff between accuracy and comprehensiveness, indicating that expanding the Signpost Conditions to include more scenarios inevitably dilutes their specificity.
 - Mean precipitation, demand increase, and evaporation rates are critical for understanding irrigation deficits under the Best Hydropower Policy.
 - Unlike the simpler Environmental Deficit, the Irrigation Deficit involves multiple factors, indicating complex hydrological and socio-economic dynamics.
 - Box 50, with high density (0.87) and low coverage (0.25), offers precise but limited scenario coverage; Box 10, with the widest coverage (0.98) and lower density (0.43), is suitable for broad surveillance; Box 20, providing a balance

Table 6.3 Best Environment Policy Analysis for Hydropower and Irrigation Deficit Scenarios

| Hydropower Deficit Scenario | | | | | |
|-----------------------------|----------|---------|--------------------|------|------|
| Box ID | Coverage | Density | Uncertainty Factor | Min | Max |
| 1 | 1.00 | 0.60 | m_mu | 0.90 | 1.04 |
| 5 | 1.00 | 0.73 | m_mu | 0.90 | 1.02 |
| 10 | 0.96 | 0.91 | m_mu | 0.90 | 0.99 |
| 15 | 0.81 | 0.99 | m_mu | 0.90 | 0.97 |
| 20 | 0.63 | 1.00 | m_mu | 0.90 | 0.95 |
| Irrigation Deficit Scenario | | | | | |
| 1 | 1.00 | 0.78 | m_mu | 0.90 | 1.04 |
| 5 | 0.97 | 0.92 | m_mu | 0.90 | 1.02 |
| 10 | 0.81 | 0.99 | m_mu | 0.90 | 0.99 |
| 11 | 0.77 | 0.99 | m_mu | 0.90 | 0.96 |

with moderate coverage (0.79) and density (0.58), is optimal for reliable scenario identification, but lacks accuracy in describing system failure.

- Box 20, employing mean precipitation and increased irrigation demand, establishes critical Signpost Conditions for effective policy formulation.
- **Overall Deficit:** Panel d) in Figure 6.8 shows a pattern similar to the hydropower deficit, with density decreasing more noticeably as coverage increases. However, the decline starts sooner and is more gradual. Similar to hydropower deficit scenarios, the highest density values are around 80 percent. It suggests that around 20 percent of the overall failure scenarios cannot be explained.
 - The primary factor is a change in seasonal amplitudes that is sufficient to cover all failure scenarios.
 - To ensure better accuracy, mean precipitation and evaporation rates must be considered.
 - Scenario box 58 offers high density and coverage. It suggests that seasonal amplitudes, mean precipitation, and evaporation rates are good Signpost Conditions.

Best Environment Policy

The focus is solely on the hydropower and irrigation deficit scenarios. It is informed by the absence of severe environmental deficits within the worst 25 percent of outcomes under this policy, demonstrating its robustness in mitigating environmental challenges across all states of the world. Thus, there is no necessity to adapt the policy specifically for environmental outcomes and overall failure scenarios.

- Both scenarios of interest demonstrate nearly identical scenario conditions. It highlights the consistent impact of mean precipitation. This suggests a major vulnerability for the Best Environment policy. Policy preference for robust environmental objective outcomes and its underlying water allocation preference probably lead to the policy's single sensitivity of mean precipitation changes.
 - Precipitation is the single most important factor that appears consistently across all scenario boxes.
 - All scenario boxes achieve high density and coverage values, with relatively similar patterns between both scenarios of interest. Irrigation deficit scenarios, with higher density values from the onset, could be even more reliable and accurate.
 - Mean precipitation is the critical Signpost Condition for the Best Environment policy.

Best Irrigation Policy

Results concentrate on Signpost Conditions for the hydropower and environmental deficit scenarios due to the lack of significant irrigation deficit scenarios under the Best Irrigation policy. Like the Best Environment and Best Tradeoff policies, they showcase the policy's robustness in coping with a broad spectrum of potential future scenarios specific to the irrigation objective.

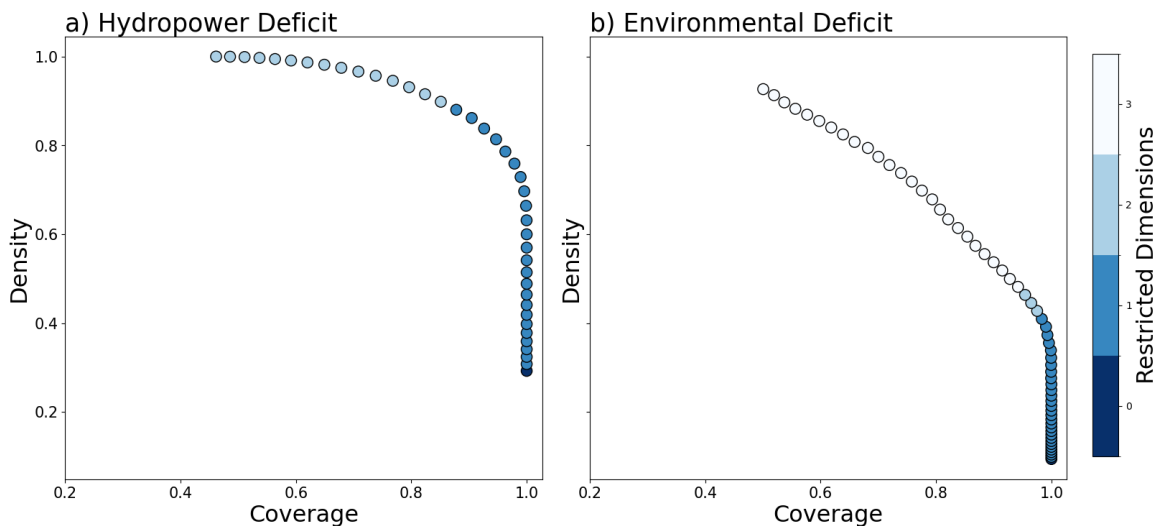


Fig. 6.7 Summary of PRIM Density - Coverage Tradeoff Plots for Best Irrigation Policy. Subplots describe the scenario of interest, which PRIM tries to describe under the Best Irrigation policy.

- **Hydropower Deficit:** The density-coverage tradeoff shows that high-density values are maintained until coverage reaches 60 percent. Beyond this point, there

is a drop in density as coverage increases to 100 percent. It indicates a more complex definition of scenarios of interest. Thus, while covering more scenarios with a broader set of Signpost Conditions is possible, the accuracy in identifying true deficit scenarios diminishes.

- Mean precipitation is the baseline Signpost Condition that is apparent in all scenario boxes.
- A combination of mean precipitation and seasonal amplitude is necessary to achieve better accuracy. For instance, while box 20 (coverage 0.96, density 0.79) is only described by the mean precipitation, box 25 provides better accuracy with a density value of 0.9, while coverage decreases to 0.85 when including seasonal amplitude.
- Mean precipitation and seasonal amplitude are critical Signpost Conditions.
- **Environmental Deficit:** Similar to the hydropower deficit, this plot shows a decrease in density with increased coverage. However, density begins to decrease almost immediately and continues steadily before it drops significantly at a coverage value of 0.9. The drop and higher number of uncertainty factors required for more accurate identifications suggest a more complex Signpost Condition for environmental deficit values.
 - Again, mean precipitation is a baseline condition that is necessary for high coverage. However, alone, it cannot provide an accurate definition of environmental deficit scenarios.
 - The same holds for the combination of mean precipitation and seasonal amplitude, only leading to density values around 0.43 for scenario box 30. It suggests a more complex Signpost Condition.
 - Adding the factor of seasonal phase shift allows for better accuracy, allowing an accuracy value of 0.72 and coverage of 0.76 in box 45.
 - Critical Signpost Conditions are described by the three factors of mean precipitation, seasonal amplitude, and seasonal phase shift.

Best Tradeoff Policy

The Best Tradeoff policy shows robust behavior in regard to irrigation deficit scenarios. Therefore, the adaptive policy structure has to be improved only when hydropower and environmental objectives are focused on. Both deficit scenarios show clear tradeoffs:

- Highest densities at lower coverage levels with hydropower deficit displaying a density of 0.95 at 55 percent coverage (Box 58), and environmental deficits showing a density of 1.00 at 43 percent coverage (Box 40). It indicates that specific Signpost Conditions might be too accurate to cover scenarios of interest, though too narrow to provide reliable scenario identification.

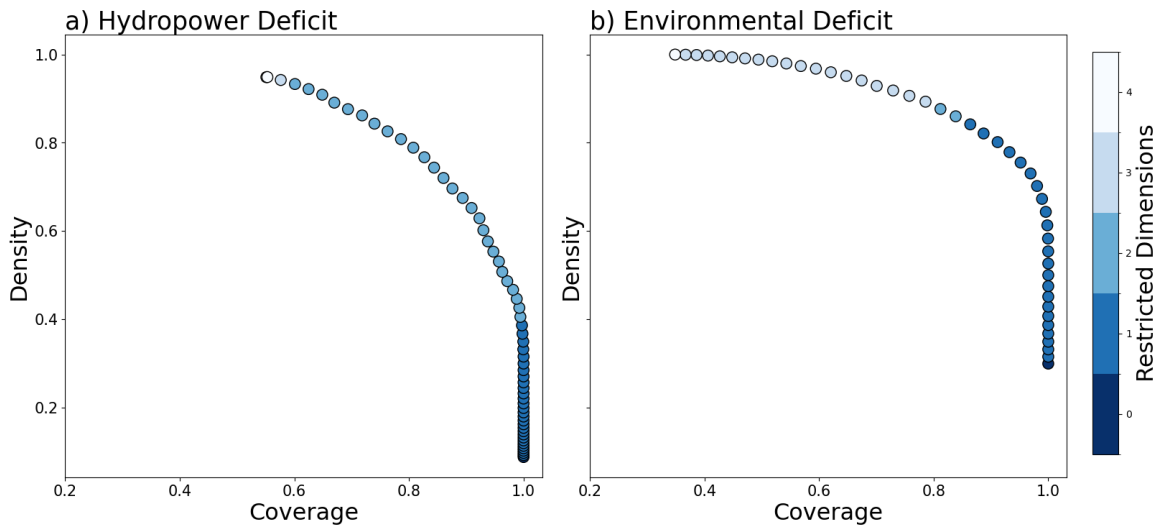


Fig. 6.8 Summary of PRIM Density - Coverage Tradeoff Plots for Best Tradeoff Policy. Subplots describe the scenario of interest, which PRIM tries to describe under the Best Tradeoff policy.

- As coverage increases, density declines. It suggests that scenarios of interest are vulnerable to more diverse conditions, making it challenging to identify suitable Signpost Conditions.
- The rate of decline differs, with the hydropower deficit experiencing a steady decrease, whereas the environmental deficit maintains a higher density (around 0.9) until about 0.8 coverage. This hints at more specific Signpost Conditions that maintain predictive accuracy over a broader range.
- For hydropower deficits, scenario boxes between 45 and 50 display a good tradeoff of accurate and reliable scenario definition. Thus, Signpost Conditions are mean precipitation and seasonal amplitude.
- Environment deficit scenarios can be defined by the single Signpost Condition of mean precipitation with accuracy and reliability above 80 percent (box 25).

In summary, each policy was analyzed according to its performance gaps across multiple scenarios of interest. Identified Signpost Conditions are summarized in Table 6.4. Precipitation is a consistent factor across all policies. This underscores its pivotal role in meeting diverse policy objectives. It further aligns with feature scoring results that emphasize its significance. However, unlike the Best Environment Policy, which depends solely on precipitation, other policies require additional factors for a comprehensive understanding of potential failures. This suggests that while precipitation is critical, it is often insufficient alone to describe all potential deficits precisely.

Multiple factors are generally necessary to accurately predict policy failures. Seasonal amplitudes frequently complement precipitation in policies like Best Irrigation and Best

Table 6.4 Summary of Signpost Conditions for Each Policy Scenario

| Policy | Scenario of Interest | Set of Signpost Conditions |
|------------------|-----------------------|---|
| Best Hydropower | Hydropower Deficit | Precipitation, Seasonal Amplitude, Evaporation Rates |
| | Environmental Deficit | Precipitation |
| | Irrigation Deficit | Precipitation, Irrigation Demand |
| | Overall Deficit | Precipitation, Seasonal Amplitudes, Irrigation Demand |
| Best Environment | Hydropower Deficit | Precipitation |
| | Irrigation Deficit | Precipitation |
| Best Irrigation | Hydropower Deficit | Precipitation, Seasonal Amplitude |
| | Environmental Deficit | Precipitation, Seasonal Amplitude, Phase Shift |
| Best Tradeoff | Hydropower Deficit | Precipitation, Seasonal Amplitude |
| | Environmental Deficit | Precipitation |

Tradeoff. This combination enhances the precision of Signpost Conditions, addressing the complex interplay of variables that affect policy outcomes.

Ultimately, the system's vulnerabilities vary by policy. The Best Hydropower policy integrates diverse conditions: precipitation, seasonal amplitudes, evaporation rates, and irrigation demand, indicating a multifaceted approach to managing the Zambezi River Basin's challenges. Conversely, the Best Environment policy is primarily sensitive to variations in precipitation, while the Best Irrigation and Tradeoff policies rely more heavily on the combination of precipitation and seasonal amplitudes to address their specific vulnerabilities.

6.3 Adaptation Tipping Points for the Zambezi River Basin

This Section presents results on the quantified Adaptation Tipping Points. Three distinct sets of Signpost Conditions are analyzed to identify final Adaptation Tipping

Point Thresholds. Each set contains the identified primary and secondary factors of precipitation and seasonal amplitude as a baseline condition. The third factor varies between evaporation rate, irrigation increase, and seasonal phase shift. Results indicate how well Signpost Conditions can identify policy-specific vulnerabilities.

- **Signpost Condition Set 1:** Precipitation, Seasonal Amplitude, Evaporation Rate
- **Signpost Condition Set 2:** Precipitation, Seasonal Amplitude, Irrigation Increase
- **Signpost Condition Set 3:** Precipitation, Seasonal Amplitude, Seasonal Phase Shift

All three sets of Signpost Conditions could accurately predict policy failure, except for the Irrigation Policy, see Table 6.5. For a comprehensive overview, see Appendix E.2.

Table 6.5 Summary of Model Accuracy Across Policy Sets

| Policy | Set 1 | Set 2 | Set 3 |
|------------------|---------|---------|---------|
| Best Hydropower | 0.6819 | 0.7060 | 0.6600 |
| Best Environment | 0.7055 | 0.6934 | 0.6913 |
| Best Irrigation | 0.01554 | 0.01580 | 0.01580 |
| Best Tradeoff | 0.8643 | 0.8602 | 0.8529 |

Under the Best Hydropower policy, Signpost Condition Set 2 demonstrated the highest model effectiveness with a Pseudo R-squared value of 0.7060. It indicates a strong correlation between the model's predictions and the observed outcomes. This reflects the model's ability to capture policy failure. Despite the relatively minor performance differences, Set 1 and Set 3 also showed strong results with values of 0.6819 and 0.6600, respectively. Across these models, both primary and secondary Signpost Conditions consistently exerted a significant negative influence on the failure probability.

In the Best Environment and Tradeoff Policies, each logistic regression model consistently reached high McFadden Pseudo R-squared values, underlining their ability to predict policy outcomes across varied settings accurately. Notably, Set 1 was identified as the most precise in these policies, achieving the highest Pseudo R-squared values. This observation implies that Set 1 models are particularly adept at accounting for the factors that influence policy success or failure in these areas.

In contrast, the logistic regression model for the Best Irrigation Policy did not accurately predict policy failure. This result is particularly striking given the insights from previous analyses suggesting that policy failure is associated with mean precipitation values around 0.9 to 0.93. Due to its inconsistent performance, the best irrigation policy has been excluded from further consideration in this analysis.

6.3.1 Identification of Adaptation Tipping Point Thresholds

The results are based on the regression models from Signpost Condition Set 1, which has slightly superior predictive accuracy. They focus on precipitation, seasonal amplitude, and evaporation rate. Contour plots offer insights into how interactions between Signpost Conditions influence the probability of policy failure.

Best Hydropower Policy

Contour plots for the Best Hydropower policy in Figure 6.9 show that mean precipitation change is critical for policy performance. As it decreases, there is a marked increase in the probability of policy failure. Seasonal amplitude and delta vaporation rate modulate the impact of precipitation decrease.

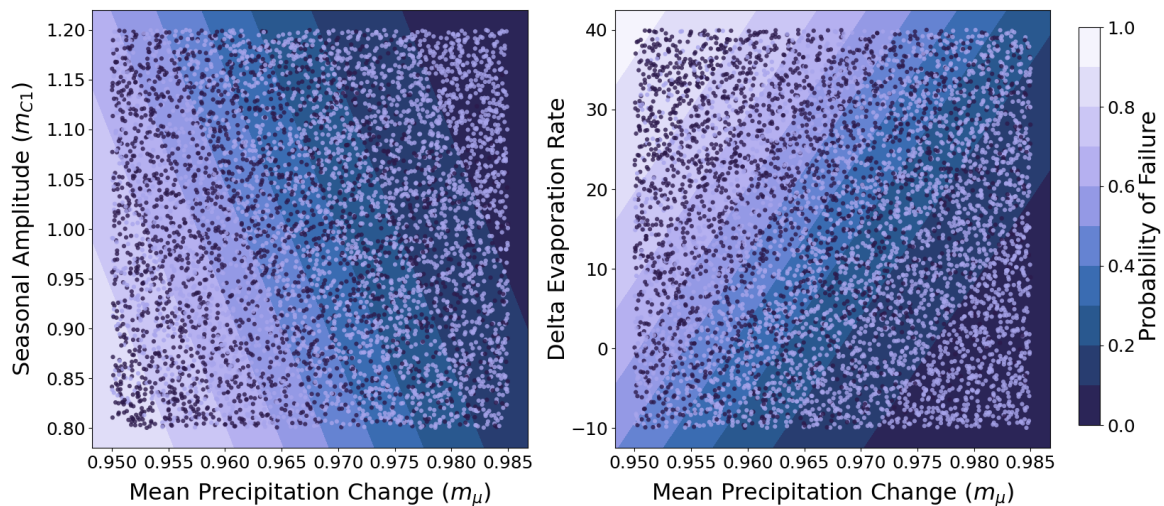


Fig. 6.9 Logistic Regression Contour Plots for Best Hydropower Policy. The contour line color indicates failure probability, with lighter shades representing higher risks. Dark dots describe policy failure.

- For the mean precipitation factor values above 0.975, failure probability remains relatively low, generally below 20 percent, indicating more stable conditions for hydropower operation.
- As the factor decreases below 0.965, there is an increase in failure probability, particularly when the seasonal amplitude factor is lower than 1.00, where the failure probability can exceed 60 percent. This suggests that reduced precipitation coupled with low seasonal amplitude significantly compromises system stability.
- Higher Seasonal Amplitudes (above 1.05) appear to mitigate risks effectively, reducing failure probabilities to around 40 percent even at the lower precipitation levels.

- Delta evaporation rates show varied impacts. Rates below 10 have a moderate influence on failure probability. As evaporation increases beyond 20, the system's vulnerability becomes more pronounced, with failure probabilities escalating above 60 percent, underscoring the system's sensitivity to higher evaporation rates under low precipitation conditions.

Best Environment Policy

Figure 6.10 displays a similar trend compared to the Best Hydropower policy vulnerabilities. A strong gradient of increasing failure probability as mean precipitation decreases is visible. Again, this pattern seems to be modulated by the levels of seasonal amplitudes and evaporation rate.

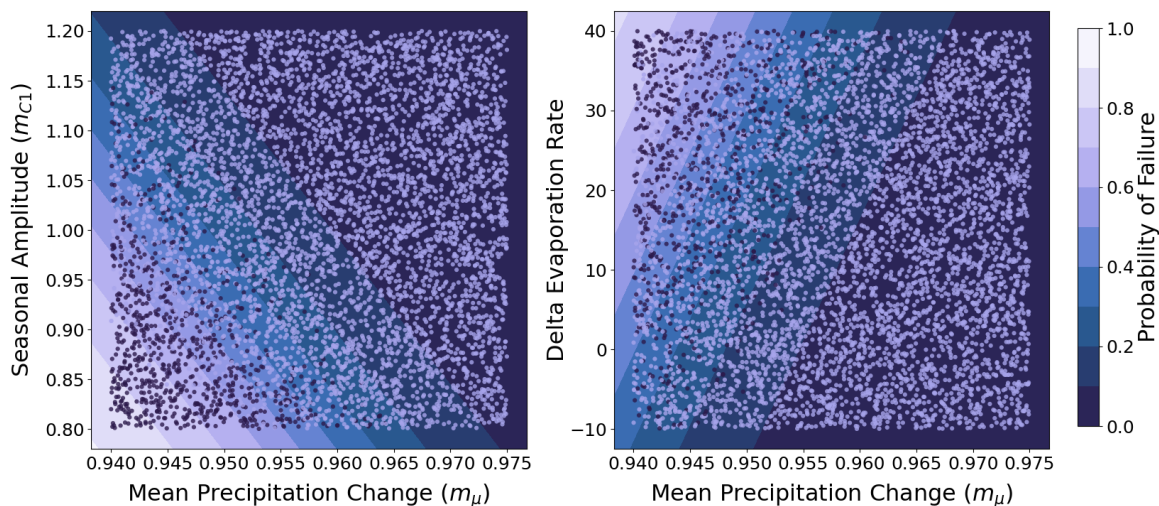


Fig. 6.10 Logistic Regression Contour Plots for Best Environment Policy. The contour line color indicates failure probability, with lighter shades representing higher risks. Dark dots describe policy failure.

- Similar to the Hydropower Policy, a decrease in precipitation correlates with higher failure probabilities in the Environment Policy. For values above 0.965, the Environment Policy maintains a low failure probability, generally below 20 percent.
- Sensitivity to changes in precipitation appears more pronounced in the Environment Policy. This suggests higher policy vulnerability to variations in precipitation.
- Higher Seasonal Amplitudes (above 1.05) buffer the probability of failure against lower precipitation levels with failure probabilities below 40 percent. However, it displays a decreased moderating effect of higher values compared to the Best Hydropower policy.

- An evaporate factor below 10 have a moderate impact on failure probability, which intensifies as the mean precipitation change decreases. When the delta evaporation rate exceeds 20, the system becomes highly vulnerable, with a significant spike in failure probabilities.
- While both policies (Best Hydro and Environment) show increased vulnerability with higher evaporation, the Environment Policy exhibits a steeper increase in failure probabilities at lower values. It could suggest a reduced moderating influence.

Best Tradeoff Policy

Figure 6.11 reveals similar patterns to the previous two policies. Policy failure displays a strong dependency on mean precipitation changes. This trend is influenced by the levels of seasonal amplitude and evaporation rates, which can either mitigate or intensify the effects of decreasing precipitation.

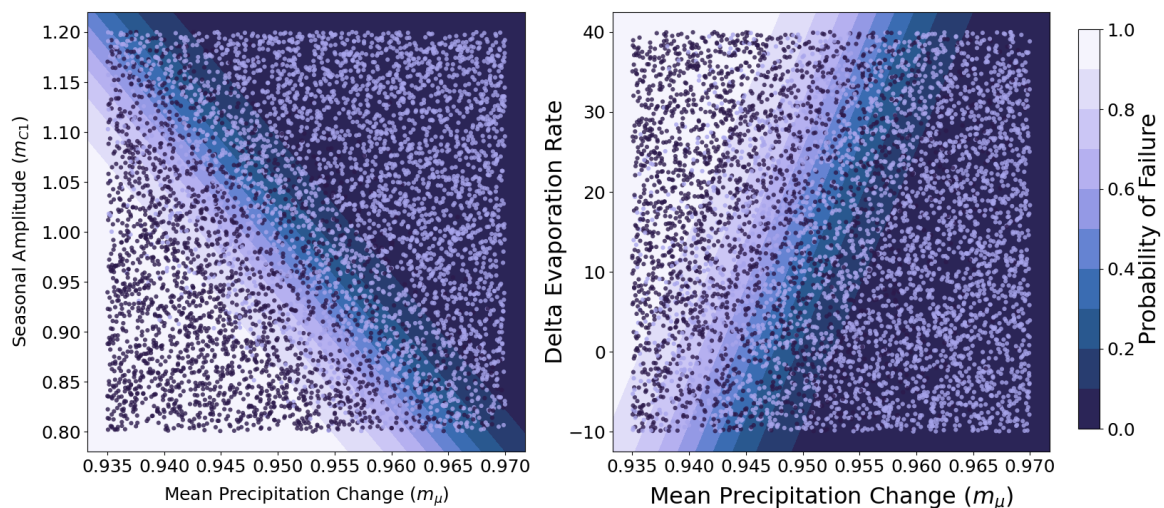


Fig. 6.11 Logistic Regression Contour Plots for Best Tradeoff Policy. The contour line color indicates failure probability, with lighter shades representing higher risks. Dark dots describe policy failure.

- Failure probability significantly increases as the mean precipitation factor decreases below 0.945.
- Compared to the other policies, boundary conditions are narrowly defined. It hints at a heightened policy sensitivity.
- Values above 1.05 serve as a buffer. Its ability to moderate the variability in precipitation makes it a stabilizing factor. Thus, higher seasonal amplitudes protect significantly against failure.

- Vulnerability to failure increases substantially when delta evaporation values exceed 10, especially at lower precipitation levels. This highlights the policy's vulnerability to both decreased precipitation and increased evaporation rates.
- Delta evaporation rates below 10 have a moderate impact on failure probability, which intensifies as mean precipitation Change decreases. When evaporation increases but 20 percent, the system becomes highly vulnerable, with a significant spike in failure probabilities.
- While both policies (Best Hydro and Environment) show increased vulnerability with higher evaporation, the Environment Policy exhibits a steeper increase in failure probabilities at lower values. It could suggest a reduced moderating influence.

Overall, the combination of Signpost Conditions demonstrated similar interactions across different policies, with varying degrees of sensitivity to each factor. Results conclude with the identification of Adaptation Tipping Point Thresholds. These are sufficient to describe vulnerabilities across all policies and thus hint at underlying systemic vulnerabilities. They reflect the system boundary condition that, when exceeded, significantly increases the likelihood of policy failure.

Adaptation Tipping Point Thresholds:

- **Mean Precipitation Change:** A threshold of 0.965 is identified across all policies, below which there is a marked increase in failure probability.
- **Seasonal Amplitude:** A threshold value of 1.05 serves as a mitigating factor, effectively reducing failure probabilities even under lower precipitation levels.
- **Delta Evaporation Rate:** A critical threshold of 20 percent increase, beyond which the vulnerability of policies increases.

6.3.2 Streamflow Patterns of Adaptation Tipping Points

Based on the scenarios of interest and critical Signpost Conditions, the analysis supports a focus on streamflow patterns as a sufficient metric for defining policy Adaptation Tipping Points. Regression model results present Adaptation Tipping Points Thresholds that inform the generation of new streamflow patterns understood as Zambezi's Adaptation Tipping Point.

Under the identified Adaptation Tipping Point Thresholds, Adaptation Tipping Point streamflow patterns exhibit a wide variety. The wide range can be explained by the interaction effects between mean precipitation changes and the seasonal amplitudes. Figure 6.12 illustrates it for the Kafue Flats catchment area; the other catchment figures can be found in Appendix E.9. Notably, there is a great streamflow decrease across all catchments during the wet season. Seasons vary from catchment to catchment. Results focus on the Max Adaptation Tipping Points streamflow conditions. Choosing

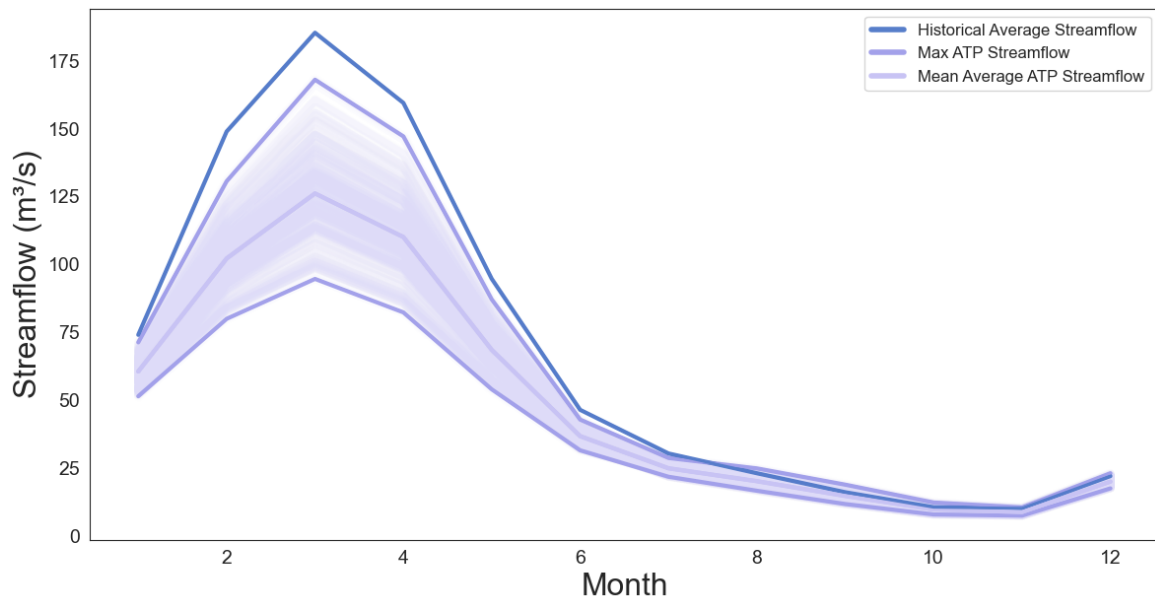


Fig. 6.12 Comparison of Monthly Average Streamflow and adaptation tipping point patterns for the Kafue Flats catchment.

this scenario displays a cautious approach that indicates adaptation once policy failure becomes more probable.

Maximum Streamflow Adaptation Tipping Point

The Maximum ATP-streamflow conditions represent streamflow patterns that, under the Adaptation Tipping Point Thresholds, exhibit the fewest differences from the current streamflow pattern. Thus, they are more likely to be reached than the mean or min ATP-streamflow conditions.

The absolute and percentage differences between average historical and Max ATP-streamflow conditions for each catchment area are depicted in Figure 6.13.

- **Seasonal Impact** is pronounced across all catchment areas with differing variability. Rainy season suffers significantly larger decreases in streamflow across all catchments, with specific months showing extreme reductions.
 - Across all catchments, the rainy season experiences the largest decreases in streamflow. Months between January and June experience a greater difference in available water. For instance, Cahora Bassa's wet season decreases by 26.59 percent, while its dry season decreases by 10.72 percent.
 - On average, the rainy season shows a decrease of 17 percent, with the Kafue Flats experiencing the lowest decrease of 16.23 percent. In contrast, the Cahora Bassa, Shire, and Bakota Gorge catchments all experience an average decrease above 20 percent, with the Cahora Bassa experiencing the

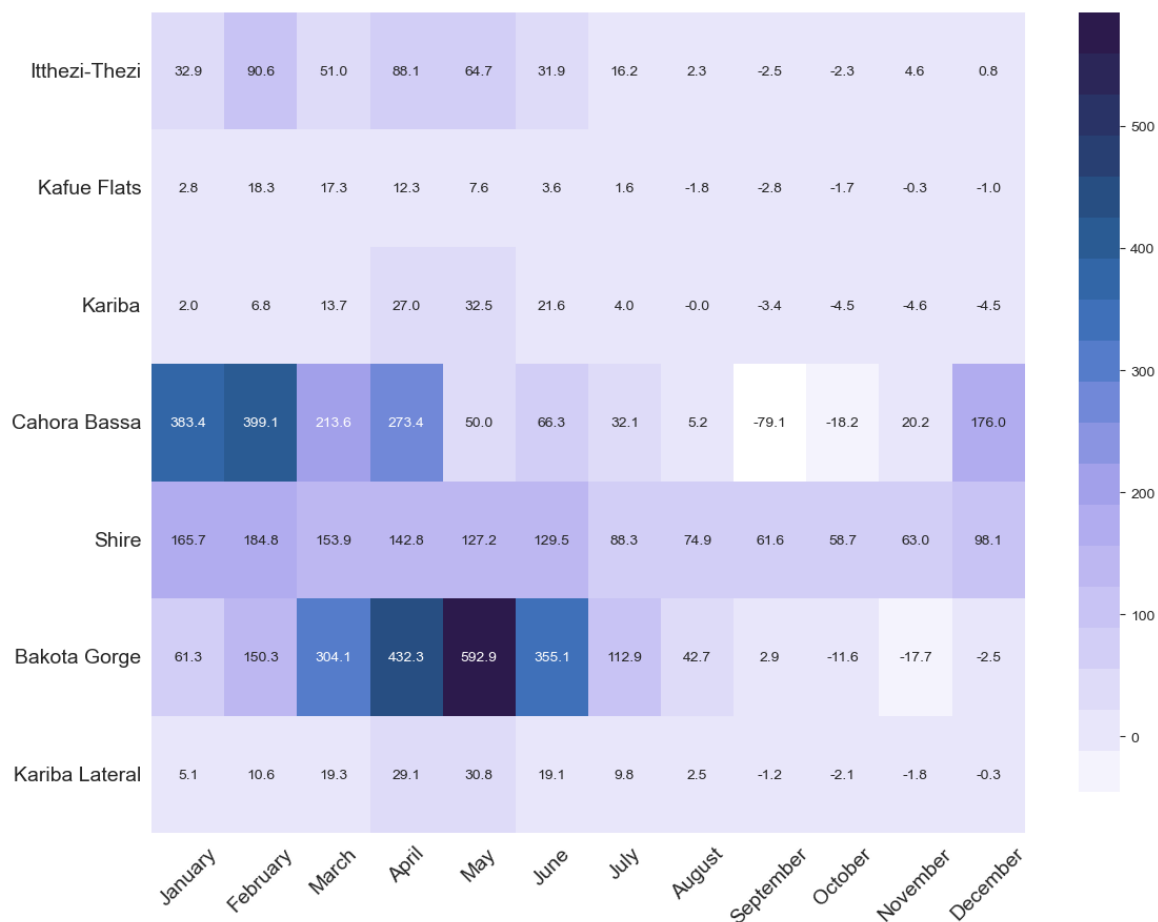


Fig. 6.13 Streamflow Pattern of the Chosen Adaptation Tipping Point Scenario with Absolute Decrease Values. The heatmap indicates the monthly decrease in streamflow across all relevant catchments compared to historical averages. The color intensity represents the absolute difference, with darker shades indicating higher values.

Bakota Gorge averaging a total decrease of 2008 m³/s compared to the historical data.

- Highest absolute reduction occurs in May, with a decrease of 593 m³/s from the Bakota Gorge catchment area.
- The dry season shows varying changes, with some catchments experiencing increases¹ and other decreases in streamflow.

¹This is most likely due to an artifact in how the streamflow data is generated. Especially low seasonal amplitude has a decreasing effect during wet seasons but also an increasing effect during the dry season; see Appendix C.5

-
- Streamflow increases are minor and cannot compensate for the great decrease during the rainy season. Overall, each catchment describes total absolute streamflow decreases.
 - **Catchments** have a different impact on the overall water balance within the system. Differences could indicate more critical catchment areas.
 - Cahora Bassa and Bakota Gorge catchments experience the most substantial impacts. It emphasizes their importance to the Zambezi River Basin's water balance.
 - Kafue Flats, Kariba, and Itthezi-Thezi catchments exhibit less extreme changes in both absolute and percentage decreases compared to Cahora Bassa and Bakota George.
 - Shire catchment displays the least variability among the studied catchments, with percentage decreases ranging from 12.9 percent in September to 23.7 percent in January. This could be attributed to Lake Malawi, which provides a consistent inflow, buffering against seasonal influence.

Chapter 7

Discussion

This thesis establishes a framework that enhances adaptive policy design for river basin management under deep uncertainty, with a specific application to the Zambezi River Basin. Integrating a Robustness Analysis with EMODPS advances a new decision-support tool that transcends Robust Planning approaches.

Integration of Robustness Analysis and EMODPS

Alternative policies were identified through a conventional EMODPS model. Epsilon non-dominated Pareto-optimal operation strategies revealed significant tradeoffs between hydropower, environmental, and irrigation goals. This was followed by a detailed characterization of key uncertainty drivers, which were then translated into quantifiable uncertainty factors and integrated into the EMODPS model. This integration laid the groundwork for an Open Exploration, which generated future States of the World across four distinct policies under varied conditions. Using Feature Scoring, PRIM, and Logistic Regression modeling, Scenario Discovery pinpointed vulnerabilities. These efforts culminated in identifying Signpost Conditions and the definition of Adaptation Tipping Point Thresholds through quantifiable streamflow patterns.

The new methodological integration in this research addresses the limitations inherent in Robust Planning while contributing to overcoming challenges in Dynamic Planning. Traditional Robust Planning is often criticized for its rigidity and inability to adapt to new information, which can lead to suboptimal policy outcomes when underlying assumptions change. The proposed approach mitigates these issues by employing Robustness Analysis not to select optimal policy alternatives but to pinpoint and respond to specific system vulnerabilities in relation to Deep Uncertainties.

Dynamic and Responsive Policy Design

The thesis enriches discussions in the realm of dynamic river basin management by identifying Signpost Conditions and quantifying Adaptation Tipping Points for the

Zambezi River Basin. It offers a nuanced perspective that prioritizes adaptability and continuous policy evolution. The thesis delineates how dynamic policies can be constructed and adjusted in response to an evolving future by characterizing key uncertainty drivers and translating these into quantifiable factors. The generation of diverse future States of the World through Open Exploration further illustrates the adaptive policy framework, enabling the identification of vulnerabilities that shape the development of Signposts and Adaptation Tipping Points.

Characterization of Signpost Conditions and Adaptation Tipping Points

Findings from the Zambezi River Basin are relevant locally and hold broader implications for global river basin management under Deep Uncertainty. Identifying mean precipitation changes and seasonal amplitude variations as primary Signpost Conditions provides a template that can be adapted to other contexts.

Critical Uncertainties

In this context, the response to the first sub-research question lays the foundational groundwork for integrating Robustness Analysis and Dynamic Planning. The exploration of the most prominent uncertainties in the Zambezi River Basin underpins the analysis. By identifying these uncertainties, the thesis delineates the critical external system factors necessary for Exploratory Modeling Analysis and enhances the capacity for anticipatory management.

Findings reveal hydroclimatic uncertainties, such as changes in precipitation patterns, potential decreases by up to 30 percent, increased inter-annual variability, and shifting seasons, are exacerbated by projected temperature rises of 1.5-3°C by mid-century. Socio-economic uncertainties, including rapid population growth expected to result in a 50 percent increase by 2050, could lead to rising irrigation demands projected to increase by 30-50 percent, which pose additional challenges. These complexities necessitate a detailed understanding of how such factors affect the basin's operating strategies.

Critical Combinations of Uncertainties

The findings related to the second sub-research question, focusing on critical vulnerability combinations, improve the dynamic policy design by identifying Signpost Conditions. The analysis reveals precipitation as a primary factor influencing all policy objectives within the Zambezi River Basin. Serving as a baseline Signpost Condition, precipitation's critical role underscores its importance in the hydrological dynamics of the Zambezi River Basin.

Seasonal changes, particularly seasonal amplitudes, complement precipitation influences on policy effectiveness. These factors notably affect the Best Irrigation and Best Tradeoff policies, highlighting their critical impact on managing seasonal water availability.

The research further identifies policy-specific vulnerabilities that suggest a policy-tailored approach. For instance, the Best Hydropower policy is influenced by diverse conditions, including Evaporation and Irrigation Demand. In contrast, the Best Environment policy responds primarily to variations in precipitation changes. In contrast, the Best Irrigation and Best Tradeoff policies require management strategies addressing precipitation and seasonal amplitude changes.

The implications of these findings shape the response frameworks necessary for dynamic river basin management. Understanding the interplay between these critical uncertainties aids in developing policy structures, including Adaptation Tipping Points. Additionally, anticipating vulnerabilities and potential policy failures is vital for proactive river basin management. This anticipatory approach is essential in mitigating adverse outcomes before they escalate into more severe challenges. A detailed understanding of uncertainty interactions also lays the foundation for quantifying Adaptation Tipping Points, which will contribute directly to answering the third sub-research question.

Quantifying Adaptation Tipping Points

The third sub-research question identifies Adaptation Tipping Points. Its focus on delineating Adaptation Tipping Points and provides actionable thresholds that signal when existing policies may become ineffective. Recognizing these thresholds allows for policy adaptation. The ability to define and respond to these tipping points ensures that adaptations are contextually relevant, preventing potential system failures.

The research identifies specific Adaptation Tipping Point Thresholds that signal policy failures. These include a mean precipitation factor threshold of 0.965, below which there is a marked increase in the likelihood of policy failure across all strategies. Additionally, a seasonal amplitude threshold of 1.05 shows that higher amplitudes can mitigate failure probabilities even under low precipitation scenarios. Furthermore, a Delta Evaporation Rate of 20 signifies a boundary beyond which policy vulnerabilities significantly increase.

Translating these thresholds into streamflow patterns enables policymakers to understand and anticipate points at which current strategies may no longer suffice. It provides a clear visual representation of when policy adjustments should be enacted. The results reveal a pronounced seasonal impact, with the rainy season experiencing significantly more significant decreases in streamflow. Notably, the wet season's streamflow across all catchments shows a substantial reduction, with an average decrease of 17 percent, highlighting critical periods of vulnerability. Specifically, the Cahora Bassa and Bakota Gorge catchments emerge as particularly sensitive, experiencing average decreases

exceeding 20 percent, with the Bakota Gorge recording an absolute reduction as high as 593 m³/s in May.

Implications for Local and Global River Basin Management

These findings gain significance in light of earlier discussions regarding projected changes in the Zambezi River Basin's precipitation patterns, anticipating up to 30 percent decreases. Such substantial alterations make the occurrence of the identified Adaptation Tipping Points not only plausible but increasingly probable.

The looming possibility of reaching Adaptation Tipping Points underscores the urgent need to explore alternative policies to which the system can adapt effectively. By characterizing Adaptation Tipping Points as specific streamflow patterns, an intriguing avenue for future research emerges. This approach could involve using these streamflow patterns as input data for subsequent EMODPS runs. This utilization would capitalize on the tendency of global approximators to overfit, which, in this context, ensures that the derived policy functions closely align with the Adaptation Tipping Point streamflow scenarios. As a result, this approach prompts a comprehensive reevaluation of existing policies, optimizing strategies that are better equipped to manage the expected hydrological changes. Therefore, using streamflow patterns to reflect Adaptation Tipping Points helps simplify complex hydrological data into actionable insights and may also enrich subsequent modeling processes that provide optimally adapted policy functions.

Conclusion and the Role of a Policy Broker

Conclusively, insights from each sub-research question provide a framework to improve the adaptive policy design that advances the management of the Zambezi River Basin. It informs proactive monitoring and dynamic adjustment of policies, addressing traditional challenges associated with Dynamic Planning, such as the complexity of continuous management and the high costs of monitoring a wide array of system variables. By clearly defining Signposts and quantifying Adaptation Tipping Points, the management process becomes more effective in addressing Deep Uncertainties.

It should be noted that choosing a diverse array of streamflow patterns to describe Adaptation Tipping Points also introduces considerable ambiguity in the decision-making process. For instance, opting for the upper boundaries of these Adaptation Tipping Point streamflow patterns suggests a more cautious approach. However, selecting lower boundaries increases the risk of policy performance falling short. This underscores that managing river basins transcends technical challenges and enters the realm of socio-technical complexities.

The process of agreeing on performance thresholds, which is critical for this framework, and agreeing on problem formulations, including setting objective constraints, necessitates extensive stakeholder involvement. While this adds complexity to decision-making, especially in a multi-objective context, it is not an unfamiliar scenario in river basin

management. The role of policy analysts as brokers between stakeholder preferences and scientific insights is critical, highlighting the dynamic interplay between knowledge and preferences in shaping policy.

This complexity should be viewed not as a limitation but as an enhancement to Dynamic Planning. Transboundary water management, often framed as a problem space fraught with competing demands and escalating conflicts, should be viewed as a solution space for continuous cooperation. Acknowledging the deeply uncertain nature of river basins like the Zambezi ensures ongoing dialogue and adaptation. Instead of striving for permanent solutions, policymakers are encouraged to foster a dynamic understanding of uncertainties. This approach is vital as it recognizes the evolving nature of challenges and promotes flexibility and responsiveness in policy frameworks.

In conclusion, adaptive policy frameworks can transform transboundary water issues from complex challenges through continuous and informed decision-making into collaborative opportunities. By embracing river basins' dynamic and uncertain waters, policymakers can address current management issues and lay a foundation for future cooperation and policy adaptation. This thesis contributes to this process by providing a decision-support tool that enhances Dynamic Planning for river basin management, which aligns with global initiatives like the 1992 Water Convention and Sustainable Development Goal 6.

Chapter 8

Conclusion and Recommendations

8.1 Conclusion

This thesis introduces a framework to enhance decision support for river basin management under Deep Uncertainty, using the transboundary Zambezi River Basin as a case study. By identifying Signpost Conditions and quantifying Adaptation Tipping Points, the research advances the dynamic policy design essential for Dynamic Planning in river basin systems.

The thesis pinpoints key uncertainties that critically impact the management of the Zambezi River Basin. The analysis revealed that a decrease in precipitation significantly influences policy outcomes, a risk that higher seasonal amplitudes can moderate. Specifically, combinations of low seasonal amplitudes and reduced precipitation consistently lead to policy failure. It enabled the identification of three sets of Signpost Conditions, which include precipitation and seasonal amplitudes as primary and secondary factors, complemented by evaporation, irrigation demand, or seasonal shifts. These conditions accurately predict policy success or failure, offering reliable and precise descriptions of the system's boundary conditions. Focusing on the combination of precipitation, seasonal amplitudes, and evaporation, the research successfully defined Adaptation Tipping Point Thresholds, such as a critical precipitation threshold of 0.965, a seasonal amplitude threshold of 1.05, and increased evaporation amounts of 20 percent. These thresholds were then translated into streamflow patterns, providing a tangible and visual means for policymakers to understand and anticipate the impacts of crossing these critical points, facilitating more informed and proactive decision-making. For the analyzed policies a common Adaptation Tipping is reached at an overall streamflow reduction of 24.2 percent, with the rainy season experiencing the most significant decreases.

The research contributes theoretically and practically to the field of river basin management under Deep Uncertainty. Theoretically, it enhances understanding of how Robustness Analysis can be applied to identify system vulnerabilities that inform

Signpost Conditions and Adaptation Tipping Points. This represents a significant advancement in addressing the complexities of Dynamic Planning and overcomes limitations inherent in traditional Robust Planning approaches. Practically, the study demonstrated the framework application. Although the Zambezi River Basin was the primary case study, the framework developed is adaptable and can be applied to other river basins.

The methodologies used throughout this study can be adapted to other river basins, each characterized by unique uncertainties that must be integrated into the modeling process. A key challenge in applying this framework elsewhere lies in accurately characterizing these uncertainties and their translation into computable factors for simulation models. This highlights the necessity of a computational model capable of conducting Open Exploration experiments. EMODPS models are a perfect fit for this task, allowing for the flexible addition of new input data, performing Open Exploration, and finding new policies optimized on quantified Adaptation Tipping Point streamflow patterns.

In conclusion, the necessity of ongoing adaptation and proactive management in river basin governance cannot be overstated. As uncertainties are profound, policy flexibility and responsiveness are crucial. This approach mitigates the risks associated with deep uncertainties and provides opportunities for enhanced cooperation and collaboration.

8.2 Recommendation

This research has substantiated the critical need for dynamic, adaptive policies tailored to the specific vulnerabilities and conditions of the Zambezi River Basin. The identification of Signposts and Adaptation Tipping Points are designed to guide the transition from traditional static models to a Dynamic Planning framework, emphasizing the importance of continuous monitoring and adaptation.

Target Monitoring of Precipitation and Seasonal Amplitudes

Given that mean precipitation and seasonal amplitudes are identified as primary drivers of system vulnerability, it is recommended that monitoring efforts be concentrated on these elements. Streamflow patterns generated during this study have pinpointed critical catchment areas like Cahora Bassa and Batoka Gorge, where streamflow changes significantly impact reservoir water balances. Monitoring should be intensified in these areas, especially during the wet season when streamflow decreases are more pronounced in absolute terms. This targeted monitoring will provide data to inform trends, suggesting when adaptation is necessary.

The Zambezi Watercourse Commission should lead the coordination of these enhanced monitoring efforts. As the transboundary river organization overseeing the Zambezi River Basin, the organization is ideally positioned to facilitate collaboration among

member states, ensuring that monitoring data is shared and used to inform decision-making across the basin. This collaborative approach will help to synchronize policies and practices.

Transboundary Stakeholder Participation

The transition to dynamic policy structures necessitates the involvement of a broad spectrum of stakeholders, extending beyond policymakers who must recognize the complex, ever-evolving challenges of river basin management, which preclude simple solutions. Instead, a continuous policy process that excels in Dynamic Planning is essential, encompassing stakeholders like reservoir operators, who traditionally rely on outdated models.

These stakeholders, particularly reservoir operators, are crucial in implementing this change and must be convinced of its benefits. These included enhanced system performance and reduced risk of system failures. Support for these stakeholders can be facilitated through training, demonstration projects, stakeholder engagement, and participatory modeling projects. It is essential to integrate the Dynamic Planning perspective into the operating minds of the Zambezi River Basin. Thus, governmental support should include the development of infrastructure and capacities that support adaptive management, such as advanced hydrological modeling tools and decision support systems.

Implementing these recommendations will require strong political will, coordinated action, and sustained investment. This might be challenging, especially in the transboundary context. However, the long-term benefits of a dynamic and collaborative river basin management framework will far outweigh the costs. By embracing Dynamic Planning with a focus on continuous adaptation, stakeholders in the Zambezi River Basin can ensure sustainable and equitable water management capable of meeting the challenges of today and tomorrow.

8.3 Limitations

While this research contributes to the improved management of the Zambezi River Basin under Deep Uncertainty, it acknowledges several limitations that may affect the generalizability and application of its findings.

The thesis focuses on the Zambezi River Basin as a case study, which limits the direct applicability of its findings to other contexts. The uncertainty characterization is specifically tailored to the Zambezi model. Consequently, the insights on Adaptation Tipping Point Thresholds derived from this study are context-specific and not universal. Additionally, the uncertainty generation process, including the scenario development, lacks validation against General Circulation Models, instead relying on the assumption that the approach meaningfully represents uncertainties at hand.

Additionally, the insights heavily depend on the accuracy with which the modeler defines the uncertainty space. This includes identifying drivers, their translation into quantifiable uncertainty factors, and their integration into the existing model, leading to potential biases if these elements are not accurately captured. Uncertainty factors were sampled using Latin hypercube sampling, which, while effective in representing the uncertainty space, fails to capture the likely interdependencies between factors. This study also considers primarily hydroclimatic uncertainties, with a limited focus on socio-economic factors, skewing the analysis towards hydrological aspects.

Moreover, using a pre-existing complex EMODPS model assumes the validity of its underlying assumptions. Additionally, the spatial dimension of the river basin management is underexplored, limiting the ability to apply findings across different geographic scales or within varied spatial contexts of the basin.

The resolution of streamflow manipulation in this model is based on monthly data, which could overlook finer temporal variations that daily data reveal, leading to less precise hydrological modeling outcomes. Furthermore, the identification of Adaptation Tipping Points is based on hydrological patterns without fully integrating socio-economic variables, which, although not deemed critical, might influence the broader context of policy adaptation.

Additionally, Adaptation Tipping Point Thresholds are defined as absolute values without considering temporal trends over moving windows, which omits the temporal dynamics of adaptation needs.

Despite these limitations, the thesis advances the field of Dynamic Planning in river basin management under deep uncertainty by providing a structured approach to leveraging Robustness Analysis to improve adaptive policy design.

8.4 Future Work

Extending the proposed framework to other river basins is essential. While this research has provided valuable insights into the Zambezi River Basin, applying and validating the adaptive policy design approach in different geographical and hydrological contexts would help strengthen the generalizability and applicability of the findings.

Further analysis within the Zambezi River Basin itself is also needed. Current research has begun to utilize data from the quantification of Adaptation Tipping Point Thresholds, but considerable scope exists to deepen this analysis. Future efforts should explore how these thresholds can directly inform and transform policy-making, mainly through the development of strategies that respond dynamically to identified streamflow patterns at critical tipping points.

Expanding the range of policies analyzed is another crucial area for future research. This thesis focused on four specific policies; however, exploring a more comprehensive

array of policy options could uncover additional robust and adaptive strategies suitable for various objectives and challenges within the river basin.

The next step is developing a comprehensive, Dynamic Adaptive Policy Plan. While the current project laid the groundwork by defining the complex policy structure, future work should identify new adaptive policies that the system can adopt as conditions evolve.

References

- Ackoff, R. L. (1979). The future of operational research is past. *Journal of the operational research society*, 30(2):93–104.
- Adger, W. N., Dessai, S., Goulden, M., Hulme, M., Lorenzoni, I., Nelson, D. R., Naess, L. O., Wolf, J., and Wreford, A. (2009). Are there social limits to adaptation to climate change? *Climatic change*, 93:335–354.
- AMCOW (2018). African Ministers’ Council on Water (AMCOW) – Count every drop, every drop counts — amcow-online.org. <https://amcow-online.org>. [Accessed 26-03-2024].
- Arnold, W., Zatarain Salazar, J., Carlino, A., Giuliani, M., and Castelletti, A. (2023). Operations eclipse sequencing in multipurpose dam planning. *Earth’s Future*, 11(4):e2022EF003186.
- Bankes, S. (1993). Exploratory modeling for policy analysis. *Operations research*, 41(3):435–449.
- Beilfuss, R. et al. (2012). A risky climate for southern african hydro: assessing hydrological risks and consequences for zambezi river basin dams.
- Bertoni, F., Castelletti, A., Giuliani, M., and Reed, P. (2019). Discovering dependencies, trade-offs, and robustness in joint dam design and operation: An ex-post assessment of the kariba dam. *Earth’s Future*, 7(12):1367–1390.
- Bloemen, P., Van Der Steen, M., and Van Der Wal, Z. (2019). Designing a century ahead: Climate change adaptation in the dutch delta. *Policy and Society*, 38(1):58–76.
- Borgomeo, E., Mortazavi-Naeini, M., Hall, J. W., and Guillod, B. P. (2018). Risk, robustness and water resources planning under uncertainty. *Earth’s Future*, 6(3):468–487.
- Borgomeo, E., Mortazavi-Naeini, M., Hall, J. W., O’Sullivan, M. J., and Watson, T. (2016). Trading-off tolerable risk with climate change adaptation costs in water supply systems. *Water Resources Research*, 52(2):622–643.
- Brown, C. and Wilby, R. L. (2012). An alternate approach to assessing climate risks. *Eos, Transactions American Geophysical Union*, 93(41):401–402.

- Bryant, B. P. and Lempert, R. J. (2010). Thinking inside the box: A participatory, computer-assisted approach to scenario discovery. *Technological Forecasting and Social Change*, 77(1):34–49.
- Celeste, A. B. and Billib, M. (2009). Evaluation of stochastic reservoir operation optimization models. *Advances in Water Resources*, 32(9):1429–1443.
- Coello, C. A. C. (2007). *Evolutionary algorithms for solving multi-objective problems*. Springer.
- Cohen, J. S. and Herman, J. D. (2021). Dynamic adaptation of water resources systems under uncertainty by learning policy structure and indicators. *Water Resources Research*, 57(11):e2021WR030433.
- Deb, K., Mohan, M., and Mishra, S. (2003). Towards a quick computation of well-spread pareto-optimal solutions. In *Evolutionary Multi-Criterion Optimization: Second International Conference, EMO 2003, Faro, Portugal, April 8–11, 2003. Proceedings 2*, pages 222–236. Springer.
- Deb, K., Pratap, A., Agarwal, S., and Meyarivan, T. (2002). A fast and elitist multiobjective genetic algorithm: Nsga-ii. *IEEE transactions on evolutionary computation*, 6(2):182–197.
- Delft High Performance Computing Centre (DHPC) (2024). DelftBlue Supercomputer (Phase 2). <https://www.tudelft.nl/dhpc/ark:/44463/DelftBluePhase2>.
- Desanker, P. V. and Justice, C. O. (2001). Africa and global climate change: critical issues and suggestions for further research and integrated assessment modeling. *Climate Research*, 17(2):93–103.
- Dessai, S., Hulme, M., Lempert, R., and Pielke Jr, R. (2009). Climate prediction: a limit to adaptation. *Adapting to climate change: thresholds, values, governance*, 64:78.
- Dewar, J. A., Builder, C. H., Hix, W. M., and Levin, M. H. (1993). *Assumption-based planning: a planning tool for very uncertain times*. Rand.
- Dias, L. F., Aparício, B. A., Nunes, J. P., Morais, I., Fonseca, A. L., Pastor, A. V., and Santos, F. D. (2020). Integrating a hydrological model into regional water policies: Co-creation of climate change dynamic adaptive policy pathways for water resources in southern portugal. *Environmental Science & Policy*, 114:519–532.
- Eckstein, D., Künzel, V., and Schäfer, L. (2021). *The global climate risk index 2021*. Bonn: Germanwatch.
- Fletcher, S., Lickley, M., and Strzepek, K. (2019). Learning about climate change uncertainty enables flexible water infrastructure planning. *Nature communications*, 10(1):1782.
- Giuliani, M., Castelletti, A., Pianosi, F., Mason, E., and Reed, P. M. (2016). Curses, tradeoffs, and scalable management: Advancing evolutionary multiobjective direct policy search to improve water reservoir operations. *Journal of Water Resources Planning and Management*, 142(2):04015050.

- Giuliani, M., Mason, E., Castelletti, A., Pianosi, F., and Soncini-Sessa, R. (2014). Universal approximators for direct policy search in multi-purpose water reservoir management: A comparative analysis. *IFAC Proceedings Volumes*, 47(3):6234–6239.
- Giuliani, M., Quinn, J. D., Herman, J. D., Castelletti, A., and Reed, P. M. (2017). Scalable multiobjective control for large-scale water resources systems under uncertainty. *IEEE Transactions on Control Systems Technology*, 26(4):1492–1499.
- Groves, D. G., Bloom, E., Lempert, R. J., Fischbach, J. R., Nevills, J., and Goshi, B. (2015). Developing key indicators for adaptive water planning. *Journal of Water Resources Planning and Management*, 141(7):05014008.
- Haasnoot, M., Kwakkel, J. H., Walker, W. E., and Ter Maat, J. (2013). Dynamic adaptive policy pathways: A method for crafting robust decisions for a deeply uncertain world. *Global environmental change*, 23(2):485–498.
- Haasnoot, M., Schellekens, J., Beersma, J., Middelkoop, H., and Kwadijk, J. C. J. (2015). Transient scenarios for robust climate change adaptation illustrated for water management in the netherlands. *Environmental Research Letters*, 10(10):105008.
- Haddeland, I., Heinke, J., Biemans, H., Eisner, S., Flörke, M., Hanasaki, N., Konzmann, M., Ludwig, F., Masaki, Y., Schewe, J., et al. (2014). Global water resources affected by human interventions and climate change. *Proceedings of the National Academy of Sciences*, 111(9):3251–3256.
- Hadka, D. and Reed, P. (2013). Borg: An auto-adaptive many-objective evolutionary computing framework. *Evolutionary computation*, 21(2):231–259.
- Herman, J. D., Quinn, J. D., Steinschneider, S., Giuliani, M., and Fletcher, S. (2020). Climate adaptation as a control problem: Review and perspectives on dynamic water resources planning under uncertainty. *Water Resources Research*, 56(2):e24389.
- Herman, J. D., Reed, P. M., Zeff, H. B., and Characklis, G. W. (2015). How should robustness be defined for water systems planning under change? *Journal of Water Resources Planning and Management*, 141(10):04015012.
- Hine, D. and Hall, J. W. (2010). Information gap analysis of flood model uncertainties and regional frequency analysis. *Water Resources Research*, 46(1).
- Hipel, K. W. and Ben-Haim, Y. (1999). Decision making in an uncertain world: Information-gap modeling in water resources management. *IEEE Transactions on Systems, Man, and Cybernetics, Part C (Applications and Reviews)*, 29(4):506–517.
- Hughes, D. and Farinosi, F. (2020). Assessing development and climate variability impacts on water resources in the zambezi river basin. simulating future scenarios of climate and development. *Journal of Hydrology: Regional Studies*, 32:100763.
- Hughes, D., Mantel, S., and Farinosi, F. (2020). Assessing development and climate variability impacts on water resources in the zambezi river basin: Initial model calibration, uncertainty issues and performance. *Journal of Hydrology: Regional Studies*, 32:100765.

- Hui, R., Herman, J., Lund, J., and Madani, K. (2018). Adaptive water infrastructure planning for nonstationary hydrology. *Advances in Water Resources*, 118:83–94.
- Hulme, M., Doherty, R., Ngara, T., New, M., and Lister, D. (2001). African climate change: 1900-2100. *Climate research*, 17(2):145–168.
- Hulme, P. E. (2005). Adapting to climate change: is there scope for ecological management in the face of a global threat? *Journal of Applied ecology*, 42(5):784–794.
- Hwang, C.-L. and Masud, A. S. M. (2012). *Multiple objective decision making—methods and applications: a state-of-the-art survey*, volume 164. Springer Science & Business Media.
- Kasprzyk, J. R., Nataraj, S., Reed, P. M., and Lempert, R. J. (2013). Many objective robust decision making for complex environmental systems undergoing change. *Environmental Modelling & Software*, 42:55–71.
- Kecskes, G. (2020). European water law and hydropolitics: An inquiry into the resilience of transboundary water governance in the european union.
- Kedida, E. G. and Arsano, Y. (2024). Challenges and prospects of transboundary river water conservation and watershed protection in ethiopia: The case of the upper blue Nile. *Heliyon*.
- Kirsch, B. R., Characklis, G. W., and Zeff, H. B. (2013). Evaluating the impact of alternative hydro-climate scenarios on transfer agreements: Practical improvement for generating synthetic streamflows. *Journal of Water Resources Planning and Management*, 139(4):396–406.
- Kling, H., Fuchs, M., and Stanzel, P. (2015). Future hydro generation in the zambezi basin under the latest ipcc climate change projections. *Int. J. Hydropower Dams Afr. Special*, 2015:23–26.
- Knight, F. H. (1921). *Risk, uncertainty and profit*, volume 31. Houghton Mifflin.
- Kollat, J. B. (2005). *The Epsilon Non-Dominated Sorted Genetic Algorithm II: A Highly Effective Multi-Objective Evolutionary Algorithm for Water Resources Applications*. PhD thesis, Pennsylvania State University.
- Kusangaya, S., Warburton, M. L., Van Garderen, E. A., and Jewitt, G. P. (2014). Impacts of climate change on water resources in southern africa: A review. *Physics and Chemistry of the Earth, Parts a/b/c*, 67:47–54.
- Kwadijk, J. C., Haasnoot, M., Mulder, J. P., Hoogvliet, M. M., Jeuken, A. B., van der Krogt, R. A., van Oostrom, N. G., Schelfhout, H. A., van Velzen, E. H., van Waveren, H., et al. (2010). Using adaptation tipping points to prepare for climate change and sea level rise: a case study in the netherlands. *Wiley interdisciplinary reviews: climate change*, 1(5):729–740.

- Kwakkel, J. H., Eker, S., and Pruyt, E. (2016). How robust is a robust policy? comparing alternative robustness metrics for robust decision-making. *Robustness analysis in decision aiding, optimization, and analytics*, pages 221–237.
- Kwakkel, J. H. and Pruyt, E. (2013). Exploratory modeling and analysis, an approach for model-based foresight under deep uncertainty. *Technological Forecasting and Social Change*, 80(3):419–431.
- Kwakkel, J. H., Walker, W. E., and Marchau, V. A. (2010). Adaptive airport strategic planning. *European Journal of Transport and Infrastructure Research*, 10(3).
- Lautze, J., Phiri, Z., Smakhtin, V., and Saruchera, D. (2017). *The Zambezi river basin: water and sustainable development*. Routledge.
- Lempert, R. J. (2003). Shaping the next one hundred years: New methods for quantitative, long-term policy analysis.
- Lempert, R. J. and Collins, M. (2007). Managing the risk of an uncertain threshold response: Comparison of robust, optimum, and precautionary approaches. *Risk Analysis*, 27(4):1009–1026.
- Maharjan, K. L. and Issahaku, Z. A. (2014). Communities and livelihood strategies: An overview. *Communities and Livelihood Strategies in Developing Countries*, pages 1–11.
- Marchau, V. A., Walker, W. E., Bloemen, P. J., and Popper, S. W. (2019). *Decision making under deep uncertainty: from theory to practice*. Springer Nature.
- Munia, H., Guillaume, J., Mirumachi, N., Porkka, M., Wada, Y., and Kummu, M. (2016). Water stress in global transboundary river basins: significance of upstream water use on downstream stress. *Environmental Research Letters*, 11(1):014002.
- Nations, U. (2009). *The United Nations World Water Development Report*. Number 3. UNESCO Pub.
- New, M., Hewitson, B., Stephenson, D. B., Tsiga, A., Kruger, A., Manhique, A., Gomez, B., Coelho, C. A., Masisi, D. N., Kululanga, E., et al. (2006). Evidence of trends in daily climate extremes over southern and west africa. *Journal of Geophysical Research: Atmospheres*, 111(D14).
- Nowak, K., Prairie, J., Rajagopalan, B., and Lall, U. (2010). A nonparametric stochastic approach for multisite disaggregation of annual to daily streamflow. *Water resources research*, 46(8).
- O’Leary, D. T., Charpentier, J.-P., and Minogue, D. (1998). Promoting regional power trade: The southern african power pool.
- Owusu, A., Zatarain Salazar, J., Mul, M., van der Zaag, P., and Slinger, J. (2022). Multi-objective trade-off analysis in operating dams for the environment: The case of the lower volta river. In *EGU General Assembly Conference Abstracts*, pages EGU22–7842.

- Pahl-Wostl, C. (2007). Transitions towards adaptive management of water facing climate and global change. *Water resources management*, 21:49–62.
- Popper, S., Griffin, J. P., Berrebi, C., Light, T., and Min, E. Y. (2009). Natural gas and israel's energy future: A strategic analysis under conditions of deep uncertainty. *RAND policy report*.
- Quinn, J. D., Reed, P. M., Giuliani, M., and Castelletti, A. (2017). Rival framings: A framework for discovering how problem formulation uncertainties shape risk management trade-offs in water resources systems. *Water Resources Research*, 53(8):7208–7233.
- Quinn, J. D., Reed, P. M., Giuliani, M., Castelletti, A., Oyler, J. W., and Nicholas, R. E. (2018). Exploring how changing monsoonal dynamics and human pressures challenge multireservoir management for flood protection, hydropower production, and agricultural water supply. *Water Resources Research*, 54(7):4638–4662.
- Rittel, H. W. and Webber, M. M. (1973). Dilemmas in a general theory of planning. *Policy sciences*, 4(2):155–169.
- Saltelli, A. and Chan, K. (2000). *Scott em: sensitivity analysis*. Wiley, 79:80.
- Savage, L. J. (1972). *The foundations of statistics*. Courier Corporation.
- Schipper, E. L. F. and Burton, I. (2009). Understanding adaptation: origins, concepts, practice and policy. *The earthscan reader on adaptation to climate change*. London, UK and Sterling, VA, USA, pages 1–9.
- Shongwe, M. E., Van Oldenborgh, G., Van Den Hurk, B., De Boer, B., Coelho, C., and Van Aalst, M. (2009). Projected changes in mean and extreme precipitation in africa under global warming. part i: Southern africa. *Journal of climate*, 22(13):3819–3837.
- Tadross, M., Hewitson, B., and Usman, M. (2005). The interannual variability of the onset of the maize growing season over south africa and zimbabwe. *Journal of climate*, 18(16):3356–3372.
- Tsoukiàs, A. (2008). From decision theory to decision aiding methodology. *European journal of operational research*, 187(1):138–161.
- Tumbare, M. J. and Authority, Z. R. (2004). The zambezi river: Its threats and opportunities. In *Zambezi River: It's Threats and Opportunities, 7th River Symposium*, volume 1.
- Turton, A. R. and Ashton, P. J. (2008). Basin closure and issues of scale: The southern african hydrological complex. *International Journal of Water Resources Development*, 24(2):305–318.
- United Nations (September 2015). United nations sustainable development summit 2015. https://sdgs.un.org/goals/goal6#targets_and_indicators. [Accessed 26-03-2024].

- United Nations, Department of Economic and Social Affairs, Population Division (2022). World population prospects 2022, file gen/01/rev1: Demographic indicators by region, subregion and country, annually for 1950-2100, instant-replacement-zero migration variant, 2022 - 2100. Online Edition. Available under a Creative Commons license CC BY 3.0 IGO.
- van Buuren, A. (2019). The dutch delta approach. *Great Policy Successes*, pages 201–217.
- Van Veldhuizen, D. A. and Lamont, G. B. (1998). Multiobjective evolutionary algorithm research: A history and analysis. Technical report TR-98-03, Department of Electrical and Computer Engineering, Air Force Institute of Technology.
- Walker, W. E., Harremoës, P., Rotmans, J., Van Der Sluijs, J. P., Van Asselt, M. B., Janssen, P., and Krayen von Krauss, M. P. (2003). Defining uncertainty: a conceptual basis for uncertainty management in model-based decision support. *Integrated assessment*, 4(1):5–17.
- Walker, W. E., Rahman, S. A., and Cave, J. (2001). Adaptive policies, policy analysis, and policy-making. *European journal of operational Research*, 128(2):282–289.
- Watkins, K. (2006). Human development report 2006-beyond scarcity: Power, poverty and the global water crisis. *UNDP Human Development Reports (2006)*.
- Watkins Jr, D. W. and McKinney, D. C. (1997). Finding robust solutions to water resources problems. *Journal of water resources planning and management*, 123(1):49–58.
- Wheeler, K. G., Basheer, M., Mekonnen, Z. T., Eltoun, S. O., Mersha, A., Abdo, G. M., Zagona, E. A., Hall, J. W., and Dadson, S. J. (2016). Cooperative filling approaches for the grand ethiopian renaissance dam. *Water International*, 41(4):611–634.
- WHO, W. H. O. (1999). Protocol on water and health to the 1992 convention on the protection and use of transboundary watercourses and international lakes, london 17 june 1999. Technical report, World Health Organization. Regional Office for Europe.
- Woodruff, M. J. and Herman, J. D. (2013). `pareto.py`: A python package for multi-objective optimization. Retrieved from <https://github.com/matthewjwoodruff/pareto.py>.
- World Bank, W. (2010). The zambezi river basin a multi-sector investment opportunities analysis. *Modeling, Analysis and Input Data; The World Bank Washington, DC: Washington, DC, USA*, 4:158.
- Zatarain Salazar, J. Z., Castelletti, A., and Giuliani, M. (2022). Multi-objective robust planning tools. In *Oxford Research Encyclopedia of Environmental Science*.
- Zatarain Salazar, J. Z., Reed, P. M., Herman, J. D., Giuliani, M., and Castelletti, A. (2016). A diagnostic assessment of evolutionary algorithms for multi-objective surface water reservoir control. *Advances in water resources*, 92:172–185.

-
- Zatarain Salazar, J. Z. S., Kwakkel, J. H., and Witvliet, M. (2024). Evaluating the choice of radial basis functions in multiobjective optimal control applications. *Environmental Modelling & Software*, 171:105889.
- Zeitoun, M., Goulden, M., and Tickner, D. (2013). Current and future challenges facing transboundary river basin management. *Wiley Interdisciplinary Reviews: Climate Change*, 4(5):331–349.
- Zitzler, E. and Thiele, L. (1999). Multiobjective evolutionary algorithms: A comparative case study and the strength pareto approach. *IEEE Transactions on Evolutionary Computation*, 3(4):257–271.
- Zitzler, E., Thiele, L., Laumanns, M., Fonseca, C. M., and Da Fonseca, V. G. (2003). Performance assessment of multiobjective optimizers: An analysis and review. *IEEE Transactions on evolutionary computation*, 7(2):117–132.

Appendix A

Zambezi Model

A.1 Zambezi Model Model Structure

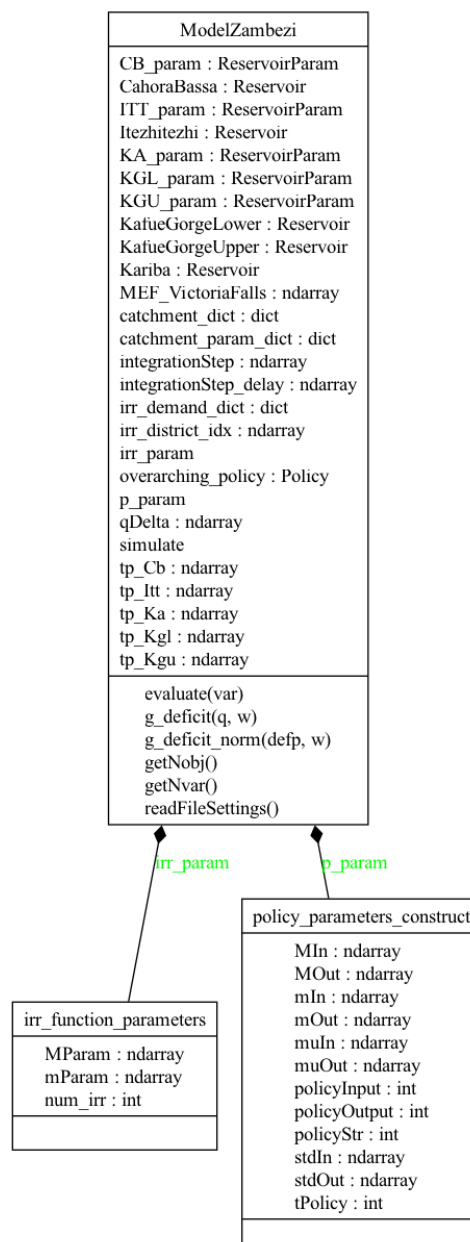


Fig. A.1 UML Overview of the Zambezi Base Case Model.

A.2 Reservoir Class Structure

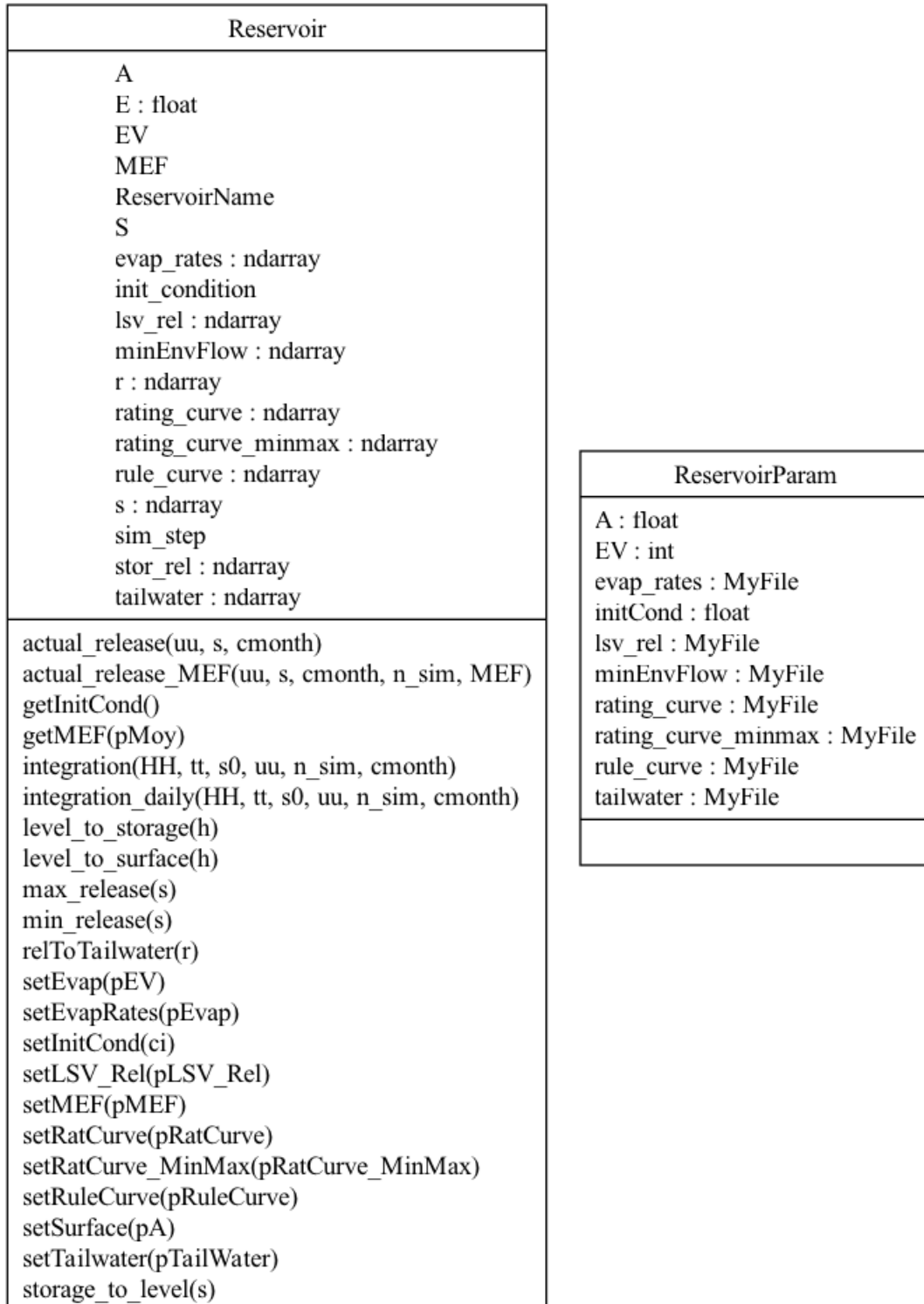


Fig. A.2 UML Overview of the Reservoir Class.

A.3 Catchment Class Structure

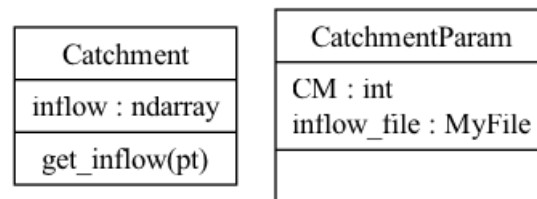


Fig. A.3 UML Overview of the Catchment Class.

A.4 Policy Class Structure

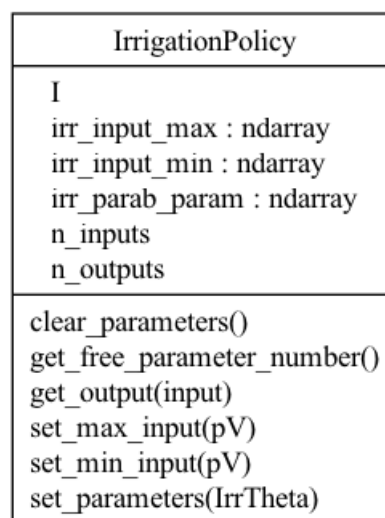


Fig. A.4 UML Overview of the Policy Class.

A.5 Utils Class Structure

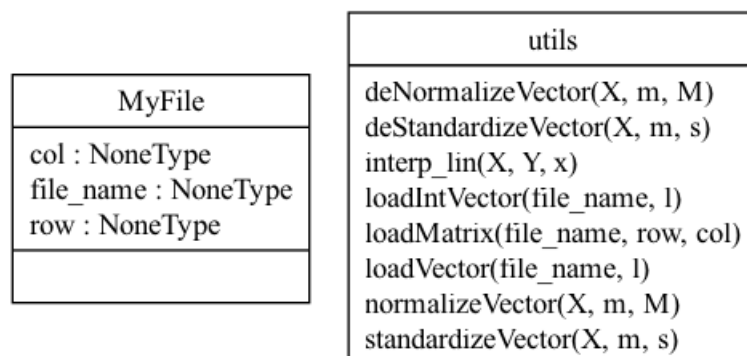


Fig. A.5 UML Overview of the Utils Class.

A.6 Smash Class Structure

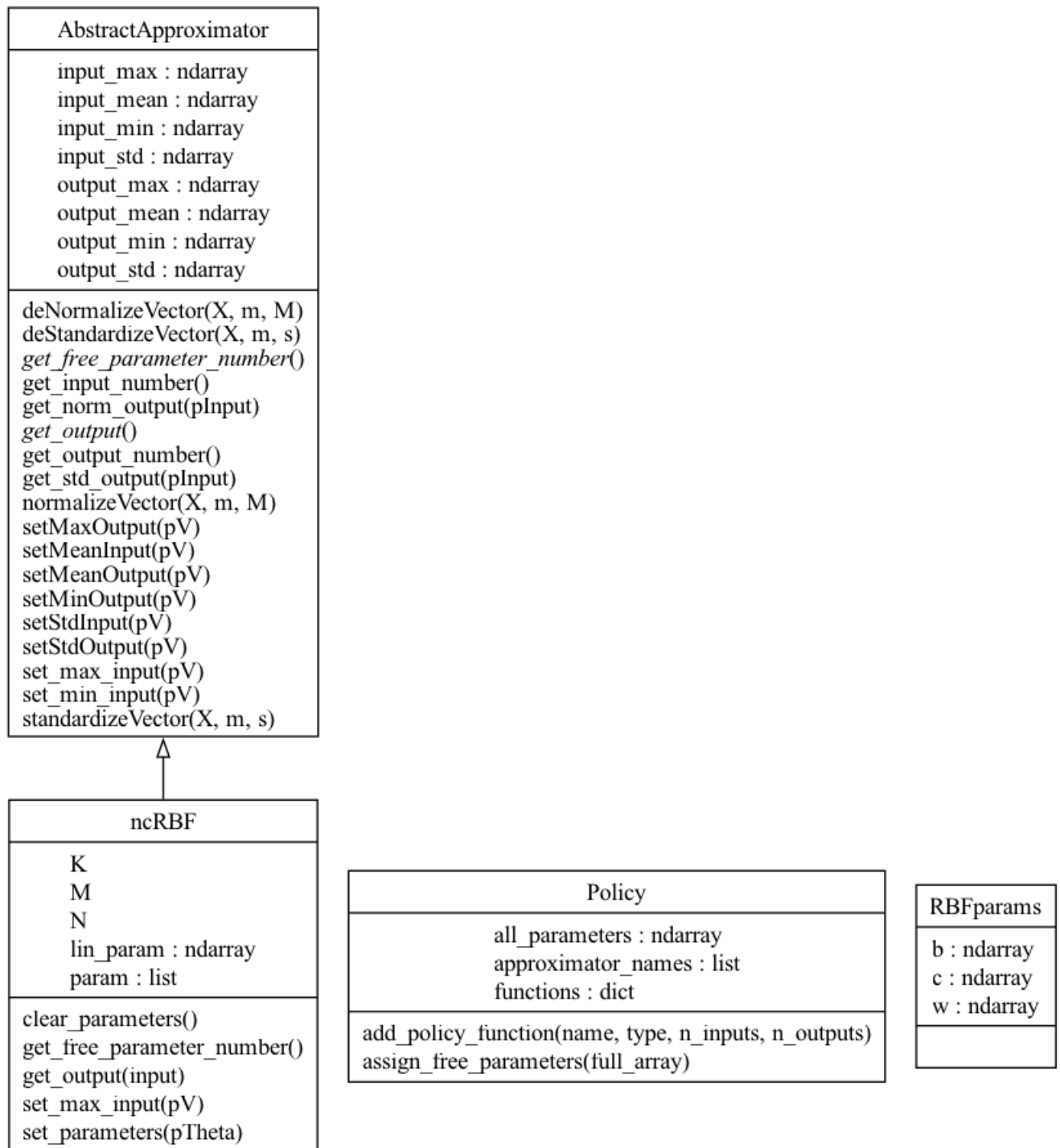


Fig. A.6 UML Overview of the Smash Class.

Appendix B

Base Case Reference Set

B.1 Base Case Pareto-Sets

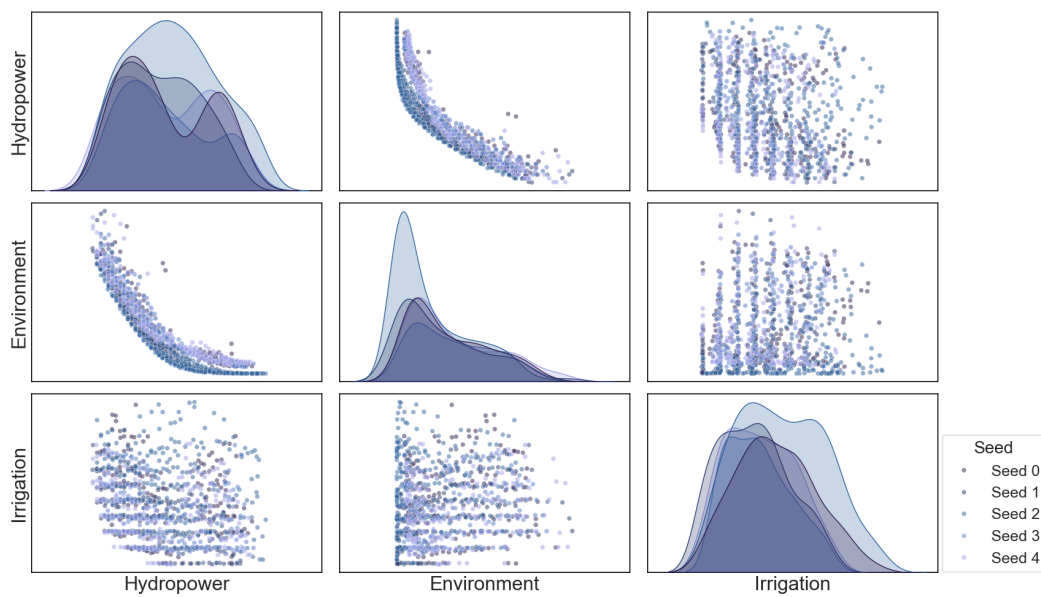


Fig. B.1 Pareto optimal solutions over five seeds across three objectives. Lower objective values indicate better performance. Values are normalized using MinMaxScaler.

B.2 Pareto-Sets across five different seeds

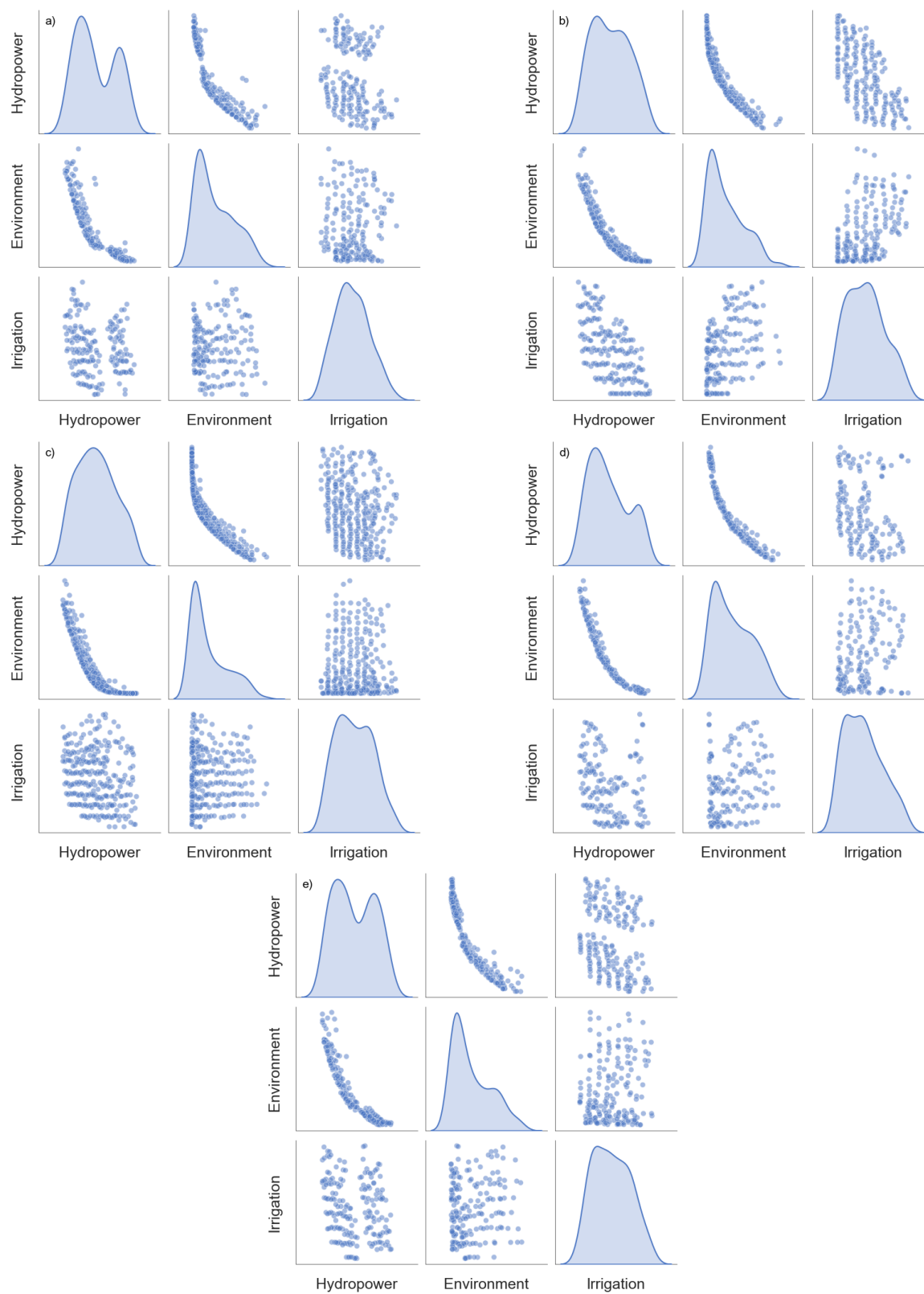


Fig. B.2 Pair plots of the five seeds using scatter plots. Pareto optimal solutions for five seeds from a) Seed 0 to e) Seed 4. The three objectives are hydropower, environment, and irrigation. Lower objective values indicate better performance. Values are normalized using MinMaxScaler.

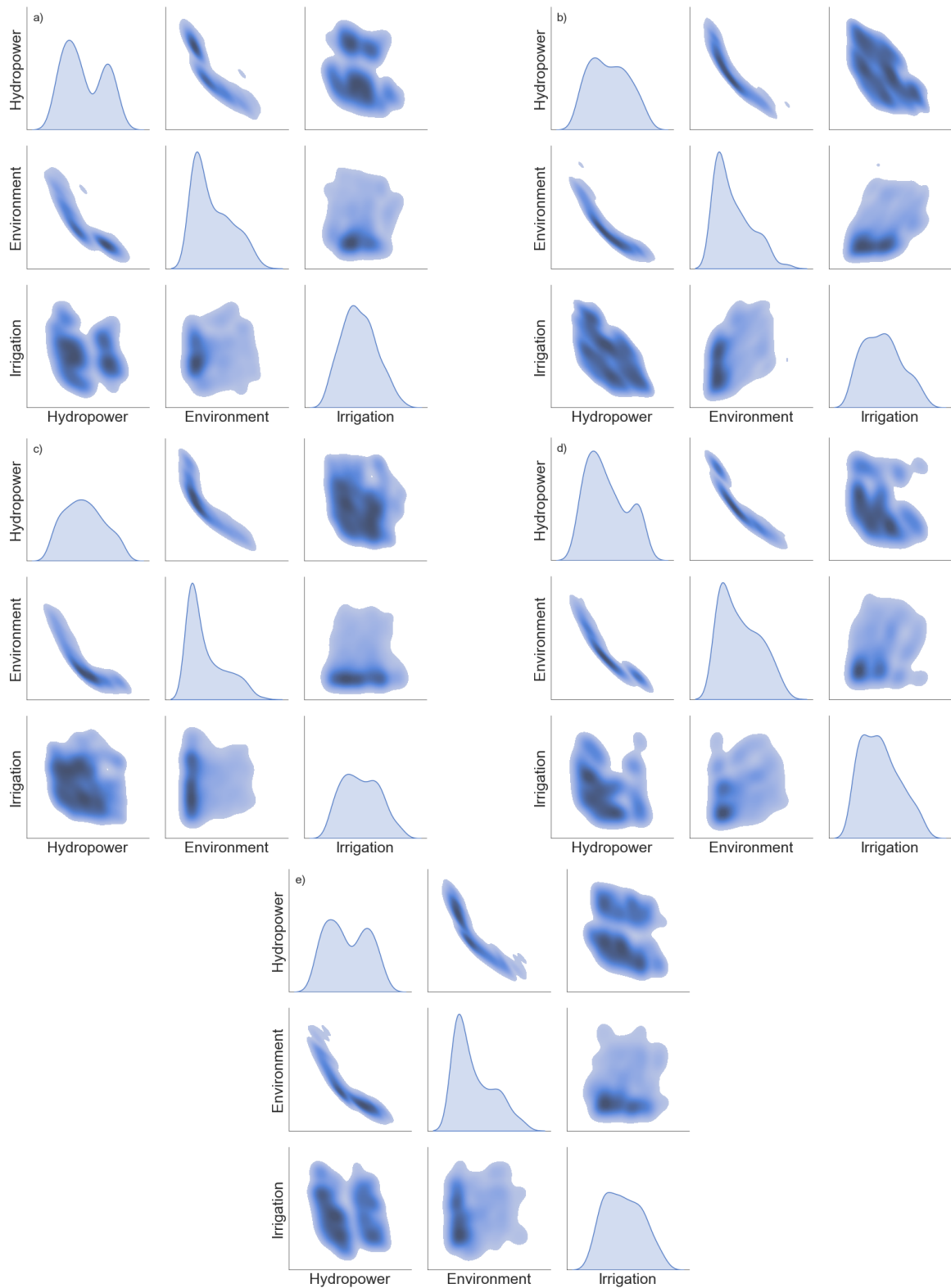


Fig. B.3 Pair plots of the five seeds using kernel density estimates. Pareto optimal solutions for five seeds from a) Seed 0 to e) Seed 4. The three objectives are hydropower, environment, and irrigation. Lower objective values indicate better performance. Values are normalized using MinMaxScaler.

Appendix C

Uncertainty Characterization

C.1 Flow Duration Curves: Historical vs. Synthetic

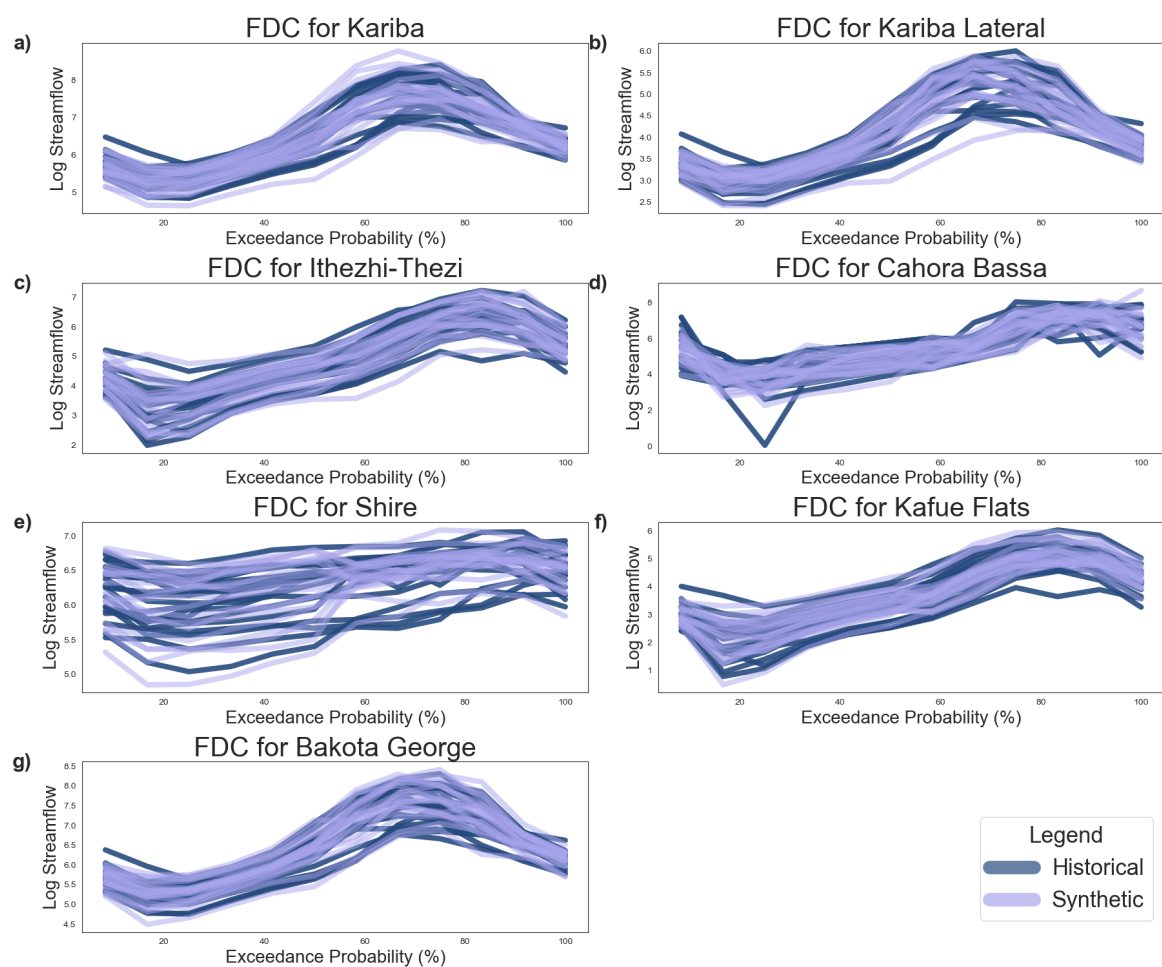


Fig. C.1 Flow Duration Curves of Historic and Synthetic Inflow Data of seven Catchments within the Zambezi River Basin. Panels (a) to (f) display the FDCs for each catchment respectively. Synthetic and historic streamflow data is log-transformed. Each curve represents an FDC over one year. In total, data consists of 20 years.

C.2 Rescaled Mean Precipitation Catchment Inflows

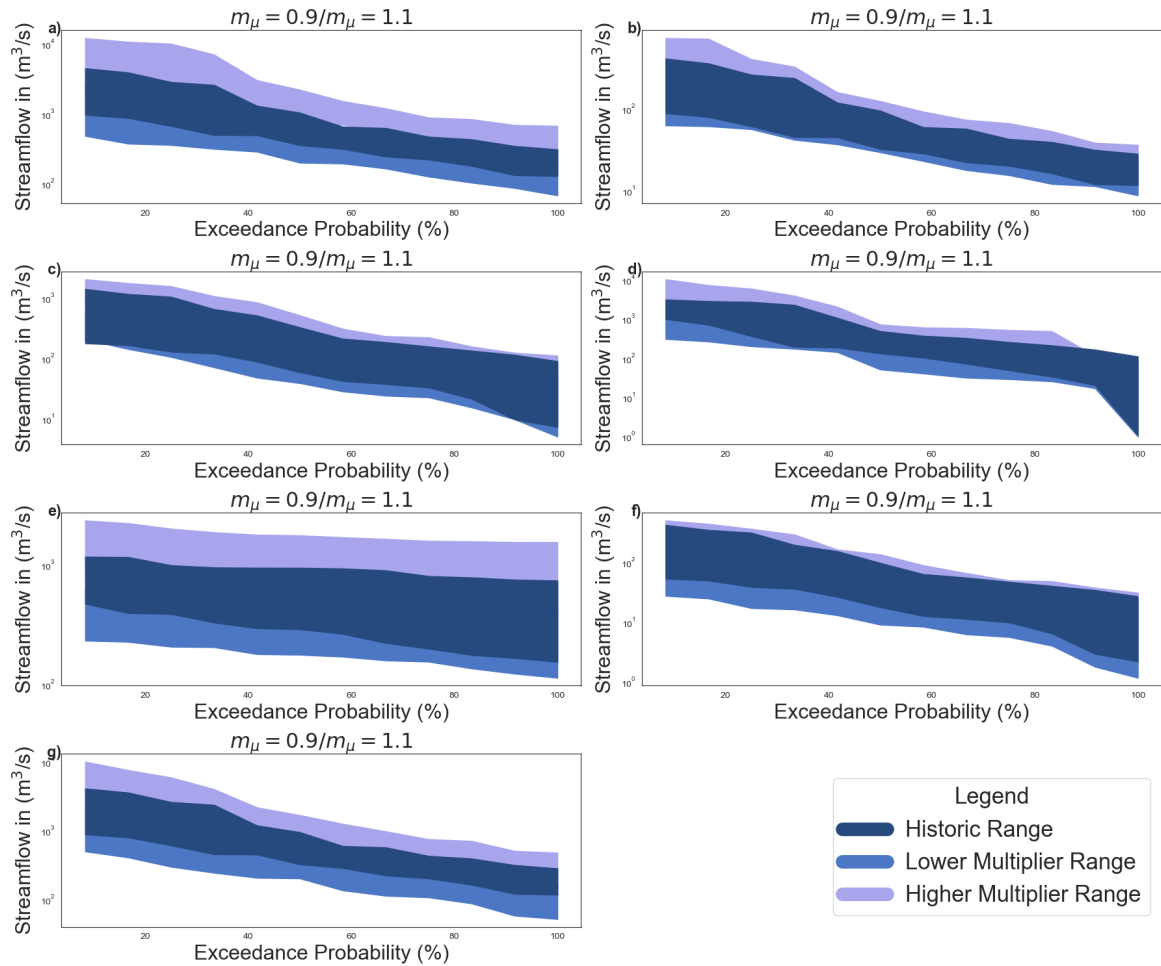


Fig. C.2 Flow Duration Curves of Historic and Rescaled Mean Precipitation Inflow Data of seven Catchments within the Zambezi River Basin. The areas between lower and upper bounds are shaded with their respective color and indicate areas of possible streamflow.

C.3 Rescaled Inter-annual Variability Catchment Inflows

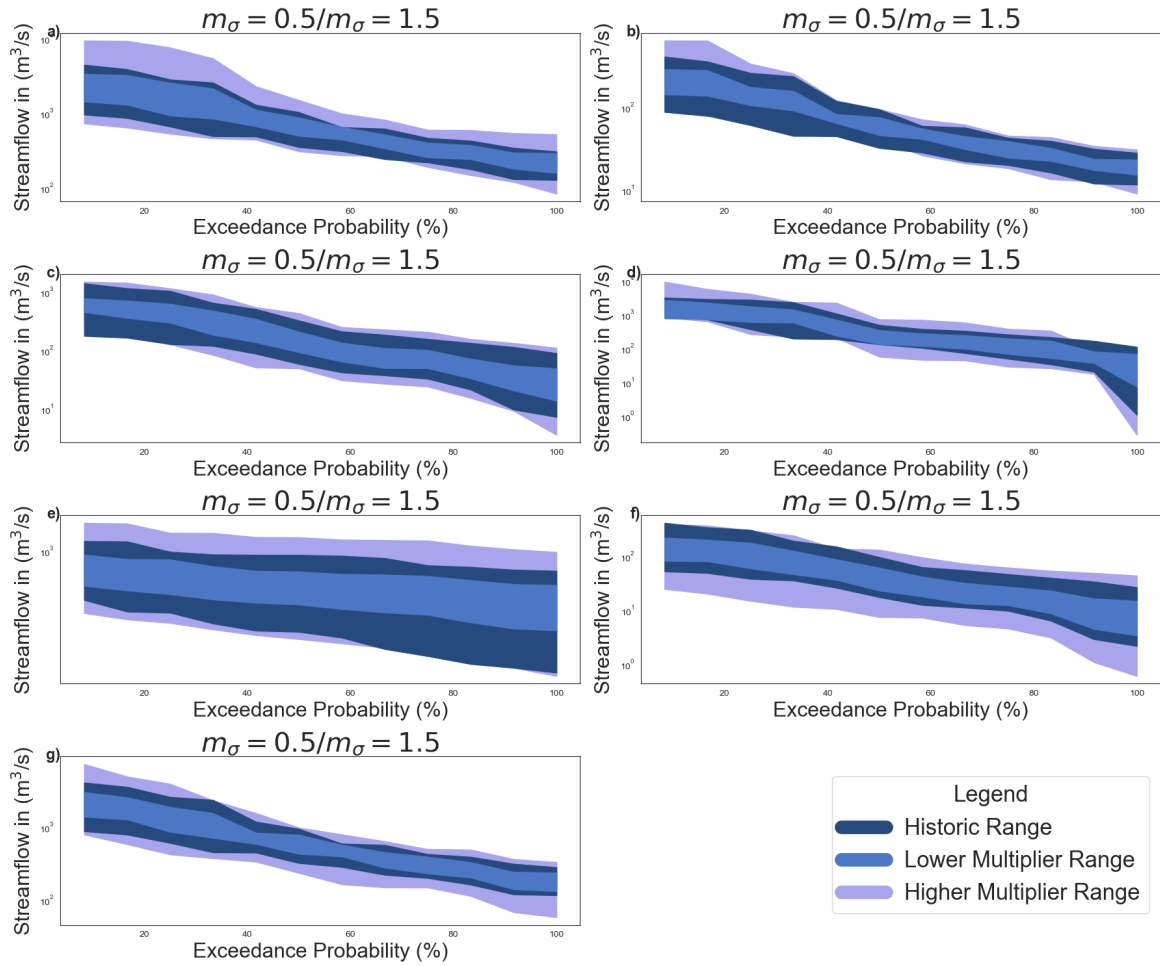


Fig. C.3 Flow Duration Curves of Historic and Rescaled Seasonal Variability Inflow Data of seven Catchments within the Zambezi River Basin. The areas between lower and upper bounds are shaded with their respective color and indicate areas of possible streamflow.

C.4 Fitted Fourier Series over Monthly Average Historical Catchment Inflows

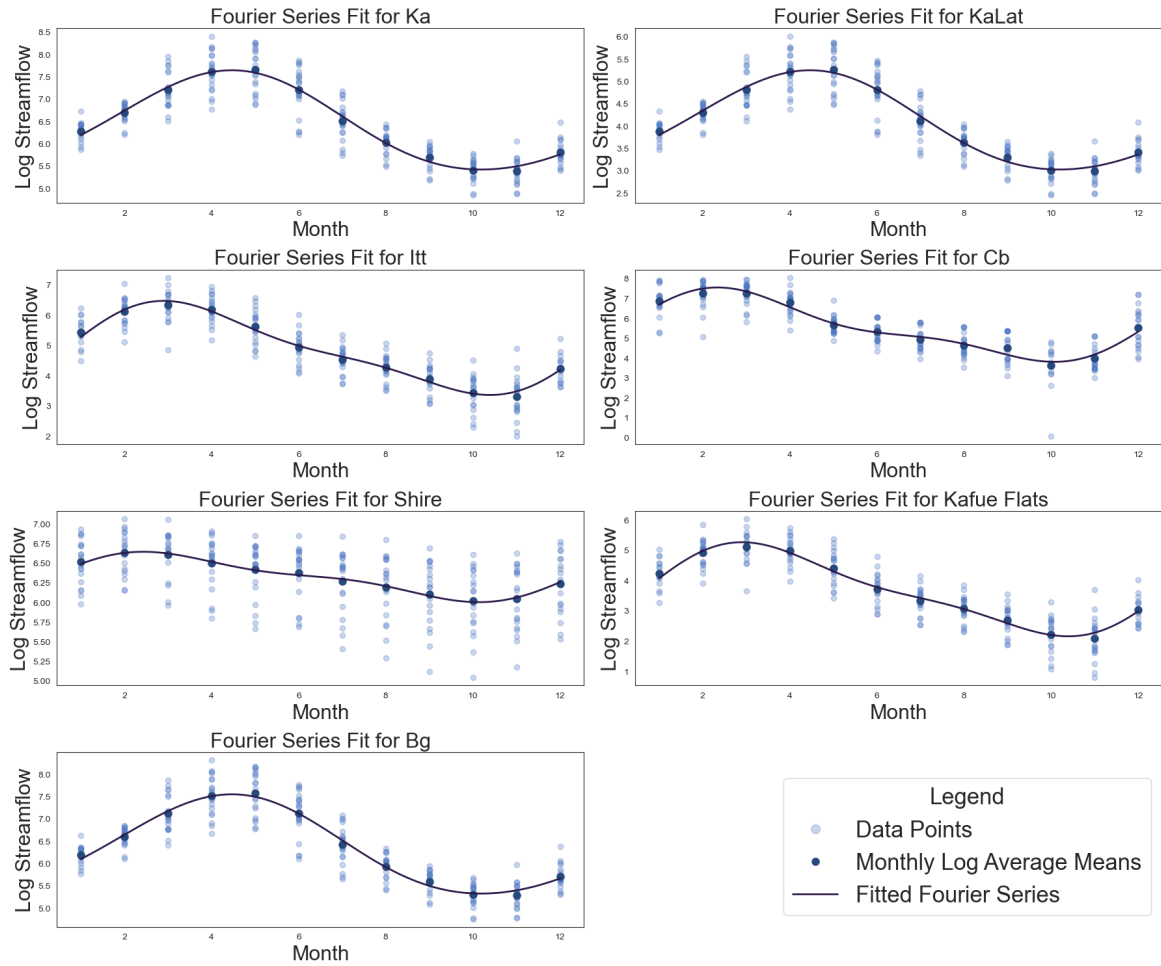


Fig. C.4 Monthly Averages of Historical Streamflow Data with Fitted Fourier Series. Each Dot represents a monthly average value, one for each year (total of 20 years). The fitted Fourier series is displayed as a line.

C.5 Rescaled Seasonal Amplitudes Catchment Inflows

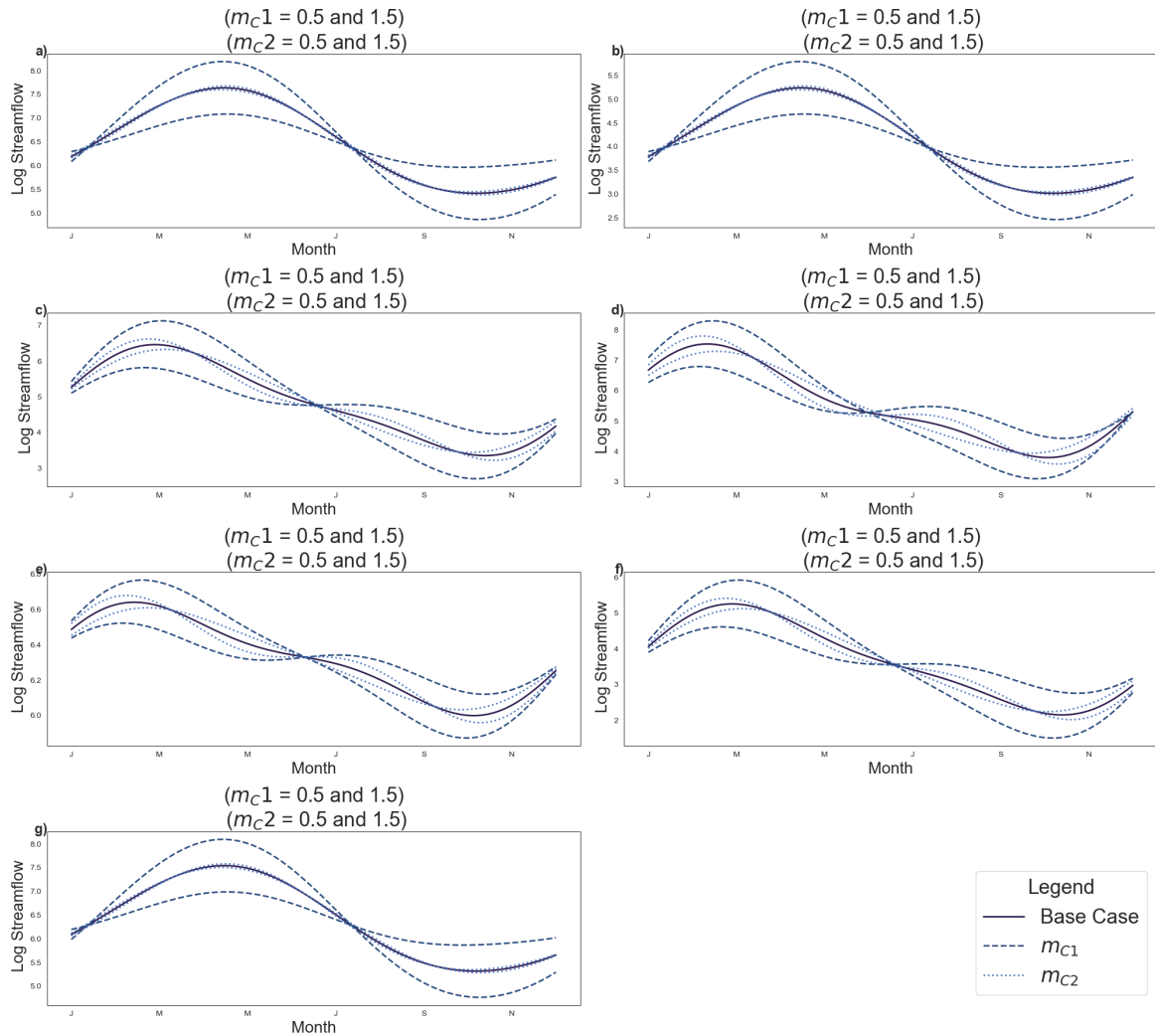


Fig. C.5 Rescaled Seasonal Amplitude Catchment Inflows of seven Catchments within the Zambezi River Basin. Different line types indicate different applied factors. Dash-Dot line representing a lower seasonal amplitude factor. Dashed Lines higher seasonal amplitude factor and solid lines original synthetic seasonal average data. Panels (a) to (f) display the catchment areas of: Kariba, Kariba Lateral, Itthezi-Thezi, Cahora Bassa, Shire, Kafue Flats, and Bakota George.

C.6 Rescaled Seasonal Shift Catchment Inflows

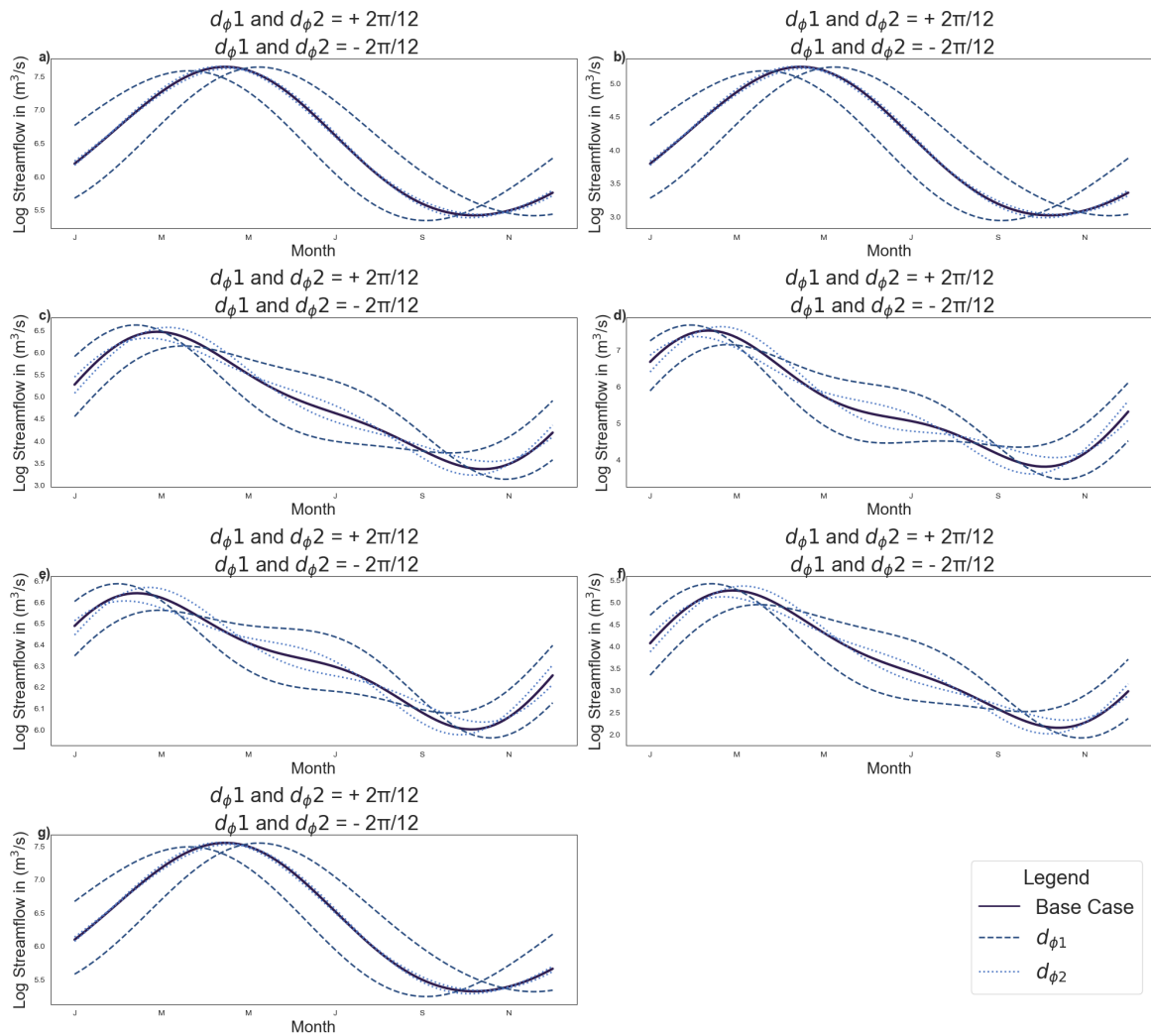


Fig. C.6 Rescaled Seasonal Phase Shift Catchment Inflows of seven Catchments within the Zambezi River Basin. Different line types indicate different applied factors. Dash-Dot line representing a lower seasonal phase-shift factor. Dashed Lines higher seasonal phase-shift factor and solid lines original synthetic seasonal average data. Panels (a) to (f) display the catchment areas of: Kariba, Kariba Lateral, Itthezi-Thezi, Cahora Bassa, Shire, Kafue Flats, and Bakota George.

Appendix D

Scenario Discovery

D.1 Scenarios of Interest

The thesis defines scenarios of interest based on their deviation from desired performance. Performance thresholds are set at the 75th percentile for each key objective: Hydropower, Environment, and Irrigation. This percentile threshold is assumed to capture the most critical scenarios. Each scenario is evaluated against the defined performance thresholds and categorized accordingly.

The distribution of scenarios of interest align with previous insights from Section 5.3.3. No performance gaps are observed for the environmental minimum flow under the Best Environment policy. Similarly, the Best Irrigation and Best Tradeoff policies effectively meet the irrigation objective, as indicated by narrow frequency distributions with peaks near low deficit values in Figure ???. Consequently, these policies are deemed robust with respect to their specific objectives and are excluded from subsequent analysis. Table D.1 summarizes policy distribution according to scenarios of interest.

Table D.1 Policy Distribution Across Different Scenarios of Interest

| Policy | Hydropower Failure | Environment Failure | Irrigation Failure | Overall Failure |
|------------------|---------------------------|----------------------------|---------------------------|------------------------|
| Best Hydropower | 1301 | 15173 | 6559 | 1134 |
| Best Environment | 14206 | - | 18441 | - |
| Best Irrigation | 7310 | 2348 | - | - |
| Best Tradeoff | 2183 | 7479 | - | - |

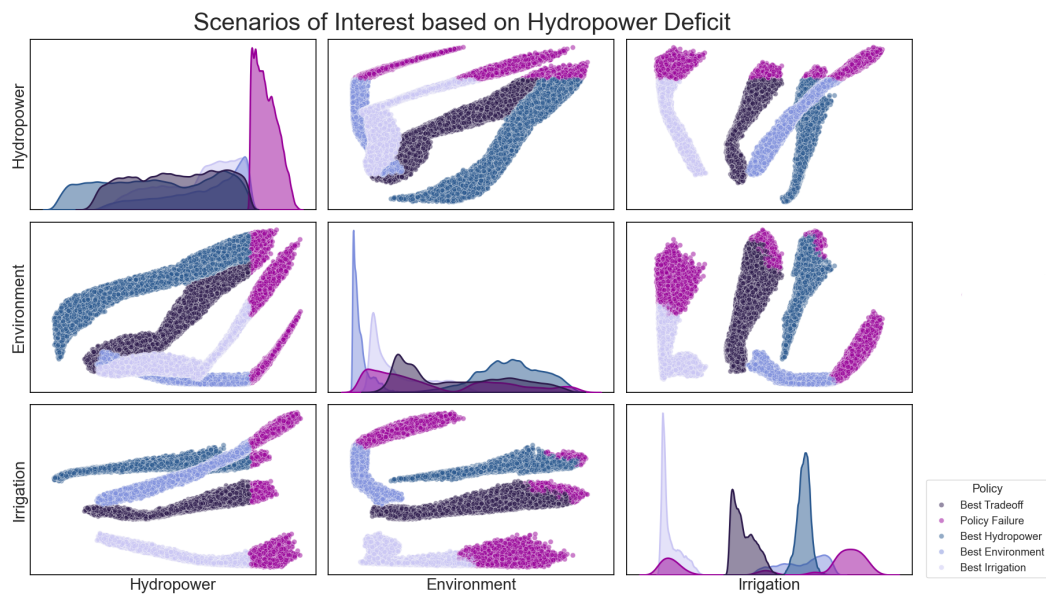


Fig. D.1 Scenarios of Interest (Hydropower Performance Failure). Dots represent objective values across 100,000 states of the world. Colors indicate policy specific scenario outcomes (25,000). Scenarios of interest describe worst 20 percent of hydropower outcomes highlighted in dark purple.

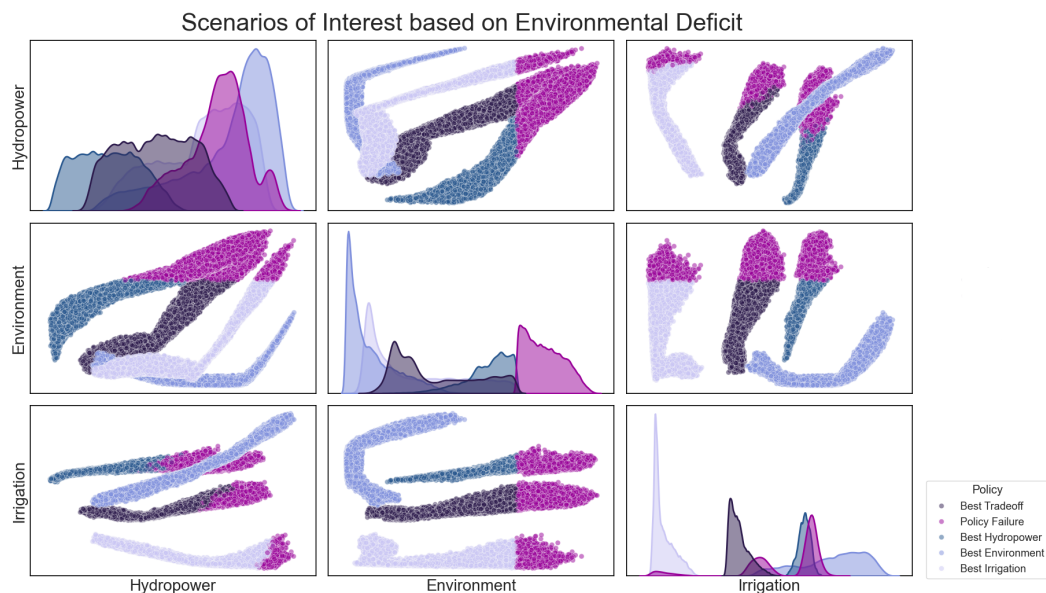


Fig. D.2 Scenarios of Interest based on Environmental Performance Failure. Dots represent objective values across 100,000 states of the world. Colors indicate policy specific scenario outcomes (25,000). Scenarios of interest describe worst 20 percent of environmental outcomes highlighted in dark purple.

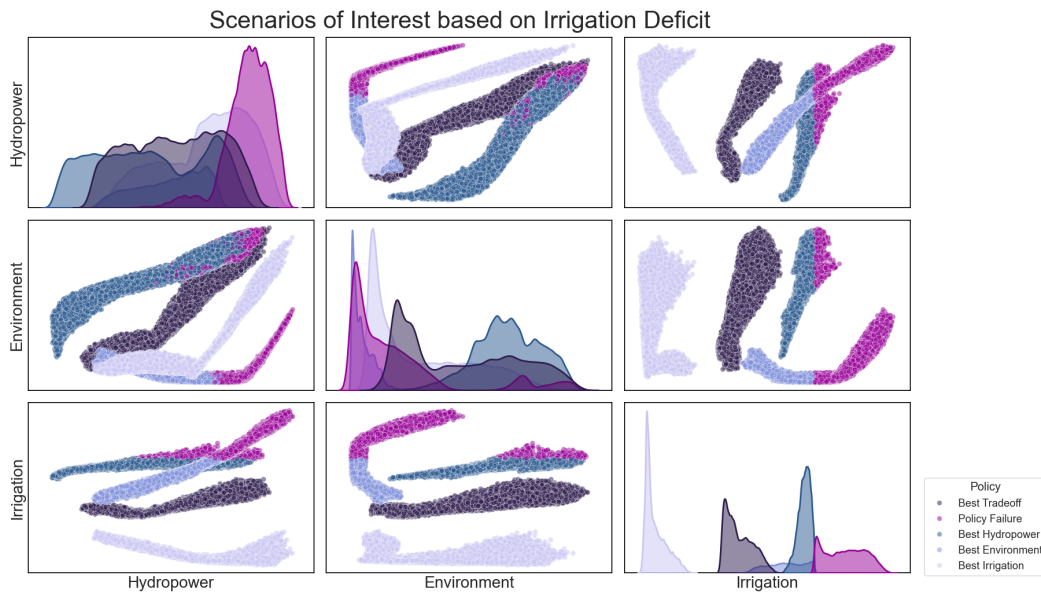


Fig. D.3 Scenarios of Interest based on Irrigation Performance Failure. Dots represent objective values across 100,000 states of the world. Colors indicate policy specific scenario outcomes (25,000). Scenarios of interest describe worst 20 percent of irrigation outcome highlighted in dark purple.

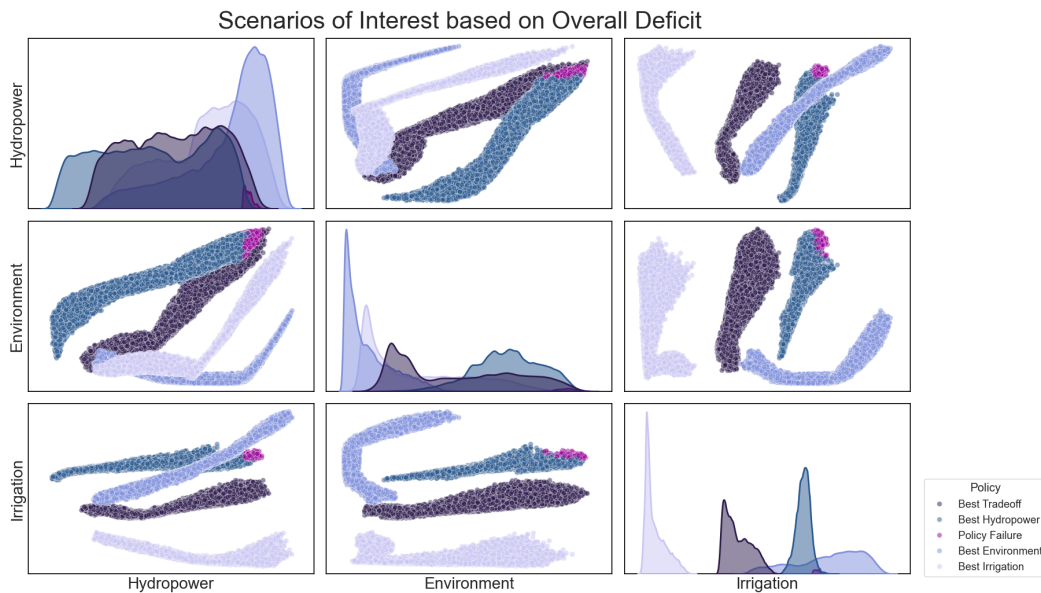


Fig. D.4 Scenarios of Interest based on Overall Performance Failure. Dots represent objective values across 100,000 states of the world. Colors indicate policy specific scenario outcomes (25,000). Scenarios of interest describe the scenarios that are in the worst 20 percent across all three objective (total number of 1134 scenarios) highlighted in dark purple.

D.2 PRIM Density-Coverage Tradeoff Plots (Best Hydropower Policy)

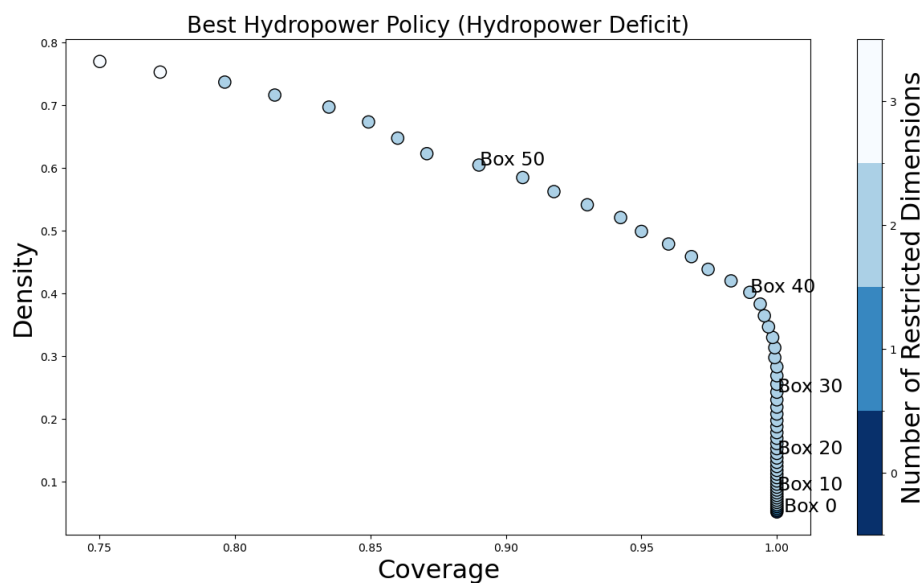


Fig. D.5 PRIM Density - Coverage Tradeoff Plot for the Best Hydropower Policy identifying hydropower deficit scenarios. Each scatter dot represents a scenario box. The color coding indicates the total number of uncertainty factors that are needed to describe the box.

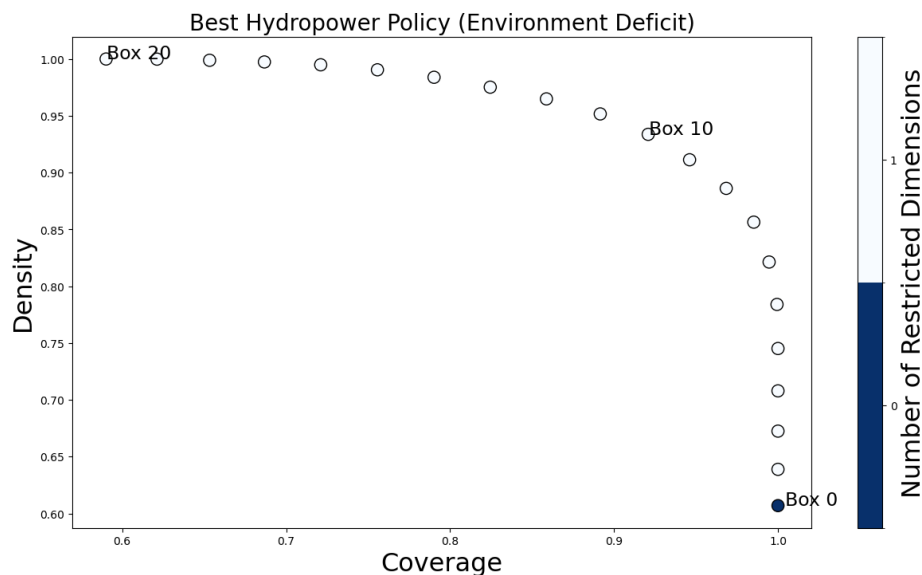


Fig. D.6 PRIM Density - Coverage Tradeoff Plot for the Best Hydropower Policy identifying environmental deficit scenarios. Each scatter dot represents a scenario box. The color coding indicates the total number of uncertainty factors that are needed to describe the box.

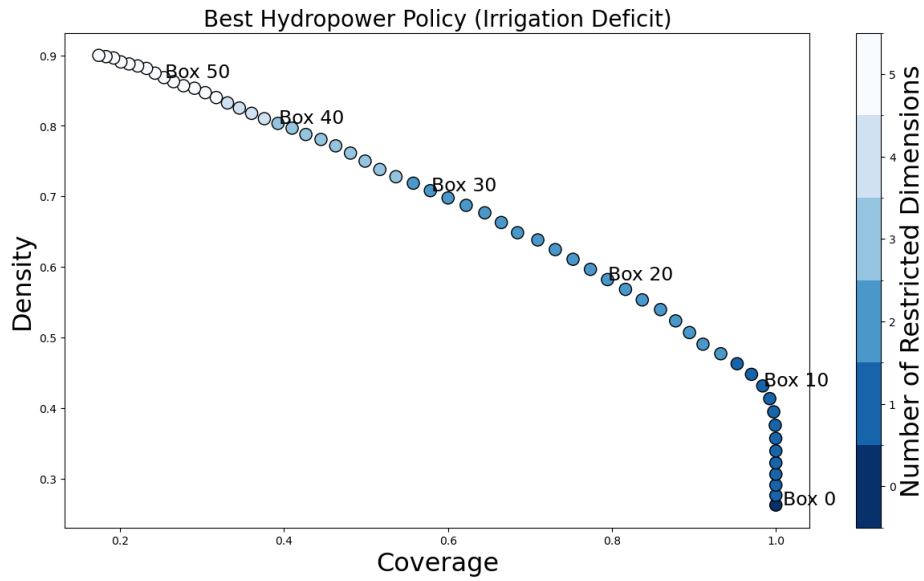


Fig. D.7 PRIM Density - Coverage Tradeoff Plot for the Best Hydropower Policy identifying irrigation deficit scenarios. Each scatter dot represents a scenario box. The color coding indicates the total number of uncertainty factors that are needed to describe the box.

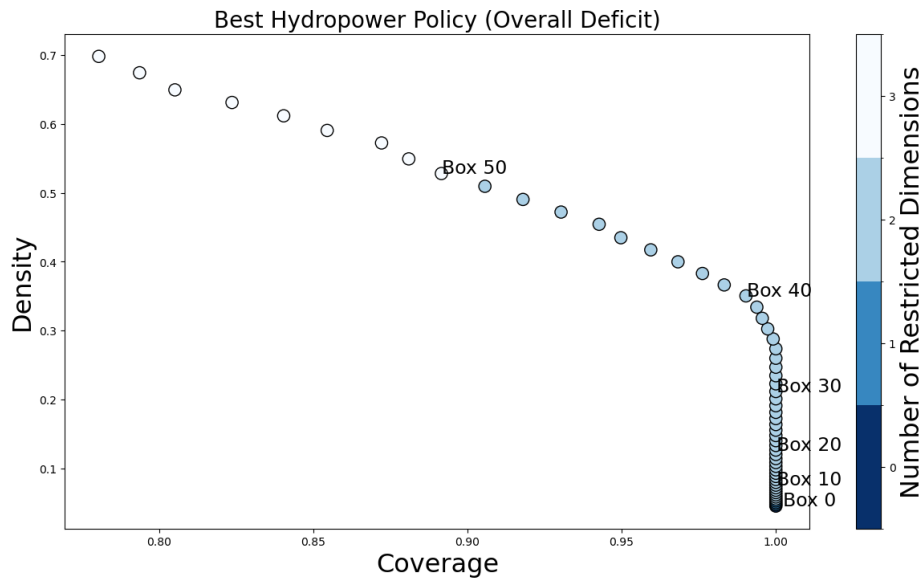


Fig. D.8 PRIM Density - Coverage Tradeoff Plot for the Best Hydropower Policy identifying overall deficit scenarios. Each scatter dot represents a scenario box. The color coding indicates the total number of uncertainty factors that are needed to describe the box.

D.3 PRIM Density-Coverage Tradeoff Plots (Best Environment Policy)

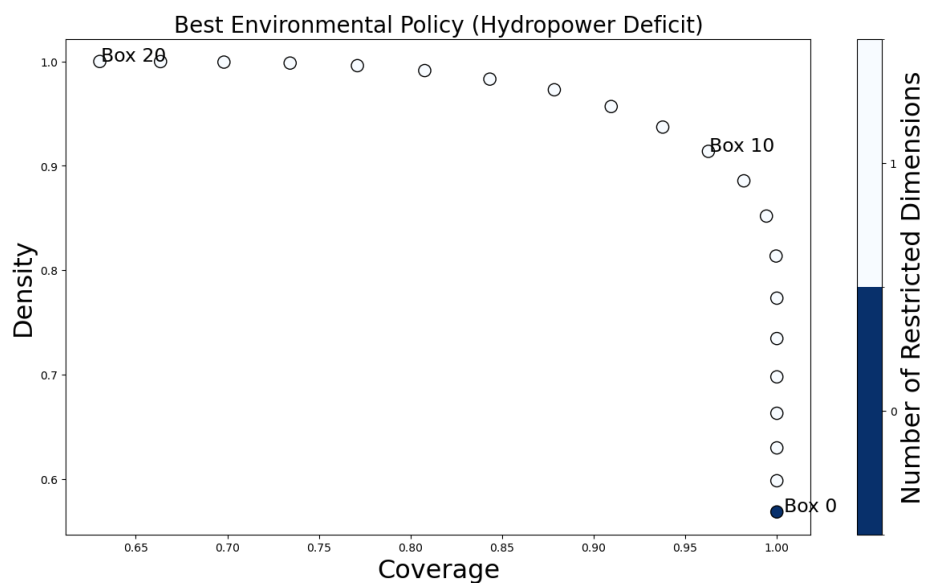


Fig. D.9 PRIM Density - Coverage Tradeoff Plot for the Best Hydropower Policy identifying hydropower deficit scenarios. Each scatter dot represents a scenario box. The color coding indicates the total number of uncertainty factors that are needed to describe the box.

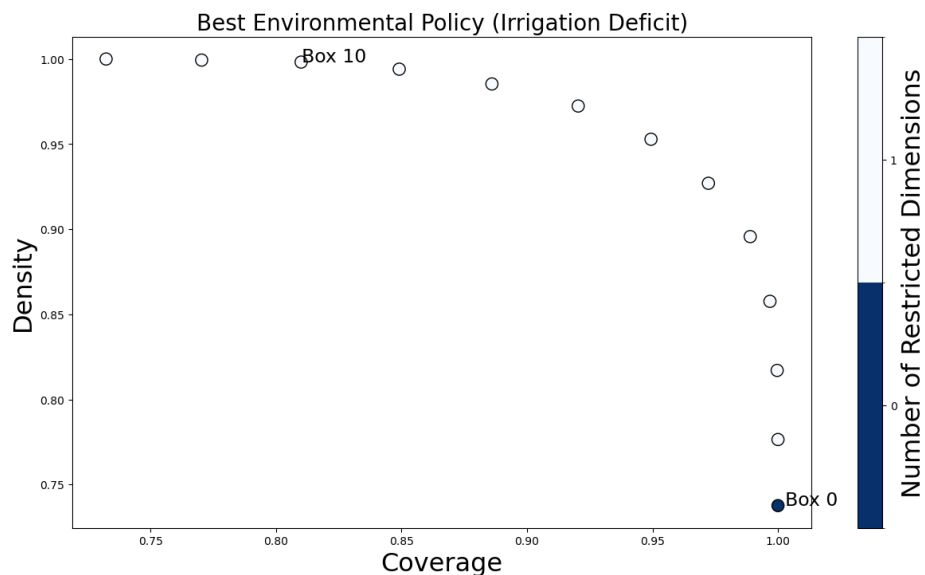


Fig. D.10 PRIM Density - Coverage Tradeoff Plot for the Best Hydropower Policy identifying irrigation deficit scenarios. Each scatter dot represents a scenario box. The color coding indicates the total number of uncertainty factors that are needed to describe the box.

D.4 PRIM Density-Coverage Tradeoff Plots (Best Irrigation Policy)

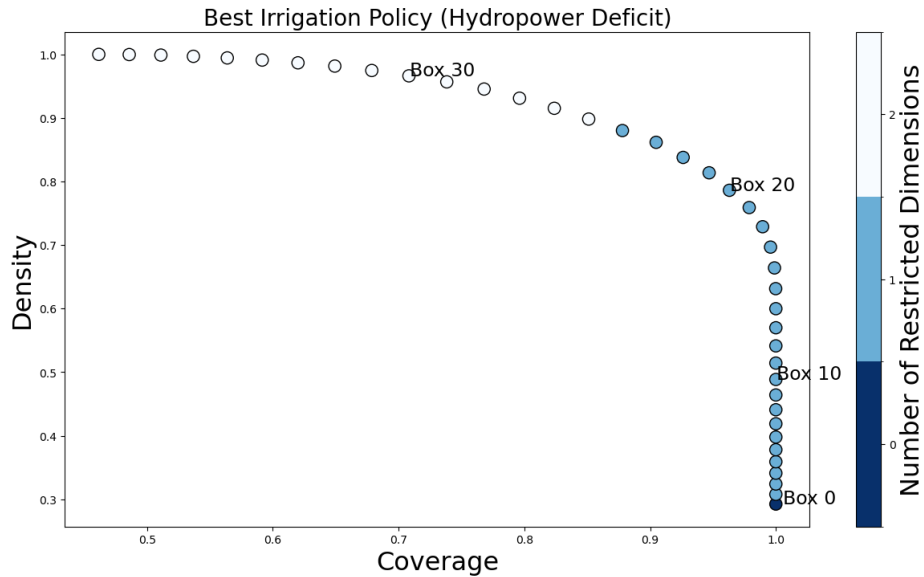


Fig. D.11 PRIM Density - Coverage Tradeoff Plot for the Best Hydropower Policy identifying hydropower deficit scenarios. Each scatter dot represents a scenario box. The color coding indicates the total number of uncertainty factors that are needed to describe the box.

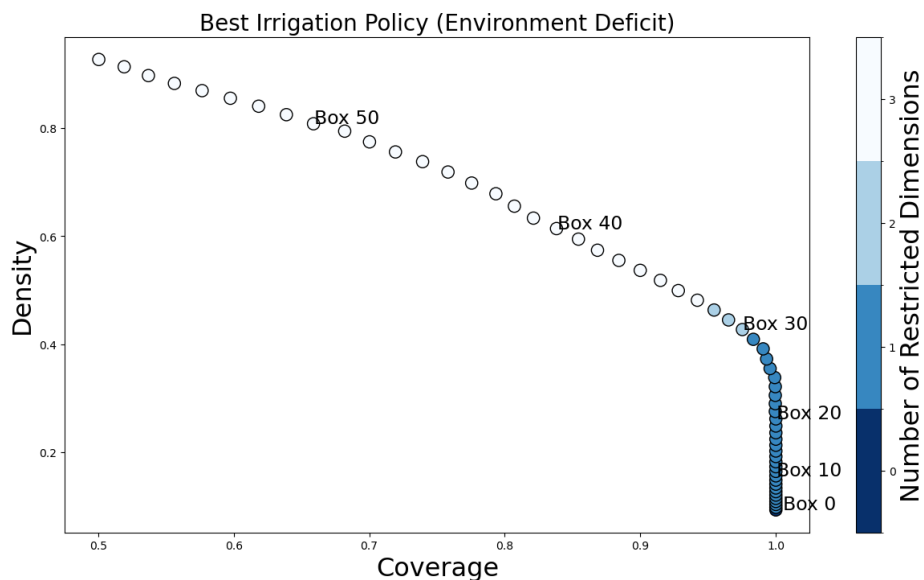


Fig. D.12 PRIM Density - Coverage Tradeoff Plot for the Best Hydropower Policy identifying environmental deficit scenarios. Each scatter dot represents a scenario box. The color coding indicates the total number of uncertainty factors that are needed to describe the box.

D.5 PRIM Density-Coverage Tradeoff Plots (Best Tradeoff Policy)

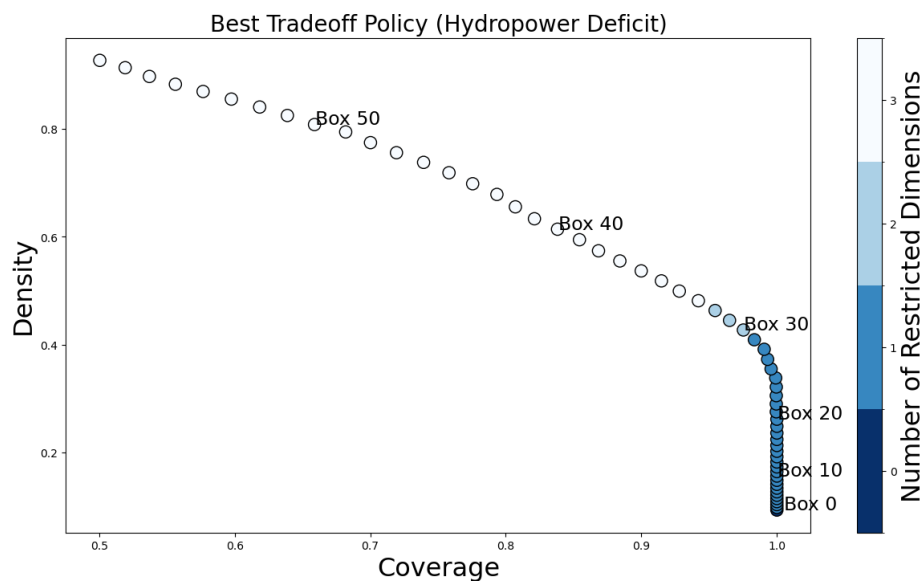


Fig. D.13 PRIM Density - Coverage Tradeoff Plot for the Best Hydropower Policy identifying hydropower deficit scenarios. Each scatter dot represents a scenario box. The color coding indicates the total number of uncertainty factors that are needed to describe the box.

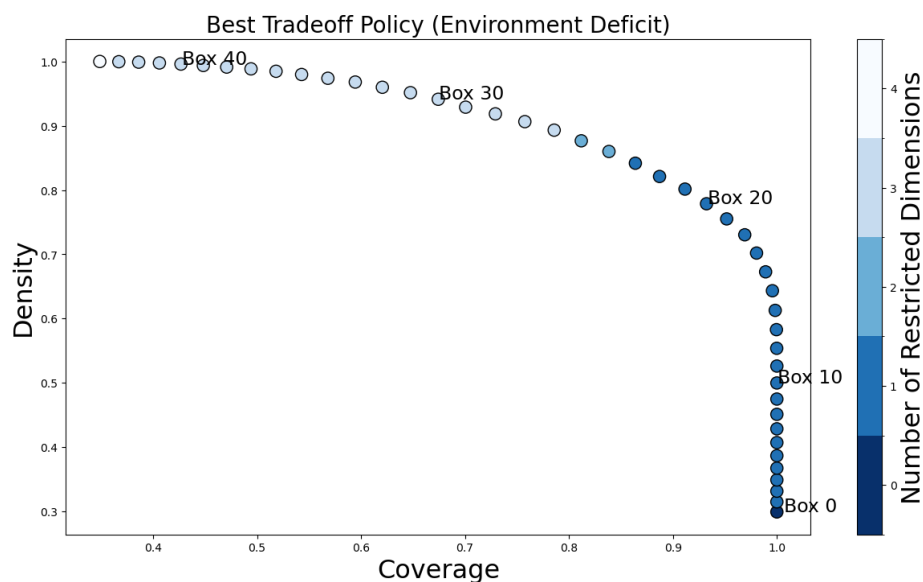


Fig. D.14 PRIM Density - Coverage Tradeoff Plot for the Best Hydropower Policy identifying environmental deficit scenarios. Each scatter dot represents a scenario box. The color coding indicates the total number of uncertainty factors that are needed to describe the box.

D.6 PRIM Scenario Box Tables

Table D.2 Best Hydropower Policy Analysis for Hydropower Deficit Scenario

| Box ID | Coverage | Density | Uncertainty Factor | Min | Max |
|--------|----------|---------|--------------------|-------|-------|
| 1 | 1.00 | 0.05 | mC1 | 0.80 | 1.18 |
| 5 | 1.00 | 0.07 | mC1 | 0.80 | 1.14 |
| | | | m_mu | 0.90 | 1.04 |
| 10 | 1.00 | 0.09 | m_mu | 0.90 | 1.00 |
| | | | mC1 | 0.80 | 1.14 |
| 15 | 1.00 | 0.11 | m_mu | 0.90 | 0.98 |
| | | | mC1 | 0.80 | 1.14 |
| 20 | 1.00 | 0.15 | m_mu | 0.90 | 0.96 |
| | | | mC1 | 0.80 | 1.14 |
| 25 | 1.00 | 0.19 | m_mu | 0.90 | 0.95 |
| | | | mC1 | 0.80 | 1.14 |
| 30 | 1.00 | 0.24 | m_mu | 0.90 | 0.94 |
| | | | mC1 | 0.80 | 1.14 |
| 35 | 1.00 | 0.31 | m_mu | 0.90 | 0.93 |
| | | | mC1 | 0.80 | 1.14 |
| 40 | 1.00 | 0.40 | m_mu | 0.90 | 0.93 |
| | | | mC1 | 0.80 | 1.10 |
| 45 | 0.95 | 0.50 | m_mu | 0.90 | 0.92 |
| | | | mC1 | 0.80 | 1.07 |
| 50 | 0.89 | 0.60 | m_mu | 0.90 | 0.92 |
| | | | mC1 | 0.80 | 1.01 |
| 55 | 0.81 | 0.72 | m_mu | 0.90 | 0.92 |
| | | | mC1 | 0.80 | 1.01 |
| 58 | 0.75 | 0.77 | m_mu | 0.90 | 0.92 |
| | | | mC1 | 0.80 | 1.01 |
| | | | delta_evaporation | -5.09 | 40.00 |

Table D.3 Best Hydropower Policy Analysis for Environment Deficit Scenario

| Box ID | Coverage | Density | Uncertainty Factor | Min | Max |
|---------------|-----------------|----------------|---------------------------|------------|------------|
| 1 | 1.00 | 0.64 | m_mu | 0.90 | 1.04 |
| 5 | 1.00 | 0.78 | m_mu | 0.90 | 1.02 |
| 10 | 0.92 | 0.93 | m_mu | 0.90 | 0.99 |
| 15 | 0.76 | 0.99 | m_mu | 0.90 | 0.97 |
| 20 | 0.59 | 1.00 | m_mu | 0.90 | 0.95 |

Table D.4 Best Hydropower Policy Analysis for Irrigation Deficit Scenario

| Box ID | Coverage | Density | Uncertainty Factor | Min | Max |
|--------|----------|---------|--------------------|-------|-------|
| 1 | 1.00 | 0.28 | m_mu | 0.90 | 1.04 |
| 5 | 1.00 | 0.34 | m_mu | 0.90 | 1.02 |
| 10 | 0.98 | 0.43 | m_mu | 0.90 | 0.99 |
| 15 | 0.89 | 0.51 | m_mu | 0.90 | 0.98 |
| | | | demand_multiplier | 1.00 | 1.03 |
| 20 | 0.79 | 0.58 | m_mu | 0.90 | 0.98 |
| | | | demand_multiplier | 1.00 | 1.02 |
| 25 | 0.68 | 0.65 | m_mu | 0.90 | 0.98 |
| | | | demand_multiplier | 1.00 | 1.02 |
| 30 | 0.58 | 0.71 | m_mu | 0.90 | 0.98 |
| | | | demand_multiplier | 1.00 | 1.01 |
| 35 | 0.48 | 0.76 | m_mu | 0.90 | 0.98 |
| | | | demand_multiplier | 1.00 | 1.01 |
| | | | delta_evaporation | -0.31 | 40.00 |
| 40 | 0.39 | 0.80 | m_mu | 0.90 | 0.98 |
| | | | demand_multiplier | 1.00 | 1.01 |
| | | | delta_evaporation | 3.61 | 40.00 |
| 45 | 0.32 | 0.84 | m_mu | 0.90 | 0.98 |
| | | | demand_multiplier | 1.00 | 1.01 |
| | | | delta_evaporation | 3.61 | 40.00 |
| | | | mC1 | 0.87 | 1.20 |
| | | | m_sigma | 0.96 | 1.20 |
| 50 | 0.25 | 0.87 | m_mu | 0.90 | 0.98 |
| | | | demand_multiplier | 1.00 | 1.01 |
| | | | delta_evaporation | 10.22 | 40.00 |
| | | | mC1 | 0.87 | 1.20 |
| | | | m_sigma | 0.96 | 1.20 |
| 55 | 0.20 | 0.89 | m_mu | 0.90 | 0.97 |
| | | | demand_multiplier | 1.00 | 1.01 |
| | | | delta_evaporation | 14.97 | 40.00 |
| | | | mC1 | 0.87 | 1.20 |
| | | | m_sigma | 0.96 | 1.20 |
| 58 | 0.17 | 0.90 | m_mu | 0.90 | 0.97 |
| | | | demand_multiplier | 1.00 | 1.01 |
| | | | delta_evaporation | 17.38 | 40.00 |
| | | | mC1 | 0.87 | 1.20 |
| | | | m_sigma | 0.96 | 1.20 |

Table D.5 Best Hydropower Policy Analysis for Overall Deficit Scenario

| Box ID | Coverage | Density | Uncertainty Factor | Min | Max |
|--------|----------|---------|--------------------|-------|-------|
| 1 | 1.00 | 0.05 | mC1 | 0.80 | 1.18 |
| 5 | 1.00 | 0.06 | mC1 | 0.80 | 1.14 |
| | | | m_mu | 0.90 | 1.04 |
| 10 | 1.00 | 0.08 | m_mu | 0.90 | 1.00 |
| | | | mC1 | 0.80 | 1.14 |
| 15 | 1.00 | 0.10 | m_mu | 0.90 | 0.98 |
| | | | mC1 | 0.80 | 1.14 |
| 20 | 1.00 | 0.13 | m_mu | 0.90 | 0.96 |
| | | | mC1 | 0.80 | 1.14 |
| 25 | 1.00 | 0.16 | m_mu | 0.90 | 0.95 |
| | | | mC1 | 0.80 | 1.14 |
| 30 | 1.00 | 0.21 | m_mu | 0.90 | 0.94 |
| | | | mC1 | 0.80 | 1.14 |
| 35 | 1.00 | 0.27 | m_mu | 0.90 | 0.93 |
| | | | mC1 | 0.80 | 1.14 |
| 40 | 0.99 | 0.35 | m_mu | 0.90 | 0.93 |
| | | | mC1 | 0.80 | 1.10 |
| 45 | 0.95 | 0.43 | m_mu | 0.90 | 0.92 |
| | | | mC1 | 0.80 | 1.07 |
| 50 | 0.89 | 0.53 | m_mu | 0.90 | 0.92 |
| | | | mC1 | 0.80 | 1.02 |
| | | | delta_evaporation | -7.41 | 40.00 |
| 55 | 0.82 | 0.63 | m_mu | 0.90 | 0.92 |
| | | | mC1 | 0.80 | 1.01 |
| | | | delta_evaporation | 1.26 | 40.00 |
| 58 | 0.78 | 0.70 | m_mu | 0.90 | 0.92 |
| | | | mC1 | 0.80 | 1.01 |
| | | | delta_evaporation | 1.26 | 40.00 |

Table D.6 Best Environment Policy Analysis for Hydropower Deficit Scenario

| Box ID | Coverage | Density | Uncertainty Factor | Min | Max |
|---------------|-----------------|----------------|---------------------------|------------|------------|
| 0 | 1.00 | 0.57 | m_mu | 0.90 | 1.04 |
| 1 | 1.00 | 0.60 | m_mu | 0.90 | 1.04 |
| 5 | 1.00 | 0.73 | m_mu | 0.90 | 1.02 |
| 10 | 0.96 | 0.91 | m_mu | 0.90 | 0.99 |
| 15 | 0.81 | 0.99 | m_mu | 0.90 | 0.97 |
| 20 | 0.63 | 1.00 | m_mu | 0.90 | 0.95 |

Table D.7 Best Environment Policy Analysis for Irrigation Deficit Scenario

| Box ID | Coverage | Density | Uncertainty Factor | Min | Max |
|---------------|-----------------|----------------|---------------------------|------------|------------|
| 0 | 1.00 | 0.74 | m_mu | 0.90 | 1.04 |
| 1 | 1.00 | 0.78 | m_mu | 0.90 | 1.04 |
| 5 | 0.97 | 0.92 | m_mu | 0.90 | 1.02 |
| 10 | 0.81 | 0.99 | m_mu | 0.90 | 0.99 |
| 11 | 0.77 | 0.99 | m_mu | 0.90 | 0.96 |

Table D.8 Best Irrigation Policy Analysis for Hydropower Deficit Scenario

| Box ID | Coverage | Density | Uncertainty Factor | Min | Max |
|--------|----------|---------|--------------------|------|------|
| 1 | 1.00 | 0.31 | m_mu | 0.90 | 1.04 |
| 5 | 1.00 | 0.38 | m_mu | 0.90 | 1.02 |
| 10 | 1.00 | 0.49 | m_mu | 0.90 | 0.99 |
| 15 | 1.00 | 0.63 | m_mu | 0.90 | 0.97 |
| 20 | 0.96 | 0.79 | m_mu | 0.90 | 0.95 |
| 25 | 0.85 | 0.90 | m_mu | 0.90 | 0.94 |
| | | | mC1 | 0.80 | 1.18 |
| 30 | 0.71 | 0.97 | m_mu | 0.90 | 0.94 |
| | | | mC1 | 0.80 | 1.14 |
| 35 | 0.56 | 0.99 | m_mu | 0.90 | 0.94 |
| | | | mC1 | 0.80 | 1.08 |
| 39 | 0.46 | 1.00 | m_mu | 0.90 | 0.93 |
| | | | mC1 | 0.80 | 1.04 |

Table D.9 Best Irrigation Policy Analysis for Environmental Deficit Scenario

| Box ID | Coverage | Density | Uncertainty Factor | Min | Max |
|--------|----------|---------|----------------------|-----------------------|----------------------|
| 1 | 1.00 | 0.10 | m_mu | 0.90 | 1.04 |
| 5 | 1.00 | 0.12 | m_mu | 0.90 | 1.02 |
| 10 | 1.00 | 0.16 | m_mu | 0.90 | 0.99 |
| 15 | 1.00 | 0.20 | m_mu | 0.90 | 0.97 |
| 20 | 1.00 | 0.26 | m_mu | 0.90 | 0.95 |
| 25 | 1.00 | 0.34 | m_mu | 0.90 | 0.94 |
| 30 | 0.98 | 0.43 | m_mu mC1 | 0.90 0.80 | 0.93 1.18 |
| 35 | 0.91 | 0.52 | m_mu mC1 dphi1 | 0.90 0.80 -0.52 | 0.93 1.16 0.47 |
| 40 | 0.84 | 0.61 | m_mu mC1 dphi1 | 0.90 0.80 -0.52 | 0.93 1.14 0.38 |
| 45 | 0.76 | 0.72 | m_mu mC1 dphi1 | 0.90 0.80 -0.52 | 0.93 1.09 0.33 |
| 50 | 0.66 | 0.81 | m_mu mC1 dphi1 | 0.90 0.80 -0.52 | 0.92 1.08 0.29 |
| 55 | 0.56 | 0.88 | m_mu mC1 dphi1 | 0.90 0.80 -0.52 | 0.92 1.03 0.24 |
| 58 | 0.50 | 0.93 | m_mu mC1 dphi1 | 0.90 0.80 -0.52 | 0.92 1.00 0.24 |

Table D.10 Best Tradeoff Policy Analysis for Hydropower Deficit Scenario

| Box ID | Coverage | Density | Uncertainty Factor | Min | Max |
|--------|----------|---------|--------------------|-------|-------|
| 1 | 1.00 | 0.09 | m_mu | 0.90 | 1.04 |
| 5 | 1.00 | 0.11 | m_mu | 0.90 | 1.02 |
| 10 | 1.00 | 0.15 | m_mu | 0.90 | 0.99 |
| 15 | 1.00 | 0.19 | m_mu | 0.90 | 0.97 |
| 20 | 1.00 | 0.24 | m_mu | 0.90 | 0.95 |
| 25 | 1.00 | 0.32 | m_mu | 0.90 | 0.94 |
| 30 | 0.99 | 0.41 | m_mu | 0.90 | 0.93 |
| | | | mC1 | 0.80 | 1.18 |
| 35 | 0.96 | 0.51 | m_mu | 0.90 | 0.93 |
| | | | mC1 | 0.80 | 1.14 |
| 40 | 0.92 | 0.63 | m_mu | 0.90 | 0.93 |
| | | | mC1 | 0.80 | 1.09 |
| 45 | 0.84 | 0.74 | m_mu | 0.90 | 0.92 |
| | | | mC1 | 0.80 | 1.05 |
| 50 | 0.74 | 0.84 | m_mu | 0.90 | 0.92 |
| | | | mC1 | 0.80 | 1.02 |
| 55 | 0.62 | 0.92 | m_mu | 0.90 | 0.92 |
| | | | mC1 | 0.80 | 1.00 |
| 58 | 0.55 | 0.95 | m_mu | 0.90 | 0.92 |
| | | | mC1 | 0.80 | 1.00 |
| | | | m_sigma | 0.95 | 1.19 |
| | | | delta_evaporation | -7.44 | 40.00 |

Table D.11 Best Tradeoff Policy Analysis for Environmental Deficit Scenario

| Box ID | Coverage | Density | Uncertainty Factor | Min | Max |
|--------|----------|---------|---|-------------------------------|------------------------------|
| 1 | 1.00 | 0.31 | m_mu | 0.90 | 1.04 |
| 5 | 1.00 | 0.39 | m_mu | 0.90 | 1.02 |
| 10 | 1.00 | 0.50 | m_mu | 0.90 | 0.99 |
| 15 | 1.00 | 0.64 | m_mu | 0.90 | 0.97 |
| 20 | 0.93 | 0.78 | m_mu | 0.90 | 0.95 |
| 25 | 0.81 | 0.88 | m_mu | 0.90 | 0.94 |
| 30 | 0.67 | 0.94 | m_mu dphi1 | 0.90 -0.52 | 0.94 0.47 |
| 35 | 0.54 | 0.98 | m_mu dphi1 mC1 | 0.90 -0.52 0.80 | 0.94 0.33 1.18 |
| 40 | 0.43 | 1.00 | m_mu dphi1 mC1 | 0.90 -0.52 0.80 | 0.93 0.17 1.18 |
| 44 | 0.35 | 1.00 | m_mu dphi1 mC1 demand_multiplier | 0.90 -0.52 0.80 1.00 | 0.93 0.14 1.18 1.03 |

Appendix E

Adaptation Tipping Points

E.1 Logistic Regression Contour Plot Best Hydropower (Hydropower Deficit)

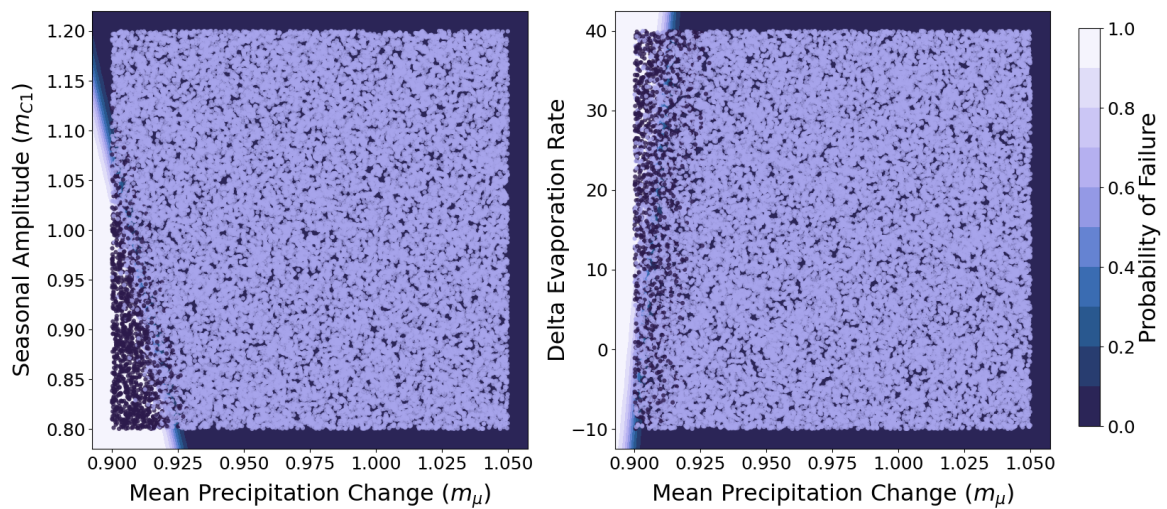


Fig. E.1 Logistic Regression Contour Plots based on Signpost Condition Set 1. The plot displays the probability for the Best Hydropower policy to fail (Scenario of Interest is Hydropower Deficit).

E.2 Logistic Regression Model Parameters (Best Hydropower Policy)

Table E.1 Logistic Regression Model Parameters of Policy Failure for Best Hydropower Policy

| Predictor | Coefficient | Standard Error | Z-Value | P-Value | 95% CI |
|-------------------------------|-------------|----------------|---------|---------|----------------------|
| Set 1 (Pseudo R-squ.: 0.6819) | | | | | |
| Intercept | 100.0384 | 1.401 | 71.404 | <0.001 | (97.292, 102.784) |
| m_μ | -101.1370 | 1.401 | -72.176 | <0.001 | (-103.883, -98.391) |
| $mC1$ | -3.5107 | 0.218 | -16.089 | <0.001 | (-3.938, -3.083) |
| δ_{evap} | 0.0478 | 0.002 | 26.017 | <0.001 | (0.044, 0.051) |
| Set 2 (Pseudo R-squ.: 0.7060) | | | | | |
| Intercept | 228.2662 | 4.369 | 52.244 | <0.001 | (219.703, 236.830) |
| m_μ | -109.5019 | 1.574 | -69.571 | <0.001 | (-112.587, -106.417) |
| $mC1$ | -3.7232 | 0.228 | -16.357 | <0.001 | (-4.169, -3.277) |
| $demand_{multi}$ | -117.4432 | 3.308 | -35.503 | <0.001 | (-123.927, -110.960) |
| Set 3 (Pseudo R-squ.: 0.6600) | | | | | |
| Intercept | 93.9826 | 1.279 | 73.480 | <0.001 | (91.476, 96.489) |
| m_μ | -94.3562 | 1.269 | -74.341 | <0.001 | (-96.844, -91.869) |
| $mC1$ | -3.2580 | 0.210 | -15.516 | <0.001 | (-3.670, -2.846) |
| $dphi1$ | -0.2230 | 0.079 | -2.807 | 0.005 | (-0.379, -0.067) |

E.3 Logistic Regression Model Parameters (Best Environment Policy)

Table E.2 Logistic Regression Model Parameters of Policy Failure for Best Environmental Policy

| Predictor | Coefficient | Standard Error | Z-Value | P-Value | 95% CI |
|-------------------------------|-------------|----------------|---------|---------|----------------------|
| Set 1 (Pseudo R-squ.: 0.7055) | | | | | |
| Intercept | 124.4312 | 1.971 | 63.120 | <0.001 | (120.567, 128.295) |
| m_μ | -123.8792 | 1.952 | -63.465 | <0.001 | (-127.705, -120.053) |
| $mC1$ | -8.3789 | 0.269 | -31.168 | <0.001 | (-8.906, -7.852) |
| δ_{evap} | 0.0404 | 0.002 | 20.235 | <0.001 | (0.036, 0.044) |
| Set 2 (Pseudo R-squ.: 0.6934) | | | | | |
| Intercept | 147.2735 | 3.773 | 39.035 | <0.001 | (139.879, 154.668) |
| m_μ | -118.5529 | 1.833 | -64.687 | <0.001 | (-122.145, -114.961) |
| $mC1$ | -7.9722 | 0.261 | -30.556 | <0.001 | (-8.484, -7.461) |
| $demand_{multi}$ | -27.2446 | 3.004 | -9.068 | <0.001 | (-33.133, -21.356) |
| Set 3 (Pseudo R-squ.: 0.6913) | | | | | |
| Intercept | 118.7568 | 1.844 | 64.411 | <0.001 | (115.143, 122.371) |
| m_μ | -117.6906 | 1.817 | -64.780 | <0.001 | (-121.251, -114.130) |
| $mC1$ | -7.9318 | 0.259 | -30.570 | <0.001 | (-8.440, -7.423) |
| $dphi1$ | -0.3860 | 0.089 | -4.357 | <0.001 | (-0.560, -0.212) |

E.4 Logistic Regression Model Parameters (Best Irrigation Policy)

Table E.3 Logistic Regression Model Parameters of Policy Failure for Best Irrigation Policy

| Predictor | Coefficient | Standard Error | Z-Value | P-Value | 95% CI |
|--------------------------------|-------------|----------------|---------|---------|------------------|
| Set 1 (Pseudo R-squ.: 0.01554) | | | | | |
| Intercept | 5.8957 | 0.311 | 18.928 | <0.001 | (5.285, 6.506) |
| m_μ | -6.7310 | 0.299 | -22.500 | <0.001 | (-7.317, -6.145) |
| $mC1$ | 0.4475 | 0.111 | 4.023 | <0.001 | (0.229, 0.666) |
| δ_{evap} | 0.0018 | 0.001 | 1.976 | 0.048 | (0.00001, 0.004) |
| Set 2 (Pseudo R-squ.: 0.01580) | | | | | |
| Intercept | 11.1727 | 1.494 | 7.479 | <0.001 | (8.245, 14.101) |
| m_μ | -6.7376 | 0.299 | -22.517 | <0.001 | (-7.324, -6.151) |
| $mC1$ | 0.4479 | 0.111 | 4.025 | <0.001 | (0.230, 0.666) |
| $demand_{multi}$ | -5.1646 | 1.436 | -3.598 | <0.001 | (-7.978, -2.351) |
| Set 3 (Pseudo R-squ.: 0.01580) | | | | | |
| Intercept | 11.1727 | 1.494 | 7.479 | <0.001 | (8.245, 14.101) |
| m_μ | -6.7376 | 0.299 | -22.517 | <0.001 | (-7.324, -6.151) |
| $mC1$ | 0.4479 | 0.111 | 4.025 | <0.001 | (0.230, 0.666) |
| $demand_{multi}$ | -5.1646 | 1.436 | -3.598 | <0.001 | (-7.978, -2.351) |

E.5 Logistic Regression Model Parameters (Best Tradeoff Policy)

Table E.4 Logistic Regression Model Parameters of Policy Failure for Best Tradeoff Policy

| Predictor | Coefficient | Standard Error | Z-Value | P-Value | 95% CI |
|-------------------------------|-------------|----------------|---------|---------|----------------------|
| Set 1 (Pseudo R-squ.: 0.8643) | | | | | |
| Intercept | 263.9196 | 5.784 | 45.628 | <0.001 | (252.583, 275.256) |
| m_μ | -259.3704 | 5.672 | -45.725 | <0.001 | (-270.488, -248.253) |
| $mC1$ | -19.0543 | 0.539 | -35.376 | <0.001 | (-20.110, -17.999) |
| δ_{evap} | 0.0753 | 0.003 | 23.699 | <0.001 | (0.069, 0.082) |
| Set 2 (Pseudo R-squ.: 0.8602) | | | | | |
| Intercept | 360.9413 | 8.789 | 41.066 | <0.001 | (343.714, 378.168) |
| m_μ | -248.1382 | 5.290 | -46.911 | <0.001 | (-258.505, -237.771) |
| $mC1$ | -18.0626 | 0.510 | -35.383 | <0.001 | (-19.063, -17.062) |
| $demand_{multi}$ | -105.9003 | 4.821 | -21.964 | <0.001 | (-115.350, -96.450) |
| Set 3 (Pseudo R-squ.: 0.8529) | | | | | |
| Intercept | 241.8064 | 5.047 | 47.908 | <0.001 | (231.914, 251.699) |
| m_μ | -236.8117 | 4.935 | -47.984 | <0.001 | (-246.485, -227.139) |
| $mC1$ | -17.2115 | 0.482 | -35.685 | <0.001 | (-18.157, -16.266) |
| $dphi1$ | -2.3623 | 0.134 | -17.632 | <0.001 | (-2.625, -2.100) |

E.6 Logistic Regression Contour Plots (Signpost Condition Set 1)

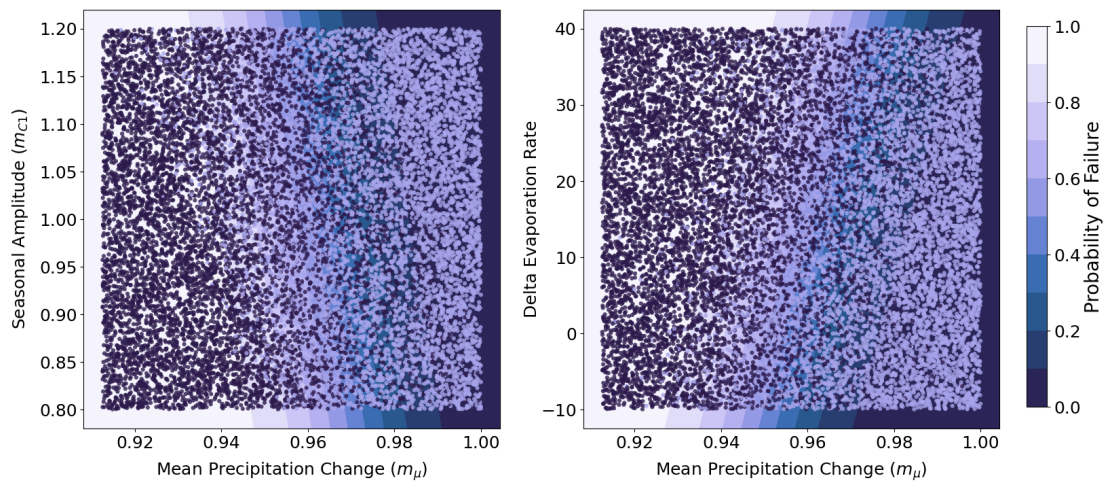


Fig. E.2 Logistic Regression Contour Plots based on Signpost Condition Set 1 (Best Hydropower Policy). The contour line color indicates failure probability, with lighter shades representing higher risks. Dark dots describe policy failure.

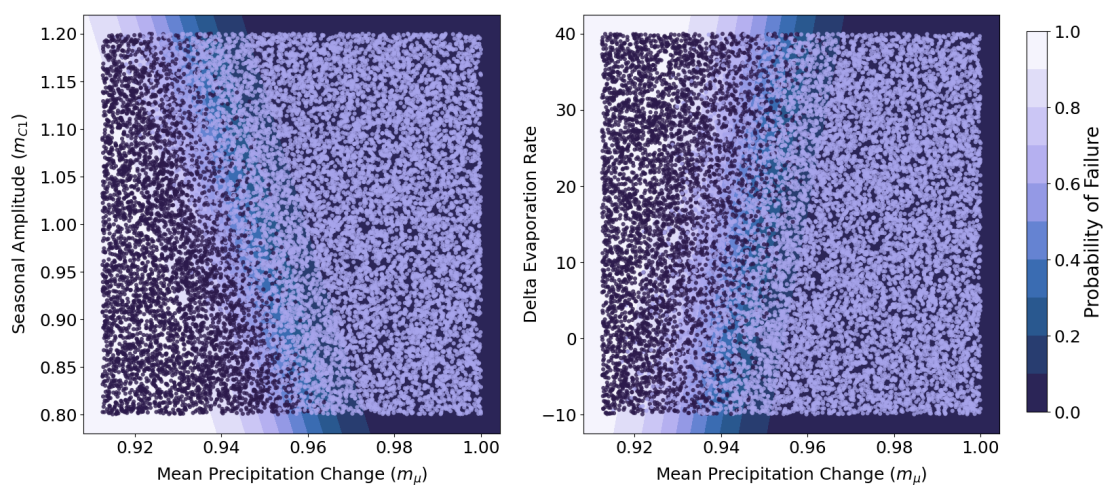


Fig. E.3 Logistic Regression Contour Plots based on Signpost Condition Set 1 (Best Environment Policy). The contour line color indicates failure probability, with lighter shades representing higher risks. Dark dots describe policy failure.

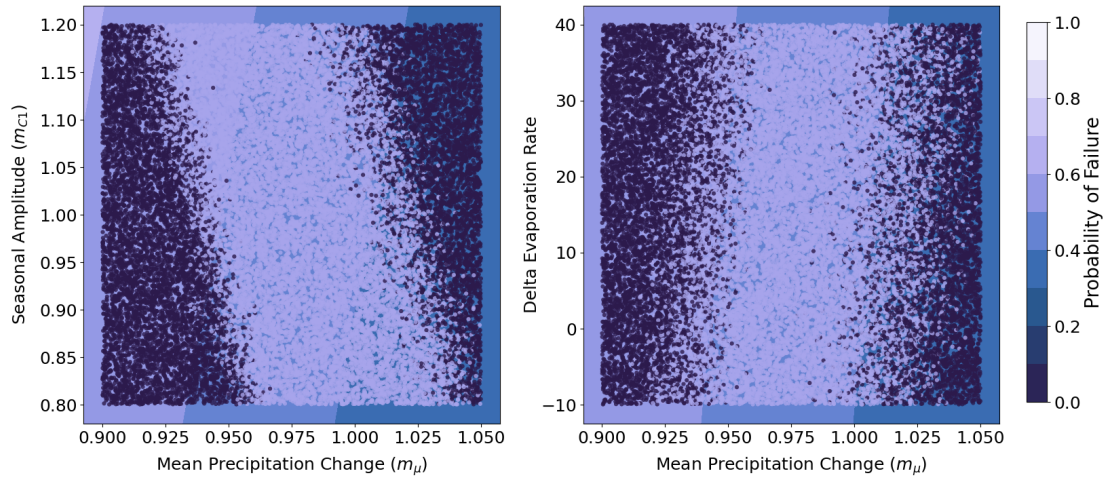


Fig. E.4 Logistic Regression Contour Plots based on Signpost Condition Set 1 (Best Irrigation Policy). The contour line color indicates failure probability, with lighter shades representing higher risks. Dark dots describe policy failure.

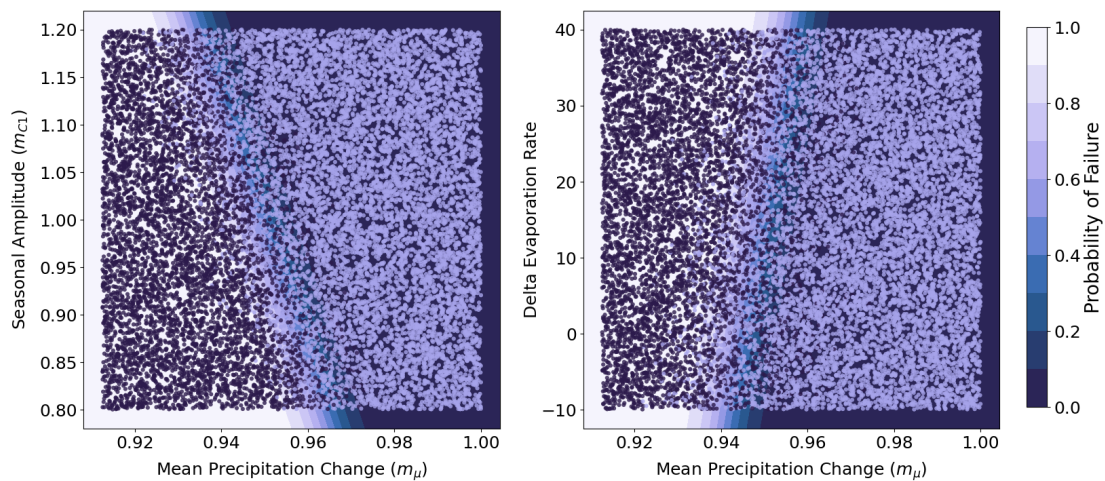


Fig. E.5 Logistic Regression Contour Plots based on Signpost Condition Set 1 (Best Tradeoff Policy). The contour line color indicates failure probability, with lighter shades representing higher risks. Dark dots describe policy failure.

E.7 Logistic Regression Contour Plots (Signpost Condition Set 2)

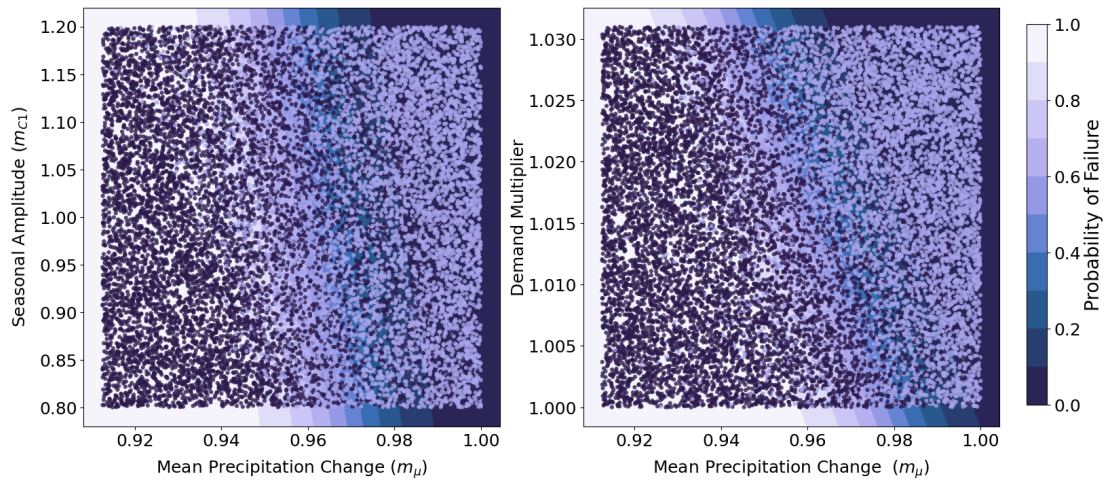


Fig. E.6 Logistic Regression Contour Plots based on Signpost Condition Set 2 (Best Hydropower Policy). The contour line color indicates failure probability, with lighter shades representing higher risks. Dark dots describe policy failure.

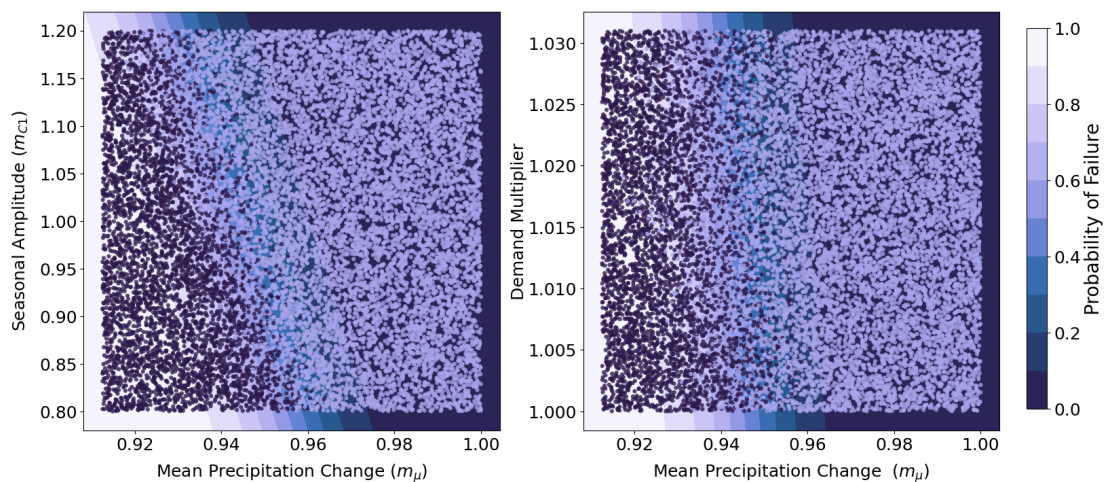


Fig. E.7 Logistic Regression Contour Plots based on Signpost Condition Set 2 (Best Environment Policy). The contour line color indicates failure probability, with lighter shades representing higher risks. Dark dots describe policy failure.

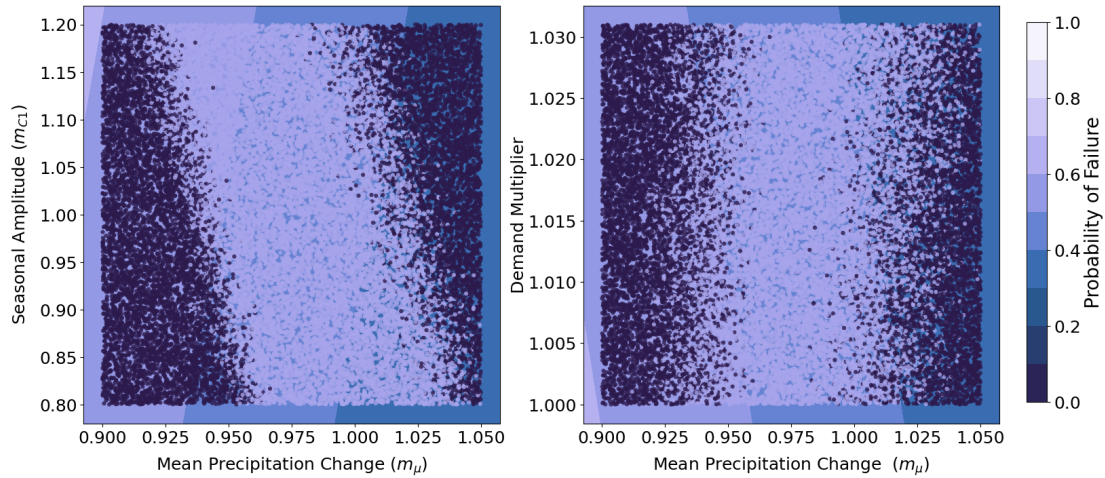


Fig. E.8 Logistic Regression Contour Plots based on Signpost Condition Set 2 (Best Irrigation Policy). The contour line color indicates failure probability, with lighter shades representing higher risks. Dark dots describe policy failure.

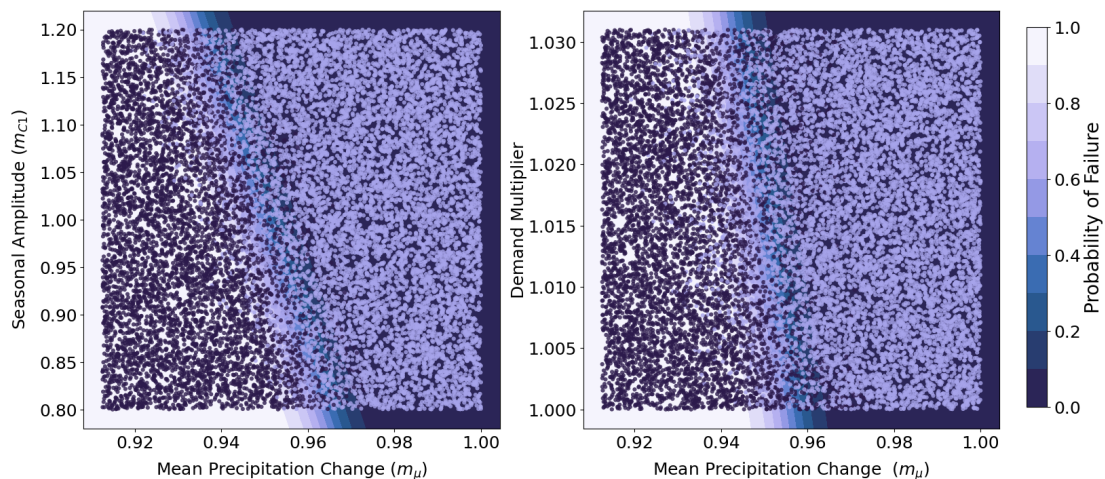


Fig. E.9 Logistic Regression Contour Plots based on Signpost Condition Set 2 (Best Tradeoff Policy). The contour line color indicates failure probability, with lighter shades representing higher risks. Dark dots describe policy failure.

E.8 Logistic Regression Contour Plots (Signpost Condition Set 3)

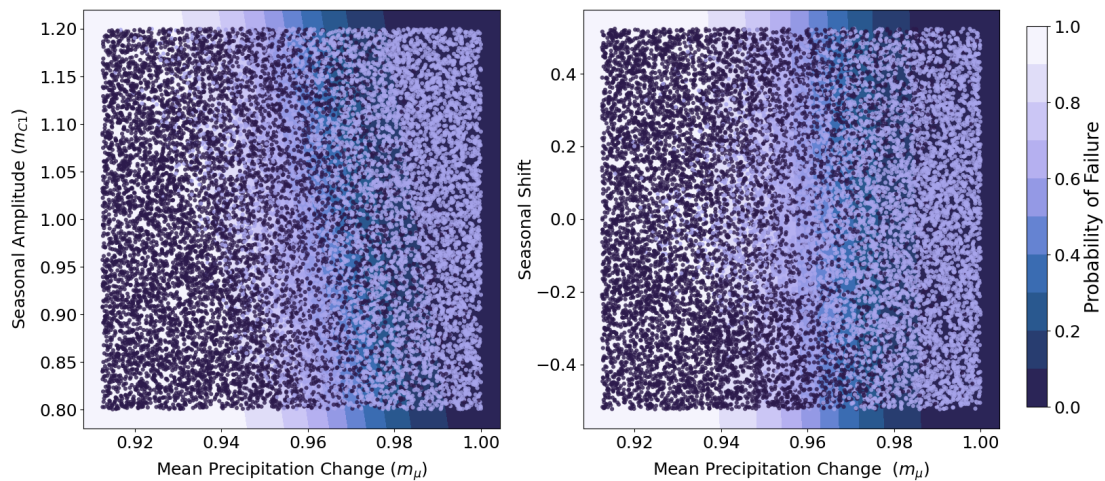


Fig. E.10 Logistic Regression Contour Plots based on Signpost Condition Set 3 (Best Hydropower Policy). The contour line color indicates failure probability, with lighter shades representing higher risks. Dark dots describe policy failure.

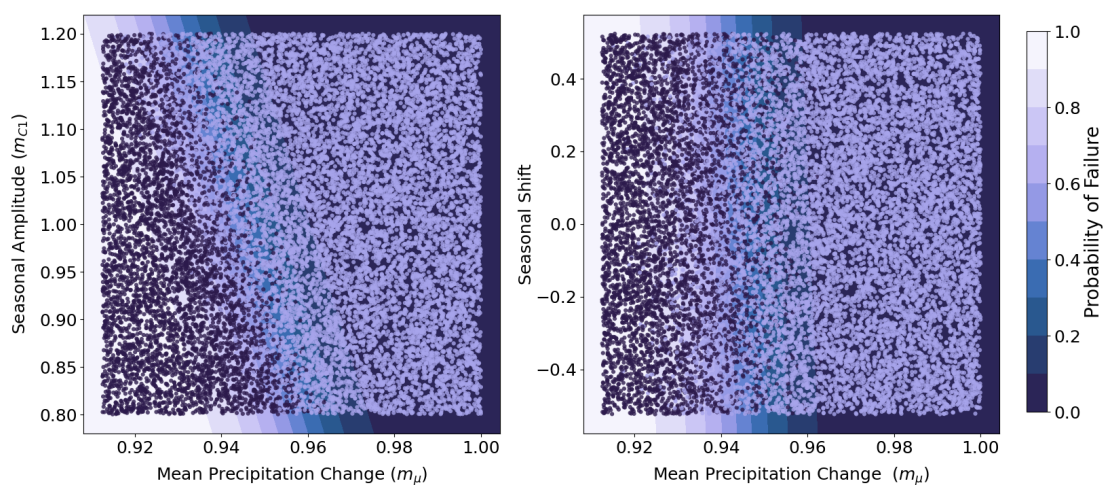


Fig. E.11 Logistic Regression Contour Plots based on Signpost Condition Set 3 (Best Environment Policy). The contour line color indicates failure probability, with lighter shades representing higher risks. Dark dots describe policy failure.

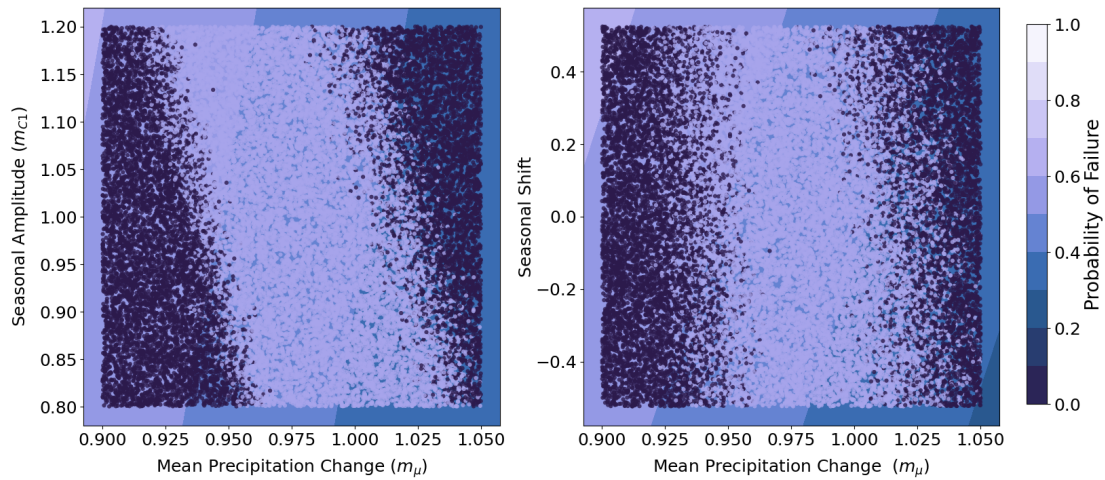


Fig. E.12 Logistic Regression Contour Plots based on Signpost Condition Set 3 (Best Irrigation Policy). The contour line color indicates failure probability, with lighter shades representing higher risks. Dark dots describe policy failure.

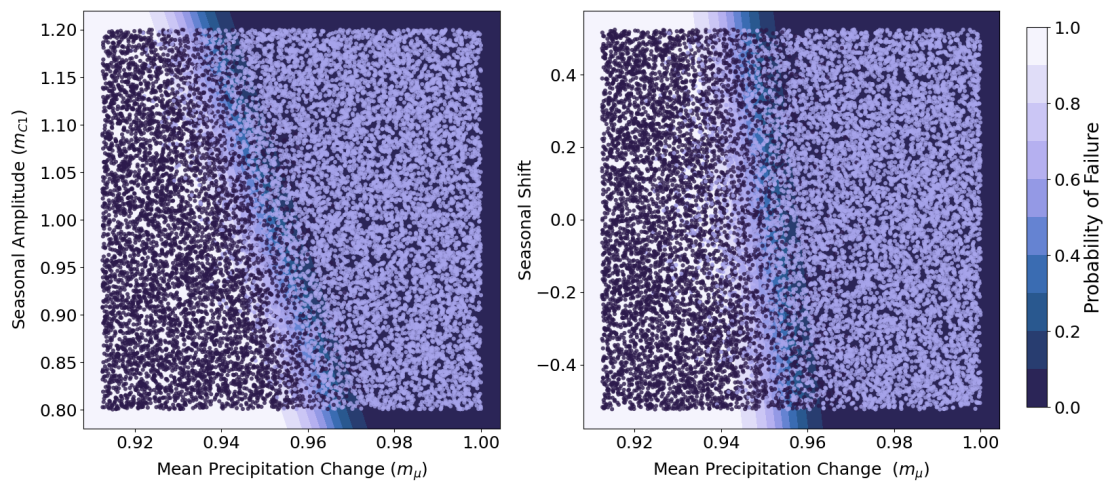


Fig. E.13 Logistic Regression Contour Plots based on Signpost Condition Set 3 (Best Tradeoff Policy). The contour line color indicates failure probability, with lighter shades representing higher risks. Dark dots describe policy failure.

E.9 Adaptation Tipping Point Streamflow Plot for ATP-Conditions

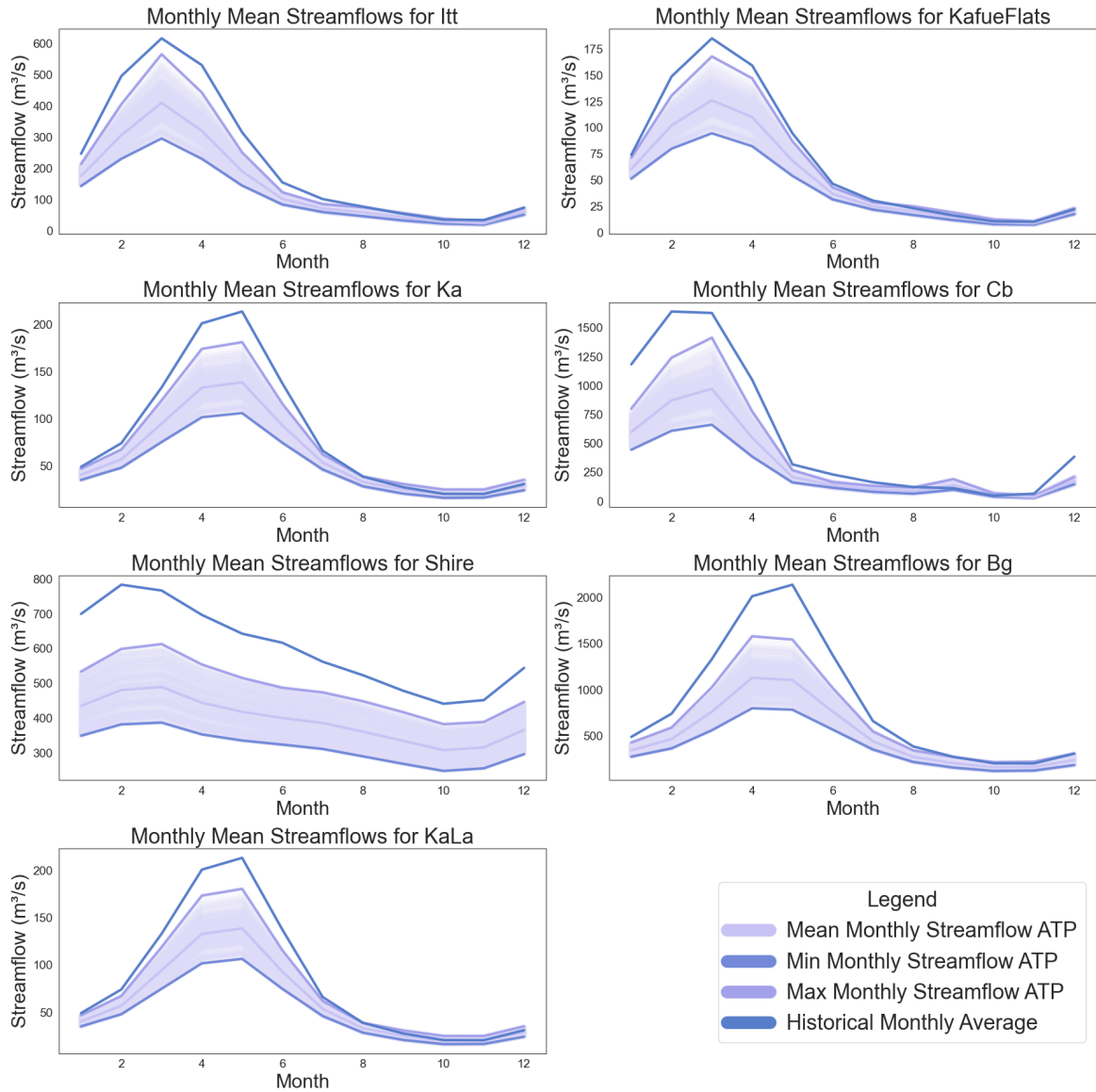


Fig. E.14 Streamflow Pattern of the Max ATP-Streamflow Condition. Comparison of historical monthly average streamflow data and Adaptation Tipping Point patterns based on the Adaptation Tipping Point Thresholds of a mean precipitation factor 0.965, and seasonal amplitudes of 1.05.

E.10 Adaptation Tipping Point Streamflow Tables for Max ATP-Condition

Table E.5 Monthly streamflow patterns for the Itt catchment comparing historical data with ATP streamflow values.

| Month | Historical | ATP Mean | ATP Max | ATP Min | Mean Diff | Max Diff | Min Diff |
|-----------|------------|----------|---------|---------|-----------|----------|----------|
| January | 246.8 | 175.5 | 213.9 | 143.4 | 71.3 | 32.9 | 103.4 |
| February | 496.1 | 306.3 | 405.5 | 230.5 | 189.8 | 90.6 | 265.6 |
| March | 617.3 | 410.2 | 566.3 | 295.9 | 207.1 | 51.0 | 321.4 |
| April | 531.2 | 320.2 | 443.1 | 230.5 | 211.0 | 88.1 | 300.7 |
| May | 315.4 | 190.5 | 250.7 | 144.5 | 124.9 | 64.7 | 170.9 |
| June | 154.8 | 101.6 | 122.8 | 83.9 | 53.2 | 32.0 | 70.9 |
| July | 101.2 | 71.1 | 85.0 | 59.8 | 30.1 | 16.2 | 41.4 |
| August | 77.0 | 58.4 | 74.7 | 46.4 | 18.6 | 2.3 | 30.6 |
| September | 53.7 | 42.4 | 56.2 | 32.6 | 11.3 | -2.5 | 21.1 |
| October | 35.3 | 28.8 | 37.6 | 22.5 | 6.5 | -2.3 | 12.8 |
| November | 34.1 | 23.7 | 29.5 | 19.4 | 10.4 | 4.6 | 14.7 |
| December | 73.5 | 60.7 | 72.7 | 51.2 | 12.8 | 0.8 | 22.3 |

Table E.6 Monthly streamflow patterns for the Kafue Flats catchment comparing historical data with ATP streamflow values.

| Month | Historical | ATP Mean | ATP Max | ATP Min | Mean Diff | Max Diff | Min Diff |
|-----------|------------|----------|---------|---------|-----------|----------|----------|
| January | 74.0 | 60.5 | 71.3 | 51.4 | 13.5 | 2.7 | 22.6 |
| February | 148.8 | 102.1 | 130.5 | 79.9 | 46.7 | 18.3 | 68.9 |
| March | 185.2 | 126.1 | 167.9 | 94.6 | 59.1 | 17.3 | 90.6 |
| April | 159.4 | 110.0 | 147.0 | 82.3 | 49.4 | 12.4 | 77.1 |
| May | 94.6 | 68.5 | 87.1 | 54.0 | 26.1 | 7.5 | 40.6 |
| June | 46.4 | 36.7 | 42.9 | 31.5 | 9.7 | 3.5 | 14.9 |
| July | 30.4 | 24.9 | 28.7 | 21.8 | 5.5 | 1.7 | 8.6 |
| August | 23.1 | 20.2 | 24.9 | 16.7 | 2.9 | -1.8 | 6.4 |
| September | 16.1 | 14.8 | 18.9 | 11.8 | 1.3 | -2.8 | 4.3 |
| October | 10.6 | 9.8 | 12.3 | 7.9 | 0.8 | -1.7 | 2.7 |
| November | 10.2 | 8.8 | 10.5 | 7.5 | 1.4 | -0.3 | 2.7 |
| December | 22.1 | 20.0 | 23.1 | 17.5 | 2.1 | -1.0 | 4.6 |

Table E.7 Monthly streamflow patterns for the Kariba catchment comparing historical data with ATP streamflow values.

| Month | Historical | ATP Mean | ATP Max | ATP Min | Mean Diff | Max Diff | Min Diff |
|-----------|------------|----------|---------|---------|-----------|----------|----------|
| January | 49.1 | 40.7 | 47.1 | 35.3 | 8.4 | 2.0 | 13.8 |
| February | 74.2 | 57.0 | 67.4 | 48.2 | 17.2 | 6.8 | 26.0 |
| March | 133.2 | 94.9 | 119.5 | 75.4 | 38.3 | 13.7 | 57.8 |
| April | 201.1 | 133.0 | 174.0 | 101.6 | 68.1 | 27.1 | 99.5 |
| May | 213.6 | 138.6 | 181.1 | 106.1 | 75.0 | 32.5 | 107.5 |
| June | 137.4 | 92.9 | 115.8 | 74.6 | 44.5 | 21.6 | 62.8 |
| July | 66.2 | 53.8 | 62.2 | 46.4 | 12.4 | 4.0 | 19.8 |
| August | 38.8 | 33.2 | 38.8 | 28.6 | 5.6 | 0.0 | 10.2 |
| September | 27.6 | 25.2 | 31.0 | 20.9 | 2.4 | -3.4 | 6.7 |
| October | 20.6 | 20.1 | 25.1 | 16.5 | 0.5 | -4.5 | 4.1 |
| November | 20.5 | 20.3 | 25.1 | 16.7 | 0.2 | -4.6 | 3.8 |
| December | 31.0 | 29.2 | 35.5 | 24.4 | 1.8 | -4.5 | 6.6 |

Table E.8 Monthly streamflow patterns for the Cahora Bassa catchment comparing historical data with ATP streamflow values.

| Month | Historical | ATP Mean | ATP Max | ATP Min | Mean Diff | Max Diff | Min Diff |
|-----------|------------|----------|---------|---------|-----------|----------|----------|
| January | 1183.8 | 598.7 | 800.4 | 444.9 | 585.1 | 383.4 | 738.9 |
| February | 1640.4 | 872.7 | 1241.3 | 608.9 | 767.7 | 399.1 | 1031.5 |
| March | 1627.7 | 971.3 | 1414.2 | 661.5 | 656.4 | 213.5 | 966.2 |
| April | 1050.1 | 548.97 | 776.7 | 385.6 | 501.1 | 273.4 | 664.5 |
| May | 317.97 | 208.8 | 268.0 | 162.4 | 109.2 | 50.0 | 155.6 |
| June | 230.7 | 138.9 | 164.4 | 116.3 | 91.8 | 66.3 | 114.4 |
| July | 163.6 | 102.7 | 131.5 | 81.3 | 60.9 | 32.1 | 82.3 |
| August | 122.5 | 86.5 | 117.2 | 65.1 | 36.0 | 5.3 | 57.4 |
| September | 111.7 | 135.8 | 190.8 | 98.8 | -24.1 | -79.1 | 12.9 |
| October | 48.1 | 50.9 | 66.4 | 39.9 | -2.8 | -18.3 | 8.2 |
| November | 64.6 | 36.0 | 44.4 | 29.5 | 28.6 | 20.2 | 35.1 |
| December | 384.5 | 175.7 | 208.5 | 146.5 | 208.8 | 176.0 | 238.0 |

Table E.9 Monthly streamflow patterns for the Shire catchment comparing historical data with ATP streamflow values.

| Month | Historical | ATP Mean | ATP Max | ATP Min | Mean Diff | Max Diff | Min Diff |
|-----------|------------|----------|---------|---------|-----------|----------|----------|
| January | 699.7 | 435.1 | 534.0 | 349.6 | 264.6 | 165.7 | 350.1 |
| February | 783.8 | 480.6 | 599.0 | 382.2 | 303.2 | 184.8 | 401.6 |
| March | 767.0 | 489.3 | 613.1 | 387.2 | 277.7 | 153.9 | 379.8 |
| April | 697.0 | 444.3 | 554.2 | 353.3 | 252.7 | 142.8 | 343.7 |
| May | 643.0 | 418.0 | 515.8 | 335.7 | 225.0 | 127.2 | 307.3 |
| June | 616.8 | 400.2 | 487.3 | 324.0 | 216.6 | 129.5 | 292.8 |
| July | 562.4 | 386.2 | 474.0 | 311.5 | 176.2 | 88.4 | 250.9 |
| August | 523.5 | 361.3 | 448.6 | 290.2 | 162.2 | 74.9 | 233.3 |
| September | 478.8 | 334.6 | 417.2 | 268.6 | 144.2 | 61.6 | 210.2 |
| October | 441.4 | 308.1 | 382.7 | 248.3 | 133.3 | 58.7 | 193.1 |
| November | 451.8 | 316.0 | 388.8 | 255.7 | 135.8 | 63.0 | 196.1 |
| December | 544.4 | 366.0 | 446.3 | 296.4 | 178.4 | 98.1 | 248.0 |

Table E.10 Monthly streamflow patterns for the Bakota George catchment comparing historical data with ATP streamflow values.

| Month | Historical | ATP Mean | ATP Max | ATP Min | Mean Diff | Max Diff | Min Diff |
|-----------|------------|----------|---------|---------|-----------|----------|----------|
| January | 491.3 | 346.3 | 430.0 | 278.3 | 145.0 | 61.3 | 213.0 |
| February | 742.1 | 468.1 | 591.8 | 367.5 | 274.0 | 150.3 | 374.6 |
| March | 1331.8 | 763.3 | 1027.6 | 562.7 | 568.5 | 304.2 | 769.1 |
| April | 2010.6 | 1128.9 | 1578.3 | 800.5 | 881.7 | 432.3 | 1210.1 |
| May | 2135.5 | 1105.5 | 1542.7 | 785.2 | 1030.0 | 592.8 | 1350.3 |
| June | 1374.5 | 765.2 | 1019.3 | 569.9 | 609.3 | 355.2 | 804.6 |
| July | 661.8 | 443.4 | 548.9 | 355.3 | 218.4 | 112.9 | 306.5 |
| August | 387.9 | 275.3 | 345.3 | 220.7 | 112.6 | 42.6 | 167.2 |
| September | 275.8 | 207.5 | 272.9 | 159.9 | 68.3 | 2.9 | 115.9 |
| October | 206.1 | 162.7 | 217.8 | 123.5 | 43.4 | -11.7 | 82.6 |
| November | 204.8 | 167.4 | 222.5 | 127.9 | 37.4 | -17.7 | 76.9 |
| December | 310.2 | 240.3 | 312.7 | 186.9 | 69.9 | -2.5 | 123.3 |